1997

Fluid inclusion studies of rare element pegmatites, South Platte District, Colorado.

Randy. Levasseur
University of Windsor

Recommended Citation

Levasseur, Randy., "Fluid inclusion studies of rare element pegmatites, South Platte District, Colorado." (1997). *Electronic Theses and Dissertations.* Paper 2129.

INFORMATION TO USERS

This manuscript has been reproduced from the microfilm master. UMI films the text directly from the original or copy submitted. Thus, some thesis and dissertation copies are in typewriter face, while others may be from any type of computer printer.

The quality of this reproduction is dependent upon the quality of the copy submitted. Broken or indistinct print, colored or poor quality illustrations and photographs, print bleedthrough, substandard margins, and improper alignment can adversely affect reproduction.

In the unlikely event that the author did not send UMI a complete manuscript and there are missing pages, these will be noted. Also, if unauthorized copyright material had to be removed, a note will indicate the deletion.

Oversize materials (e.g., maps, drawings, charts) are reproduced by sectioning the original, beginning at the upper left-hand corner and continuing from left to right in equal sections with small overlaps. Each original is also photographed in one exposure and is included in reduced form at the back of the book.

Photographs included in the original manuscript have been reproduced xerographically in this copy. Higher quality 6" x 9" black and white photographic prints are available for any photographs or illustrations appearing in this copy for an additional charge. Contact UMI directly to order.

NOTE TO USERS

The original manuscript received by UMI contains pages with indistinct and slanted print. Pages were microfilmed as received.

This reproduction is the best copy available

UMI

FLUID INCLUSION STUDIES OF RARE ELEMENT PEGMATITES, SOUTH PLATTE DISTRICT, COLORADO

by

Randy Levasseur

A Thesis
Submitted to the Faculty of Graduate Studies and Research
through the Department of Earth Sciences
in Partial Fulfillment of the Requirements
for the Degree of Master of
Science at the
University of Windsor

Windsor, Ontario, Canada
1997

ABSTRACT

Over fifty granite-hosted pegmatites occur in the South Platte district, located in the northern portion of the 1.01 Ga Pikes Peak batholith in the Rocky Mountain Front Range of central Colorado. Many of these pegmatites are concentrically zoned and enriched in fluorite, REE, Y and Nb, relative to the host granite, and may be classified as NYF pegmatites. Rare-element mineralization principally occurs in a core-margin zone as vein and replacement assemblages comprising albite, fluorite, hematite, muscovite and a variety of rare-element minerals, including samarskite, allanite, monazite, bastnaesite and gadolinite.

Laser-excited emission (fluorescence) spectra indicate early, massive, core-margin fluorite (probably magmatic) in many instances contains higher concentration of REE than later hydrothermal white, clear and purple fluorite which replace it. The latter fluorite is associated with rare element minerals which have sequestered the REE released from the massive fluorite during fluid-fluorite interaction. This indicates that at least some of the rare elements in the mineralized zones have been derived from earlier, magmatic concentrations. Some later hydrothermal, rare element mineral-free fluorite contains very high concentrations of REE, possibly requiring intrinsically high rare element contents in the hydrothermal fluids.

Fluid inclusion studies of both magmatic and hydrothermal phases reveal that four compositionally distinct hydrothermal fluid types have permeated the pegmatites. These are: (1) Low salinity aqueous fluids (0 - 12 equiv. wt. % NaCl

+ CaCl$_2$); (2) Intermediate salinity aqueous fluids (18 to 24 equiv. wt.%); (3) High salinity aqueous fluids (26 to 30 equiv. wt. %); and (4) Low salinity, CO$_2$-bearing fluids.

Data from primary inclusions within hydrothermal fluorite indicate that the rare-element mineralization was formed from low salinity (<10 equiv. wt. % NaCl + CaCl$_2$), orthomagmatic fluids at temperatures of at least 340 to 500°C. The other fluid types occur exclusively in secondary inclusions, and post-dated the early, low-salinity fluid. The intermediate salinity fluid is present in all the pegmatites studied and likely represents a distinct, district-wide fluid infiltration event. The high salinity and carbonic fluids are, for the most part, restricted to the same pegmatites and are possibly genetically related to one another through immiscibility. Modelling of the compositions of halite-bearng inclusions in the H$_2$O-NaCl-CaCl$_2$ system indicates two compositionally-distinct high-salinity fluids; one with around 3 wt % CaCl$_2$ and another with around 11 wt % CaCl$_2$. These two fluids are distributed differently within the pegmatites and their compositional differences possibly reflect separate fluid-rock interaction histories, the Ca-poor fluid having interacted with fluorite-rich assemblages.

DEDICATION

To she who is responsible for this thesis to exist,
by simply having been there - all of the time.
My love forever Shannon

To my grandfather Henderson. Your wisdom,
kindness, generosity, and jokes will be missed.
I wish you could of been here.

Acknowledgments

I would like to express my deepest gratitude to Dr. Iain Samson who suggested, supervised, and financed this project (through an NSERC research grant). I thank him for the numerous hours he assisted me both in the field and in the lab; without his expertise this project could not have been completed. I would also like to thank my other committee member, Dr. I. Al-Aasm for his help, guidance and encouragement. Special thanks go to Gema Olivo for the SEM-EDS analysis, Ingrid Churchill for assisting in staining techniques, and Bob Burruss for help with sampling and discussion about the South Platte pegmatites.

Thanks also to my fellow colleagues Ryan Walker, Ian Kerr, Chris Lauzon and Debby MacDonald who assisted this project with their input and direction.

Sincere thanks are also due to all of my friends (especially Randy Hadland for his support and constant work projects), the Sigma Chi Fraternity and fellow graduate students at the U.O.W. and elsewhere who helped me retain my sanity, or insanity, depending on the situation at hand.

Finally I am most grateful to my fiancee for her encouragement to pursue this goal and patience to see it through and to my family for their enduring faith, support, and encouragement.

TABLE OF CONTENTS

LIST OF TABLES

LIST OF FIGURES

Chapter 1: Introduction

Introduction

The South Platte pegmatite district is located within the eastern half of the Buffalo Park intrusive centre, which lies within the 1010 Ma Precambrian Pikes Peak batholith in the Front Range of Colorado (Fig. 1). The central portion of this district comprises an area of about 80 km^2 which contains over 50 concentrically-zoned, rare element pegmatites, many of which have been mined on a small scale (Simmons and Heinrich, 1975, 1980). These pegmatites are enriched in rare earth elements (REE), Y, U and Nb.

Pegmatites in general may be classified on the basis of their mineralogy, chemistry, internal structure, parental granitoid chemistry, and pressure-temperature conditions of crystallization (Cerny, 1991a). The South Platte pegmatites belong to the rare element NYF (Niobium-Yttrium-Fluorine) class. In most of the South Platte pegmatites the primary minerals have, in-part, been replaced by hydrothermal fluorite, albite and a variety of rare element minerals including samarskite, bastnaesite, allanite, monazite and synchisite (Simmons and Heinrich, 1975; Brewster, 1986), which typically occur at, or close to, the margin between the quartz core and the intermediate zones of the pegmatites. Rare earth elements are used as superconductors and space exploration.

Although rare element mineralization is commonly hosted by, or associated with, igneous plutons, the mineralization, particularly REE

mineralization, is in fact often hydrothermally deposited (e.g. Sorenson, 1974; Lira and Ripley, 1990, Salvi and Williams-Jones, 1990; Campbell et al, 1995). The relatively little data that exists on the character of the fluids responsible for hydrothermal rare element mineralization indicate that the chemistry of the fluids is highly variable, and is generally characterized by moderate to high salinity aqueous fluids (15 - 90 wt. % NaCl) with variable amounts of CO_2, CH_4 and higher hydrocarbons (Lira and Ripley, 1990; Salvi and Williams-Jones, 1990; Campbell et al., 1995). Both internal (magmatic)(Lira and Ripley, 1990; Campbell et al., 1995) and external (formation waters)(Salvi and Williams-Jones, 1990) sources have been suggested for these fluids. As far as the author is aware, the only study dealing with the chemistry of fluids in pegmatites of a similiar character to those in the South Platte District (i.e. REE and Y rich) is that of Salvi and Williams-Jones (1992) on the Strange Lake deposit. Quartz in these pegmatites host a variety of fluid inclusion types ranging from moderate salinity aqueous (~14 to 27 wt. %) to hydrocarbon-rich, aqueous-poor fluids. However the rare element minerals in the Strange Lake pegmatites are magmatic rather than hydrothermal so that they are not directly analagous to the South Platte occurrences. Because the South Platte pegmatites are characterized by hydrothermal rare element mineralization within pegmatites, they afford an excellent opportunity to study hydrothermal magmatic fluids close to their source, prior to any interaction with country rocks or external fluids.

2
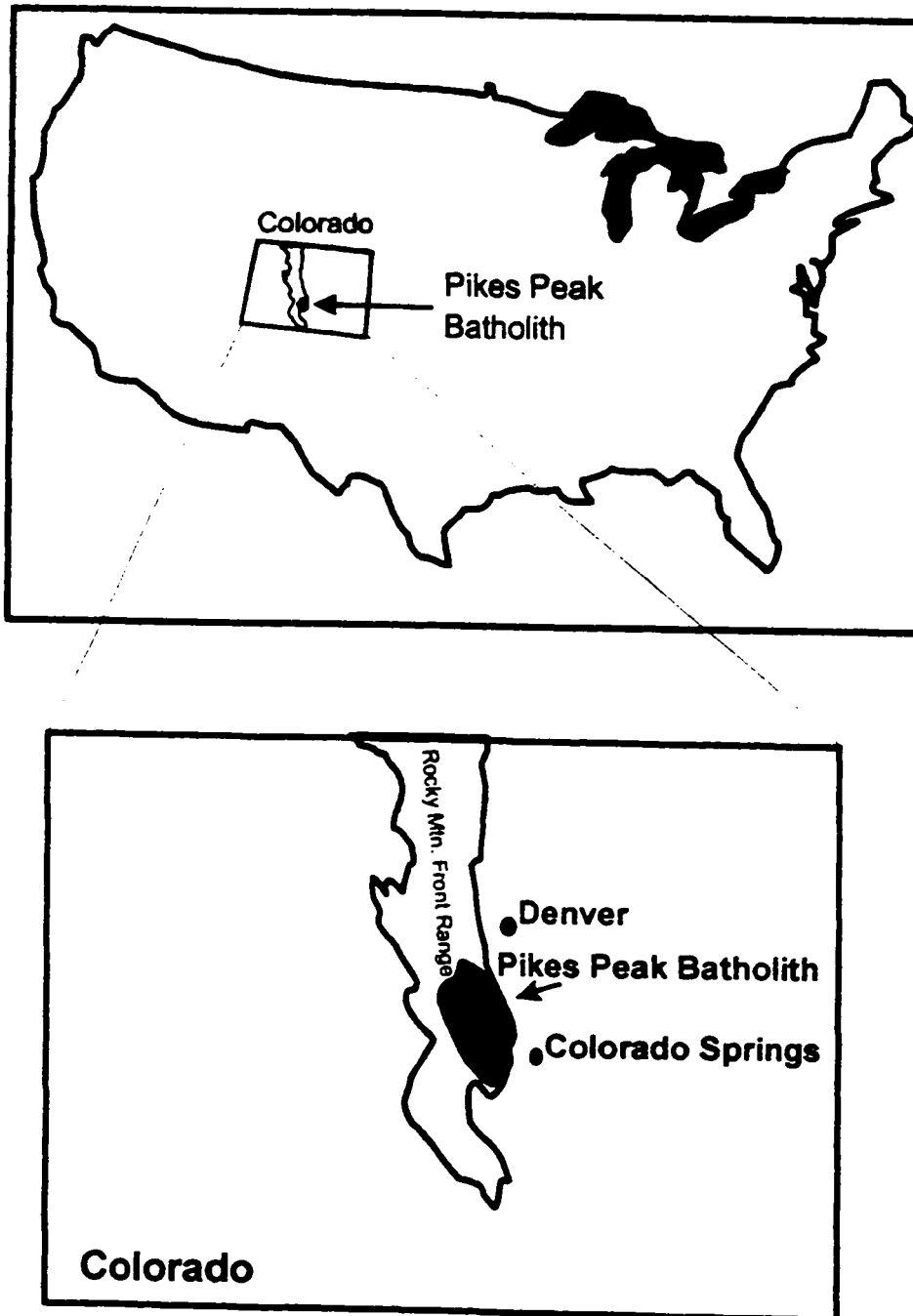
Figure 1. General location map of Pikes Peak batholith within the continental United States (modified from Brewster, 1986).

The hydrothermal minerals associated with the REE enrichments in the South Plate pegmatites contain abundant fluid inclusions (Simmons and Heinrich, 1980). Simmons and Heinrich (1980) recognized two types of inclusions based on their composition and degree of filling. The first type are liquid-vapour inclusions with a vapour phase comprising 2 - 30% of the inclusion volume. These inclusions typically occur within quartz and fluorite and contain little or no CO_2. Salinities range from 1 to 40 wt. % with large salt cubes present in the higher salinity inclusions. The second type are gas-rich inclusions with 40 - 95% vapour and these are restricted to core quartz. These inclusions occur only in quartz and are further subdivided into: 1) inclusions which homogenize to the vapour phase, 2) those which homogenization to the liquid phase and 3) those which exhibit critical homogenization. Simmons and Heinrich (1980) suggest that primary aqueous liquid-vapour inclusions are present in early green fluorite and primary inclusions in quartz include both aqueous and CO_2-rich types.

Daughter minerals were examined only in the first type of inclusion, and include halite, sylvite, anhydrite, synchisite and a carbonate solid (Simmons and Heinrich, 1980). Halite and sylvite are present in inclusions in both quartz and fluorite, whereas anhydrite is restricted to inclusions in fluorite. Some gas rich inclusions were also seen to contain unidentified minerals possibly carbonates. The liquid-vapour inclusions in green fluorite were believed to be primary, and homogenized between 98 and 324°C. The liquid-vapour quartz-hosted inclusions homogenized between 100 and 308 °C whereas the gas-rich inclusions

homogenized between 300 and 431°C, although most of the latter decrepitated prior to homogenization (Simmons and Heinrich, 1980).

Simmons and Heinrch (1980) concluded that core-margin green fluorite formed at temperatures above 340 °C and core quartz above temperatures of 430 °C. They also suggested that immiscibility between aqueous and carbonic fluids occurred during core quartz formation. However they could not resolve the discrepency between homogenization temperatures of the two fluid types and the interpreted primary origin for both. Furthermore, they questioned their interpretation of many of the inclusions in quartz as primary because this would require precipitation of the quartz core from hydrothermal fluids, which, on mass balance grounds, would be very difficult to achieve in a closed pegmatitic system. This also calls into question the primary origin of their inclusions in fluorite, based on the homogenization temperature data.

Objectives and Methodology

The principal objectives of this study are to determine the physico-chemical characteristics of the fluids responsible for rare-element mineralization in the South Platte pegmatites, how the nature of the fluids evolved within the pegmatites, and how the fluids varied between pegmatites.

Ideally, internally-derived fluids would be trapped as primary inclusions at various stages in the crystallization of the pegmatite. The location of the rare element zones at the core-margin indicates that they formed after crystallization

of the wall and intermediate zones. However, they could have formed prior to, during, or after crystallization of the core. If rare element mineral deposition occurred prior to core formation, the responsible fluids should be absent from the core quartz, whereas if the rare element zones formed after most of the core had formed, the fluids should be present within the core quartz as secondary (and possibly primary) inclusions. The underlying premise in testing such models is that the character of the hydrothermal fluids released from a crystallizing pegmatitic magma evolve with time, so that early fluids can be distinguished from those exsolved later. This seems a reasonable prediction to make based on other studies of pegmatites (e.g. London 1986a,b,c, 1987)

Four rare element pegmatites were chosen for this study: Oregon 3, Luster 1½, White Cloud and Lesser White Cloud. These four represent pegmatites from the western and eastern groups within the northern part of the South Platte district and include the two pegmatites with the best rare element mineralization (Oregon 3 and White Cloud). Seventy thin sections were prepared from samples from these four pegmatites. A subset of these samples were then prepared as doubly polished wafers for fluid inclusion analysis. Petrographic and mineralogical studies were carried out to provide a petrologic and paragenetic framework for the fluid inclusion studies.

Optical microscopy was used to study the mineralogy and textures of samples, as well as the distribution and characteristics of fluid inclusions. Mineral identification was also achieved using X-ray diffraction (XRD). Feldspars

were distinguished using XRD and staining. A scanning electron microscope with an energy dispersive analyser (SEM-EDS) was used to identify small crystals within fluorite.

Simmons and Heinrich (1980) describe a variety of fluorite types within the South Platte pegmatites, some of which contain high concentrations of REE. In order to characterize and compare the various fluorite types, and to gain some insight into their REE contents, laser-induced fluorescence studies of the fluorites were carried out. Recently, the potential value of laser-generated fluorescence spectra from fluorite has been recognized (Iliev et. al., 1988, Burruss et al., 1992). Substantial amounts of REE may substitute for calcium in fluorite (Bill and Calas, 1978) and these ions produce a series of intense narrow emission bands when excited by laser radiation (Burruss et al., 1992). Iliev et al. (1988) and Burruss et al. (1992) have used Raman spectrometers to obtain REE fluorescence spectra in natural fluorites and have attempted to assign observed bands to individual REE ions. Burruss et al. (1992) have also demonstrated a positive correlation between peak height and REE concentration.

Fluid inclusions were used to obtain information on the chemistry of the hydrothermal fluids in the pegmatites. Samples from all the pegmatite zones were studied, however, most analyses were carried out on inclusions in hydrothermal minerals in the rare element-rich replacement zones and from the quartz core. Fluid compositions were determined using both low and high temperature microthermometry. Low temperature phase equilibria provided

salinity estimates and qualitative information on the nature of the electrolytes in aqueous inclusions and on the composition and concentrations of gases. Compositional information was also obtained using high temperature phase equilibria, specifically, daughter mineral dissolution temperatures. The methods used in estimating fluid inclusion compositions are discussed at the appropriate points in the text.

Chapter 2: Geology

Pikes Peak Batholith

The Pikes Peak batholith lies within the Precambrian core of the Rocky Mountain Front Range in central Colorado (Fig. 1). It is a composite, anorogenic pluton composed mostly of granite and quartz monzonite which has been dated at 1040 Ma (Hedge, 1970). It intrudes predominantly Proterozoic quartzo-feldspathic gneiss, granitic rocks, amphibolite, and mica schist of the Idaho Springs Formation, which have been dated at 1450 to 1750 Ma (Peterman and Hedge, 1968; Barker et al., 1975).

The intrusive rocks within the Pikes Peak batholith are subalkalic to peraluminous, contain very little MgO (<0.20%), and have high FeO/Fe_2O_3 ratios, averaging around 2.5 (Barker et al., 1975). The batholith has been subdivided into three intrusive centres based on the structures and textures of the intrusive rocks (Hutchinson, 1972); these are the Buffalo Park, Lost Park, and Pikes Peak centres (Fig. 2). The Buffalo Park pluton, which hosts the South Platte pegmatites, shows evidence of being reversely zoned, with a more felsic outer zone composed of biotite granite and a more mafic centre of quartz monzonite (Simmons et al., 1987). In addition to the pegmatites, late-stage features include quartz veins, fluorite veins and aplite dikes.

9
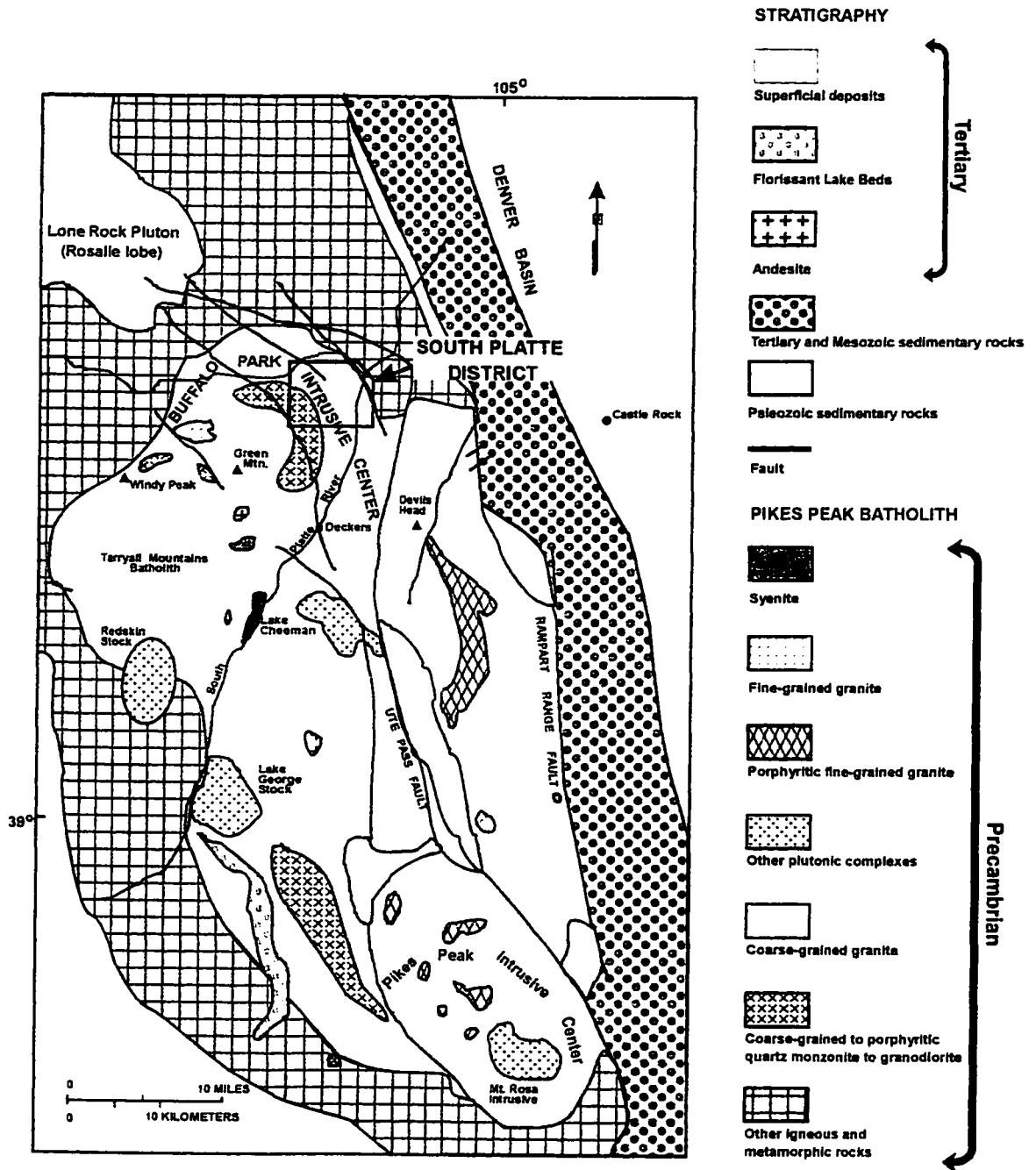
Figure 2. Geologic map of Pikes Peak batholith showing Buffalo Park intrusive center and the location of the South Platte pegmatite district (modified from Simmons et al., 1987).
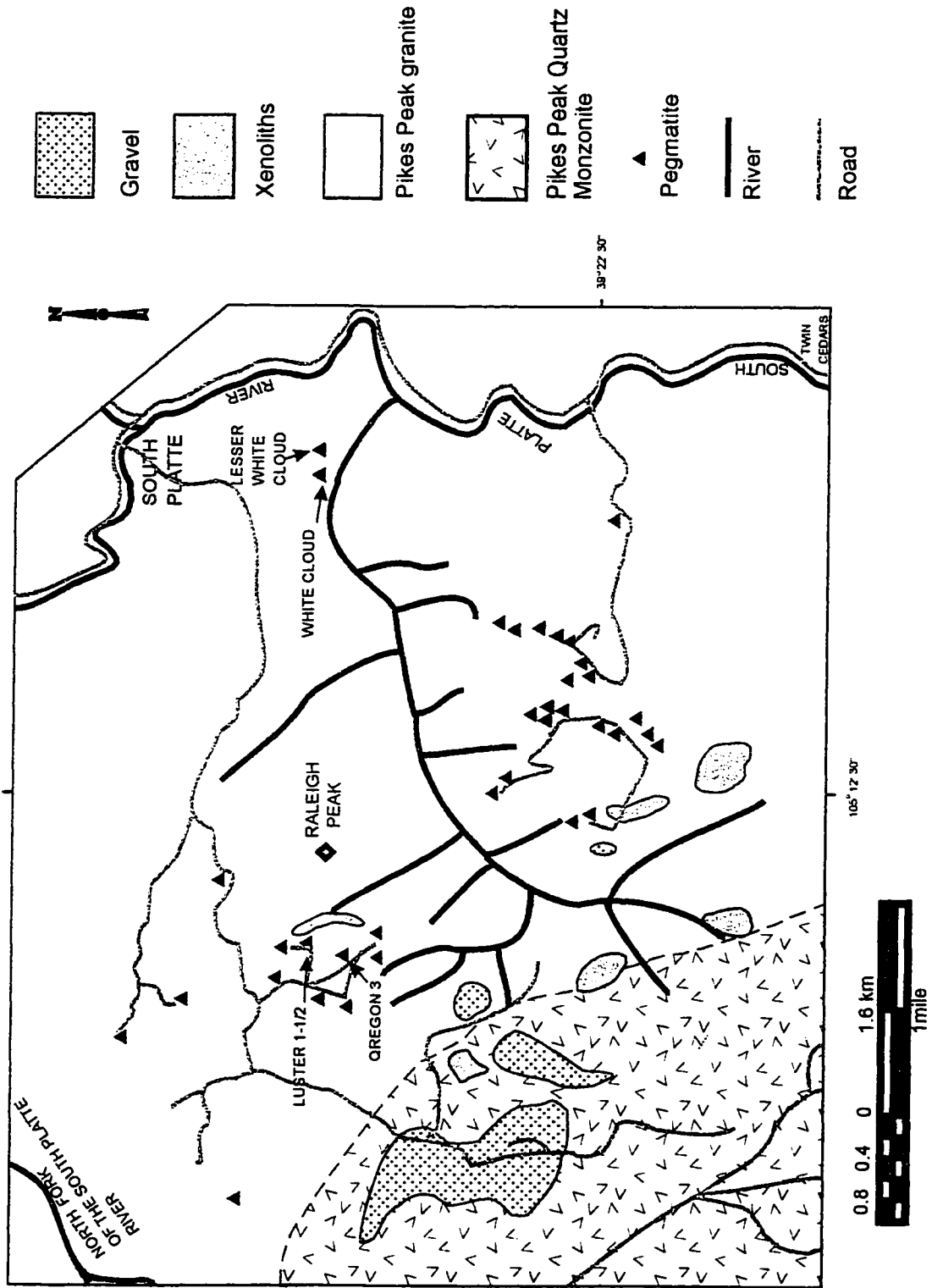
Figure 3. Geologic map of the South Platte pegmatite district, showing location of selected pegmatites (modified from Simmons and Heinrich, 1975).

11

South Platte Pegmatites

More then 50 pegmatites are exposed in an 80 km^2 area southwest of the former town of South Platte (Fig. 3). The pegmatites occur in three main groups, with the highest concentration west and south of Rayleigh Peak (Fig. 3). A northern group of pegmatites occurs at an elevation of around 2400 meters, a southern group at around 2200 meters and an eastern group at around 2100 meters. In addition to those pegmatites shown on Figure 3, numerous smaller pegmatites occur in the area along with many aplite dikes. The latter may contain small pegmatitic zones and miarolitic cavities that are compositionally similar to the host aplites. The aplite dikes are typically less than a meter in width (Simmons and Heinrich, 1980). The following description of the pegmatites comes primarily from Simmons and Heinrich (1980) and Simmons et al. (1987).

Primary Zones

Two end-member pegmatite types, polyzonal and bizonal, can be distinguished on the basis of external shape and the number and nature of internal zones (Fig. 4). The polyzonal pegmatites (Fig. 4a) have an inverted teardrop shape in cross section and are roughly circular in plan view. They contain up to six mineralogically distinct primary zones and, in addition, secondary replacement units (Table 1).

12

Table 1. Primary Zones of Polyzonal Pegmatites

Zone	Size	Main Minerals	Textural Features
Border	1-2" thick	Quartz, Microcline-Perthite	aplitic to micrographic texture
Wall	50% of pegmatite	Quartz, Microcline-Albite, ±Biotite	graphic texture
Outer-Intermediate	2% of pegmatite	Microcline, Quartz	giant biotite crystals
Intermediate	15% of pegmatite	Microcline-Albite	
Core margin	3% of pegmatite	Quartz, Fluorite, REE-Y-Nb	green to blue fluorite
Core	30% of pegmatite	Quartz	
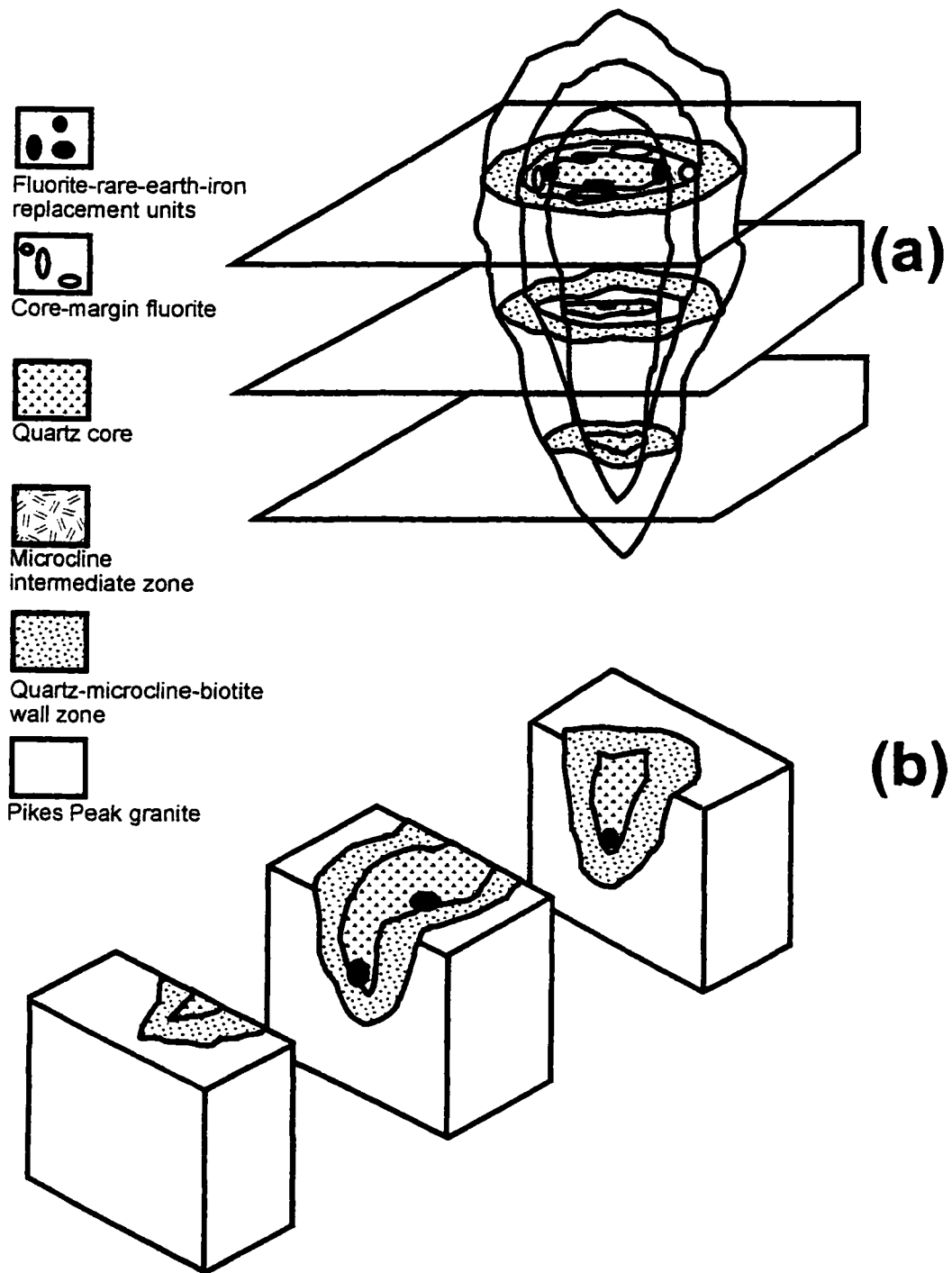
Figure 4. Idealized block diagram of the internal structure of the polyzonal and bizonal pegmatites (modified from Simmons et. Al., 1986).

14

The border zone is typically thin or absent and is granitic in composition. The wall zone comprises biotite graphic granite and is typically the largest zone. The intermediate zone mostly comprises microcline, with up to 20% "perthitic white albite" (Simmons and Heinrich, 1980; Simmons et al., 1987), which occurs as small blebs and veins. Whether this represents antiperthite or an intergrowth of albite and perthite is not clear, and was not studied. A microcline-quartz-biotite outer-intermediate zone may be developed as discontinuous pods between the wall and intermediate zones, in which the biotite may be very coarse grained. Scattered pods of green or blue fluorite ± quartz occur between the intermediate zone and the core. These are referred to as the core-margin zone. These fluorite pods may be enclosed by quartz, feldspar, or both and are best developed in the Oregon 3 pegmatite. Brecciated feldspar fragments occur along and adjacent to the feldspar-fluorite contact, and in some instances angular feldspar fragments are completely enclosed by fluorite. The fluorite also appears as small veins within the feldspar. The core of these polyzonal pegmatites generally only comprises quartz but may contain minor microcline, or veins of albite or fluorite. Simmons (1973) reported that the polyzonal pegmatites average 57% wall zone, 13% intermediate zone, and 29% quartz core by volume

The bizonal pegmatites (Fig. 4b) are usually vertical to steeply dipping and elliptical to planar in cross section. These pegmatites consist of only a wall zone and a composite quartz-microcline core. In the bizonal pegmatites, the cores

occupy a larger proportion of the pegmatite than in the polyzonal pegmatites and consist on average of 52% wall zone and 47% quartz-microcline core, by volume.

Secondary Units

Both pegmatite types contain small secondary, largely replacement, hydrothermal units. These are dominated by albite, fluorite, hematite and a variety of rare element minerals (Table 2), and are superimposed on the primary zonal sequence (Simmons and Heinrich, 1971, 1975, 1980). The polyzonal pegmatites are usually more extensively replaced by secondary minerals then the bizonal pegmatites. In the polyzonal pegmatites, field evidence indicates a correlation between the size of the replacement units and their position within the pegmatite. The larger replacement units are found where primary zones are inclined at shallow angles away from the center of the pegmatite, whereas replacement units are smaller where dips are steeper or inclined toward the center of the pegmatite. These units replace the primary minerals and are generally located along the core margin of the pegmatites.

Albite is the most abundant of the secondary minerals and, according to Simmons and Heinrich (1980), typically replaces perthite, particularly near the core-margin. However, it also occurs throughout the wall and intermediate zones. The albite occurs as disseminated patches or in veins. The veins commonly consist of bladed aggregates of cleavelandite; whereas the isolated irregular patches are a granular, "sugary" albite and may pseudomorph the primary minerals. In a few places, most notably in the Luster 1½ pegmatite, the albite

16

Table 2. Replacement minerals identified in the South Platte pegmatites (after Simmons and Heinrich,1987).

Compositional Class	Mineral Formula	Mineral[1]
Simple Oxides	Fe_2O_3	Hematite
	MnO_2	(Pyrolusite)
Multiple Oxides	$(Y,Ln,U,Th,Fe)(Nb,Ta,Fe,Ti)_2O_6$	Samarskite
	$(Y,Ce,U,Th,Zr,Fe)(Nb,Ta,Ti)O_4$	Fergusonite
	$(Y,U,Fe)(Ta,Nb)O_4$	(Yttrotantalite)
	$(Va,Na,Ce)_2(Nb_2O_6)(OH,F)$	(Pyrochlore)
Halides	CaF_2	Fluorite
	$(Y,Ln,Ca)F_2$	Yttro-fluorite
	MgF_2	(Sellaite)
Carbonates	$(Fe,Mg,Mn)CO_3$	(Siderite)
	$CaCO_3$	(Calcite)
	$CaLa(CO_3)_2F$	Synchisite
	$(Ln)CO_3F$	Bastnaesite
	$Th(Ca,Ln)(CO_3)_2F_2 \cdot 3H_2O$	Thorbastnaesite
Sulfide	FeS_2	(Pyrite)
	MoS_2	Molybdenite
Sulfate	$CaSO_4$	(Anhydrite)
Phosphates	$(Ce,La,Th)(PO_4,SO_4)$	Monazite
	YPO_4	Xenotime
	$Ca(UO_2)_2(PO_4)_2 \cdot 10\text{-}12H_2O$	(Autunite)
Silicates	$KAl_2(Si_3AlO_{10})(OH)_2$	Muscovite
	$NaAlSi_3O_8$	Albite
	$Al_4Si_4O_{10}(OH)_8$	Kaolinite
	$ThSiO_4$	Thorite
	$(Th,U)SiO_4$	Uranothorite
	$(Th,U)(Si.P)O_{4-x}(OH)_{4x}$	(Thorogummite)
	$(Th,U,Ln)SiO_4$	Cyrtolite
	$ZrSiO_4$	Zircon
	$(Y,Ca)_2FeBe_2Si_2O_{10}$	Gadolinite
	$Y_3Si_3O_{10}(OH)$	(Thalenite)
	$(Ln,Ca,Y)_2(Al,Fe)_3(SiO_4)_3(OH)$	Allanite
	$Be_3Al_2Si_6O_{18}$	(Beryl, Bertrandite)

[1] Very rare species in parentheses;   Ln (Lanthanides) = REE

has been altered to kaolinite, particulary along core-margin units directly adjacent to the core.

Simmons and Heinrich (1980) recognized six types of fluorite in the pegmatites: green, purple, colourless, white, brown and grey. As noted in the previous section, they interpreted the green fluorite (core-margin) as being primary. Inclusion-rich purple fluorite is the most common type of replacement fluorite, which occurs as veins, small patches, or disseminated in quartz, perthite and green fluorite. Inclusion-free purple fluorite occurs in late vugs perched on quartz and microcline. Colourless, white, and brown fluorite are also present in the replacement units in minor amounts. Grey, yttrian fluorite occurs as anhedral masses within the replacement units where it principally replaces primary fluorite.

Hematite is common throughout the replacement units as a fine coating on crystal surfaces and as impregnations in other replacement minerals. Primary biotite is also replaced by hematite to varying degrees. Most of the hematite is related to fracturing. Greenish-yellow muscovite is also common as a late-stage replacement mineral and is commonly intergrown with purple fluorite.

The more abundant rare element minerals are samarskite, allanite, gadolinite, bastnaesite, fergusonite, monazite, xenotime, synchisite and yttrian fluorite. These minerals commonly occur as aggregates and disseminations within the replacement units.

Samarskite is present in the core-margin, typically in the more extensively albitized zones. Gadolinite and allanite are associated with purple fluorite. The

gadolinite crystals are black to greenish black and are usually embedded in fluorite and yttrofluorite. The allanite crystals occur as shiny black radioactive masses and, unlike gadolinite, is found as isolated anhedral crystals enclosed in altered and discoloured perthite. Fergusonite occurs in the outer-intermediate zones in rare euhedral to subhedral crystals and more commonly as anhedral masses interleaved with giant biotite crystals and within fractures. Bastnaesite is associated with accessory allanite and gadolinite which it replaces to varying degrees. Synchisite occurs as dark-red, fine-grained, granular masses intimately associated with fluorite, hematite, yttrofluorite, quartz, and sericite. These intergrowths appear to be late-stage alteration products of monazite, xenotime, allanite, gadolinte, and thalenite (Brewster, 1986; Wayne, 1986). In addition, synchisite replaces both quartz and fluorite, and has been observed as pseudomorphs after fluorite.

Heavy REE (HREE)-rich samarskite and yttrian fluorite are more abundant in the northern polyzonal pegmatites than in the southern bizonal pegmatites, which are characterized by the presence of light REE (LREE)-rich minerals such as allanite and bastnaesite (Brewster, 1986; Simmons et al., 1987).

In addition to the replacement units, other secondary features are present within the pegmatites. These includes steeply-dipping zones of shearing and fracturing which are commonly stained reddish-brown by limonite and hematite and may contain vugs within which secondary quartz has crystallized (Simmons et. al., 1987). "Primary" vugs or miarolitic cavities occur in the cores of both

types of pegmatite. These can be distinguished from the later fracture zones (secondary vugs) by the absence of shearing and the presence of euhedral crystals. Primary vugs in the quartz cores contain only clear and smoky quartz, whereas those in composite cores (quartz + microcline) can contain both quartz and microcline. The vuggy crystals are typically stained with dusty hematite and in rarer cases contain small cubes of purple fluorite.

Chapter 3: Results

Petrography of the Samples Studied

Sampling was focused on the core and core-margin units. A few samples were taken from the wall zone for comparison.

The textures and mineralogy of the wall zone samples are typical of those described by Simmons and Heinrich (1980), comprising of an intergrowth of medium to coarse-grained quartz and K-feldspar, in many cases displaying a graphic texture.

Most samples from the core consist of massive quartz. The quartz can be classified into three basic types: milky, clear and smoky. Most samples comprise milky quartz with only a few examples of completely clear quartz. In those samples which contain both types, there is a gradation from one to the other. Smoky quartz is typically found in the core-margin zone, but also occurs in the wall zone. At Lesser White Cloud, massive smoky quartz is developed in the core where it is in contact with an albite-fluorite-rare element replacement unit. This distribution of smoky quartz suggests that in the core and core-margin, it developes as a replacement of core or wall zone quartz.

The core margin units are the most mineralogically and texturally diverse aspects of the pegmatites. The core margin zones are primarily exposed on the vertical walls of the quarries, making it difficult to determine the relationships between core quartz and the core-margin units.

Three abundant types of fluorite are discernable in hand specimen within samples from the core-margin zone: green, white/clear and purple. Green fluorite, which is most abundant at Oregon 3, is massive and coarse grained, and forms large masses within the core-margin zones. In the White Cloud pegmatite, this massive fluorite is white or whitish-green. Purple and white/clear fluorite occur as veins (1 mm to several cm in width) and patches (up to 5 cm across) within green fluorite, quartz, and wall zone K-feldspar (Fig. 5a). Figure 5a shows massive green fluorite being veined by purple fluorite and being replaced by purple and white fluorite. Within the core-margin zones, this replacement fluorite post-dates massive milky quartz, which could either be wall zone quartz or core quartz. Purple fluorite may either form discrete veins within green fluorite and K-feldspar or occur as replacement patches in the same minerals. At White Cloud and Lesser White Cloud, white/clear fluorite typically occurs as veins and patches in quartz and K-feldspar, but also replaces and veins the more massive white to greenish-white fluorite (Fig. 5b). Figure 5b shows K-feldspar being replaced by patchy albite and being veined by albite-fluorite and rare element minrals. Distinguishing early and late white/clear fluorite at White Cloud is often difficult both in hand specimens and in thin sections. At Oregon 3, and to a lesser extent in the White Cloud pegmatites, white fluorite occurs as patches in association with purple fluorite. In some samples, it is best developed around purple fluorite veins and patches and is clearly an alteration of the green fluorite. In other

22
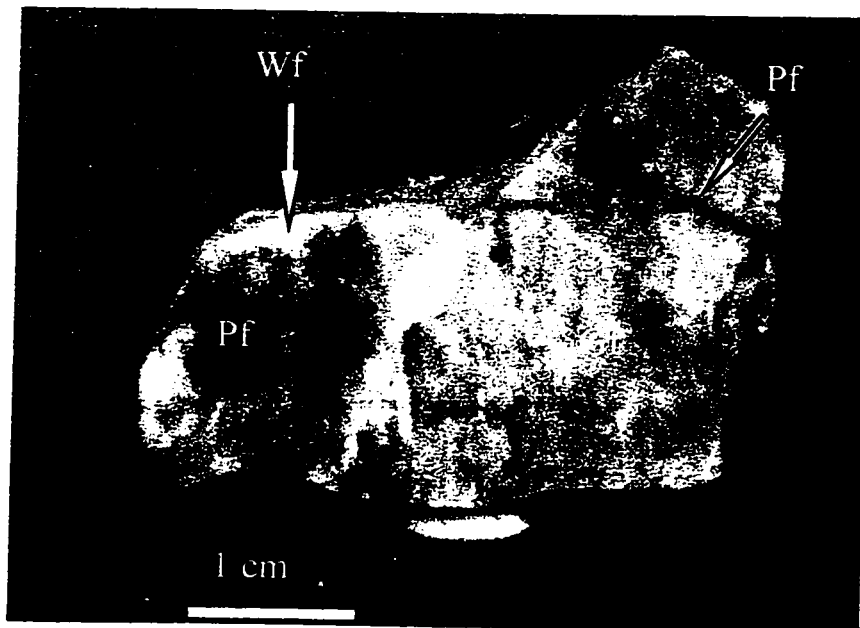
Figure 5a. Replacement of Green Fluorite (GF) by purple (PF) and white (WF) fluorite. Oregon 3.
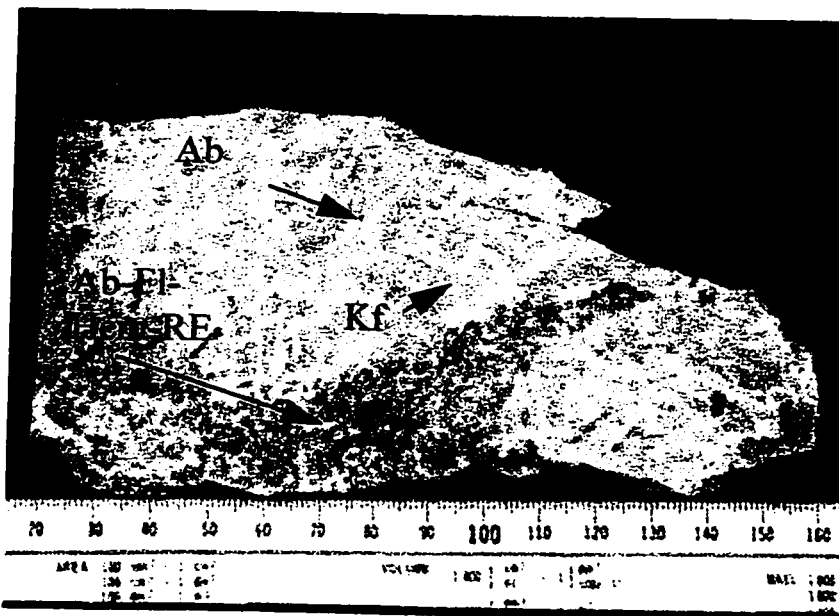
Figure 5b. Albite-fluorite-RE replacement of intermediate zone K-feldspar. Lesser White Cloud.

cases white, clear and purple fluorite occur as vug fillings. These may either comprise early, medium-grained, purple fluorite with later, coarse-grained, white fluorite or coarse-grained, white and purple zoned crystals. Particularly in the replacement examples, the white and purple fluorites grade into one another and in detail consist of a patchy intergrowth of the two types. Although in most samples white and purple fluorite deposition are related, in some samples there appears to be a clear fluorite which post-dates the purple fluorite.

White fluorite which has replaced green fluorite almost always contains abundant birefringent solid inclusions. Analysis of some of these solids using SEM-EDS identified bastnaesite, parasite and apatite (Fig. 6). In addition, Simmons and Heinrich (1980) report the presence of monazite, xenotime, gadolinite and allanite as inclusions in their clear and purple fluorite. In addition to occurring as inclusions in fluorite, rare element minerals form coarser grained aggregates, typically in association with white and purple fluorite veins or patches, both within K-feldspar and fluorite. The rare earth minerals in these aggregates include samarskite, allanite, bastnaesite, monazite and gadolinite

Albite occurs as a pervasive replacement of wall zone K-feldspar, producing a fine grained sugary aggregate, as rims on K-feldspar crystals or as anastomosing veins within the K-feldspar.

Disseminated muscovite is common as a replacement of albite and K-feldspar. Although muscovite often occurs in mineralized samples it is probably just as abundant in intermediate and wall zone feldspar in the absence of fluorite

24

or rare element minerals. This indicates that it represents a separate, later event. Similarly, hematite is very common in all the zones of the pegmatite. In some fluorite-rich samples it occurs in narrow veins which cross-cut purple fluorite veins, indicating that it also is a late event. In addition to the samples obtained from the pegmatites, a sample was taken from a granite-hosted quartz vein, 50 m northwest
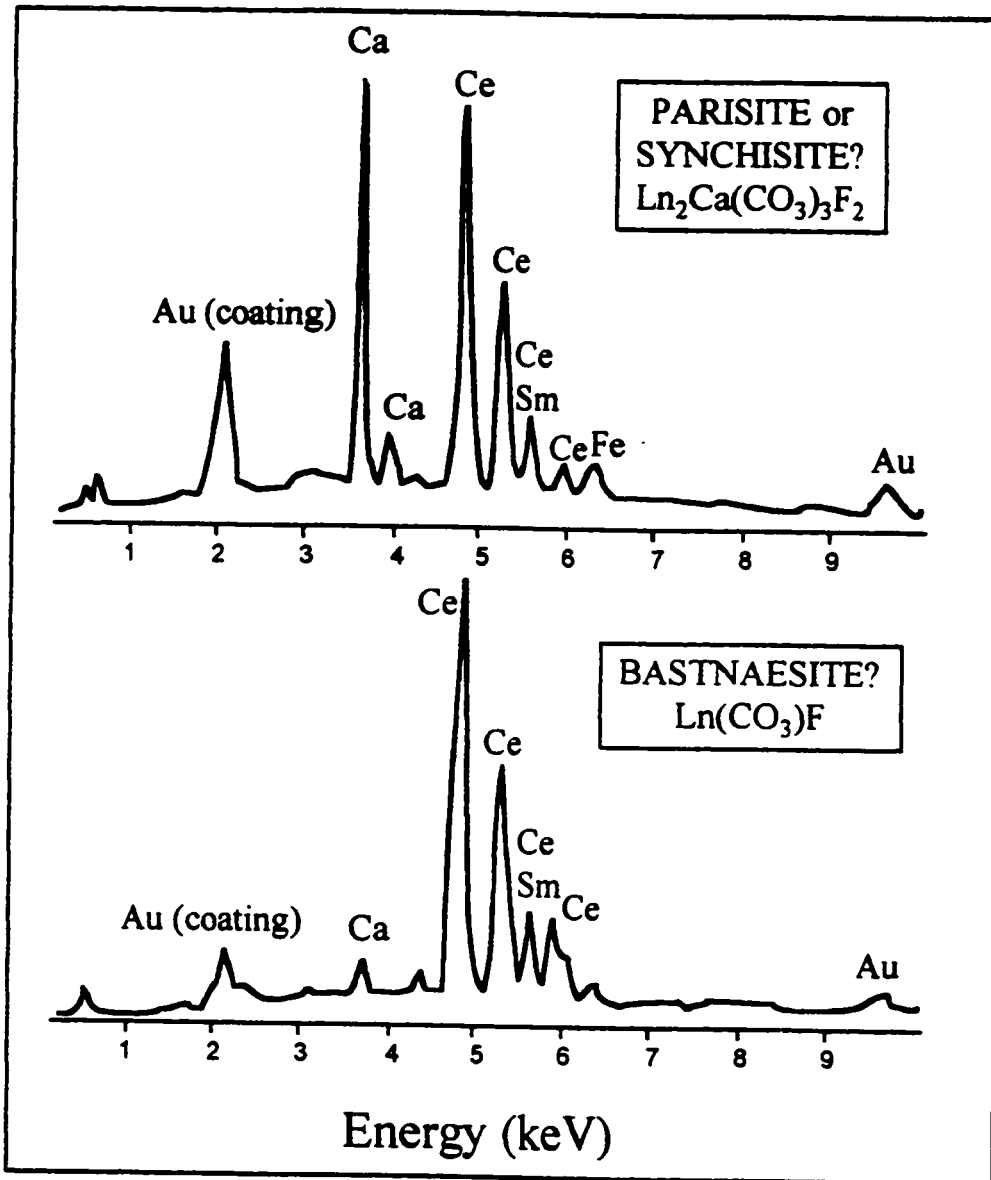
Figure 6. SEM-EDS analysis of solid inclusions in Clear-Purple Fluorite.

of the White Cloud pegmatite. This vein is 10 to 15 cm wide and comprises massive to vuggy white quartz.

Laser-induced Fluorescence in Fluorite

Fluorescence spectra of green, white, clear, and purple fluorite from White Cloud and Oregon 3 are presented in Figures 7 to 10. Individual peaks represent photon emissions from specific rare earth elements within the fluorite structure. All of the fluorite spectra presented from a given sample were collected under identical conditions (given on the spectra) so that differences in intensity reflect the concentrations of rare earth elements in the fluorite (Burruss et al., 1992). Positions of the main luminescence peaks are given in Table 3 along with rare earth ions tentatively assigned to some of the peaks after Burruss et al. (1992).

Sample 55b from Oregon 3 contains early, massive green fluorite which has been replaced by purple and white fluorite. In addition, this sample contains minor amounts of a late, clear fluorite which occurs interstitially to euhedral purple fluorite. It can be seen from Figure 6 that the late, clear fluorite provided the most intense spectra indicating that it contains the highest concentrations of rare earth elements. In contrast, the replacement purple and white fluorite yielded a relatively weak response indicating significantly lower concentrations of rare earth elements. The massive green fluorite gave an intermediate response. Although

26

peak intensities vary significantly between the various fluorites, the positions and relative intensities of peaks are very similar.

Sample 51 comprises a vug containing zoned purple and white/clear fluorite with a late-stage clear fluorite that occurs in small vugs between the fluorite euhedra and as a vein which cross-cuts both the white and purple fluorite. As with sample 55b, the early white
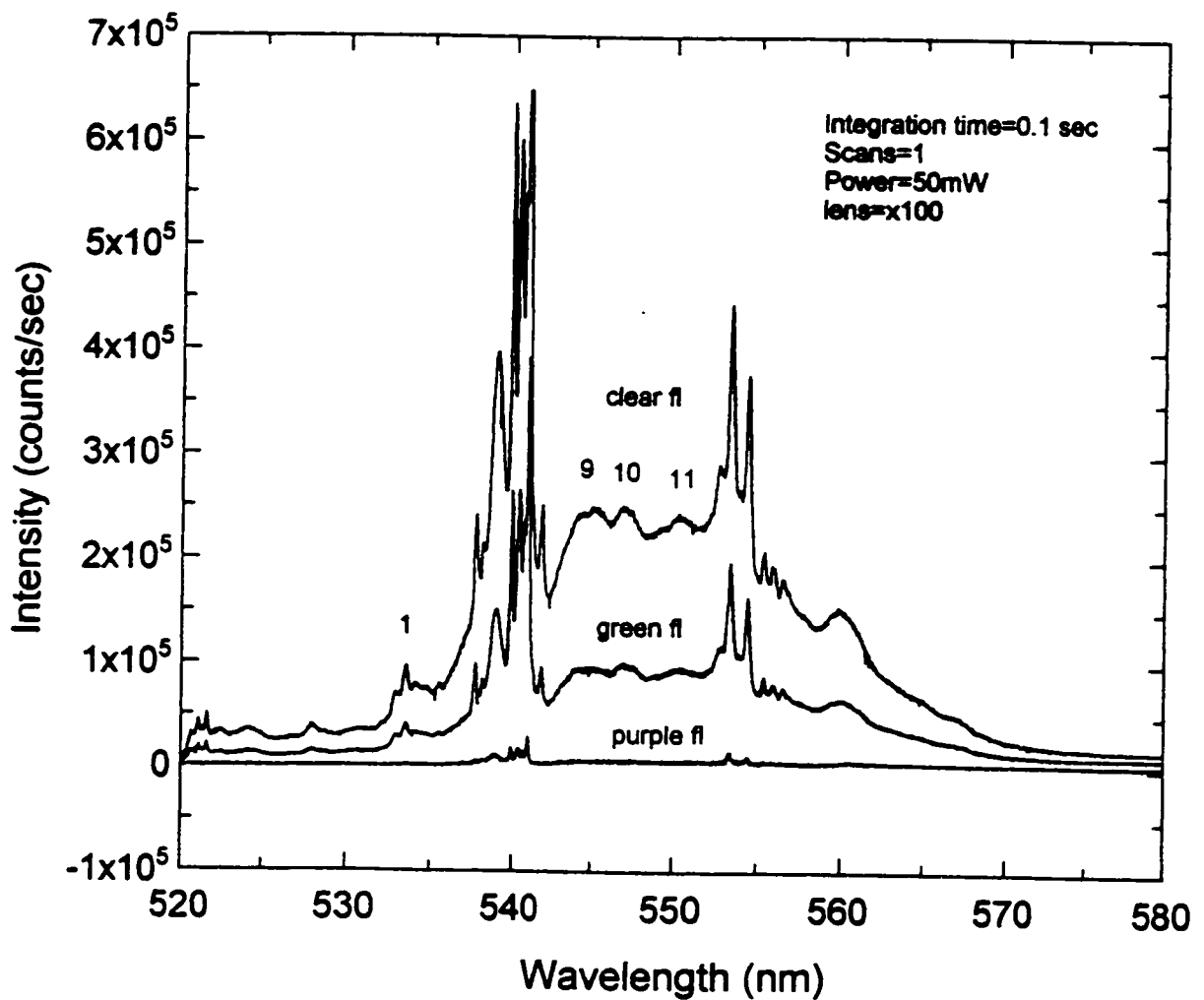
Figure 7a. Fluorescence spectra from Sample 55b.
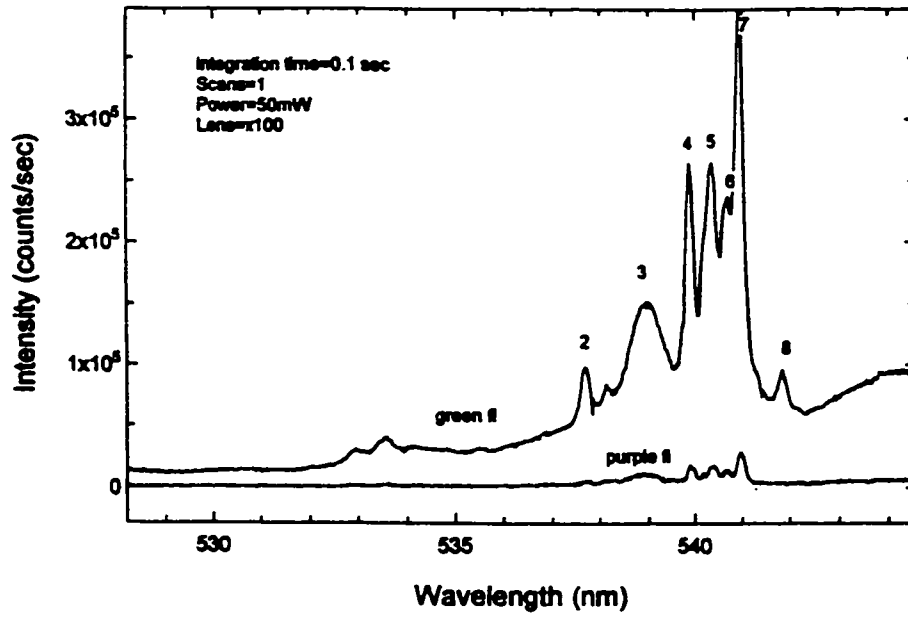
Figure 7b. Fluorescnece spectra of purple and green fluorite from sample 55b (529-544 nm).
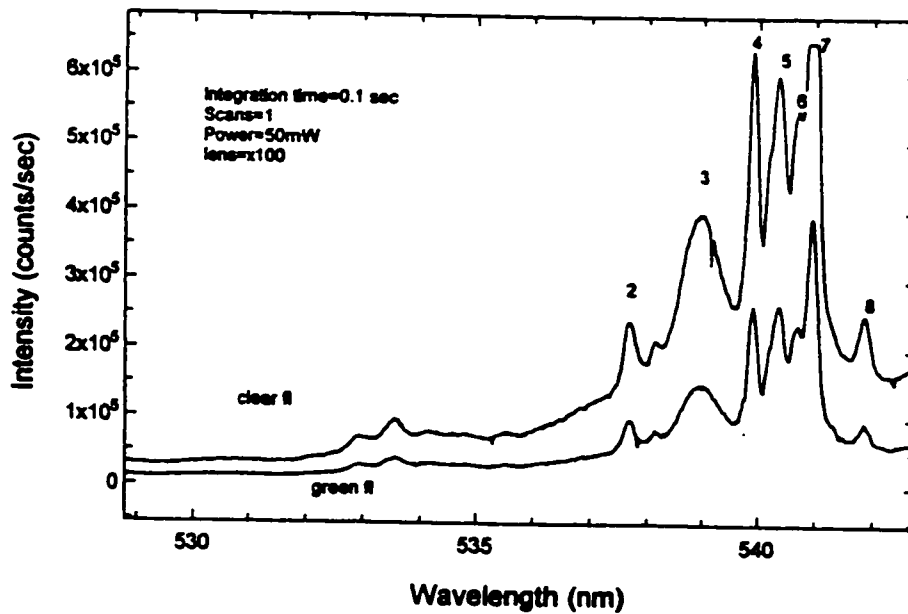
Figure 7c. Fluorescence spectra of green vs clear fluorite from sample 55b (529-542).

28

and purple fluorite give a weak response and the later, clear fluorite a much stronger response (Fig. 8). In fact, under theses particular analytical conditions, no REE fluorescence peaks are seen for the purple fluorite. Note that the spectra from sample 51 were not collected under exactly the same conditions as those from sample 55b so that a direct comparison of intensities cannot be made. The peak positions and relative intensities of the late clear fluorite are very similar to those in the spectra from 55b, however, the peak positions in the white fluorite spectrum are very different from any of the other fluorites analyzed.

As was noted in the previous section, distinguishing early and late fluorite at White Cloud is difficult because of their similar appearance, however, generally speaking, the early massive fluorite is cloudy and the later fluorites clear. Figure 9 shows spectra obtained from an early, massive white (cloudy) fluorite, and later clear and purple fluorite from sample 82. It can be seen that the clear fluorite has variable REE contents: one spectrum has higher, and another lower intensities than the white fluorite. The purple fluorite has the highest intensities of the fluorites analyzed from this sample. The relationship between early massive fluorite and late clear is obviously more complicated than at Oregon 3. Notably, unlike at Oregon 3, the purple fluorite has higher intensities than any of the other fluorite types. Unlike the Oregon 3 fluorites, there are some differences in peak intensities between the White Cloud fluorites. Whereas the white and clear fluorites are similar, the purple fluorite has several peaks which are more prominent than in the other types, namely peaks 6, 8, and 12 (Fig. 9).

29
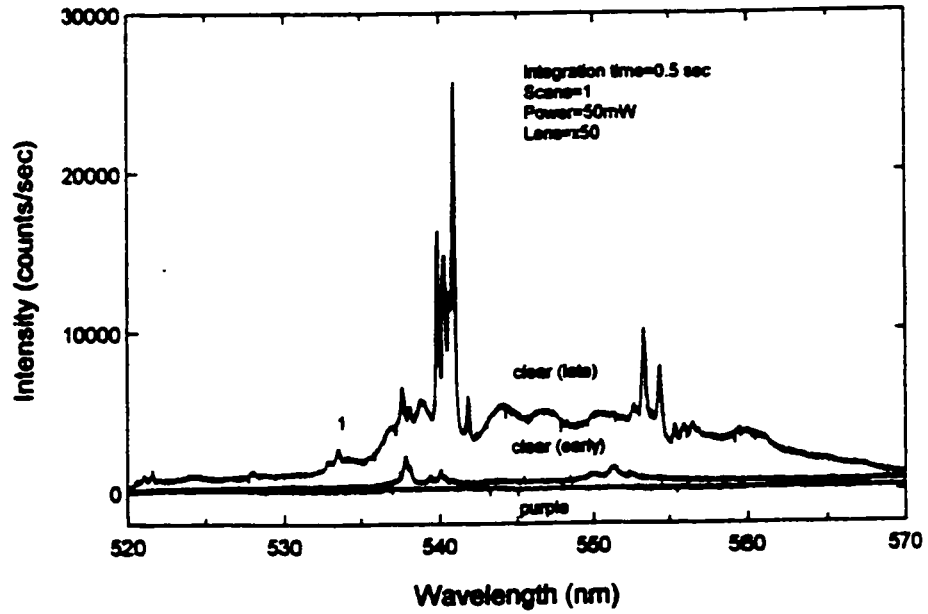
Figure 8a. Fluoresence spectra from sample 51.
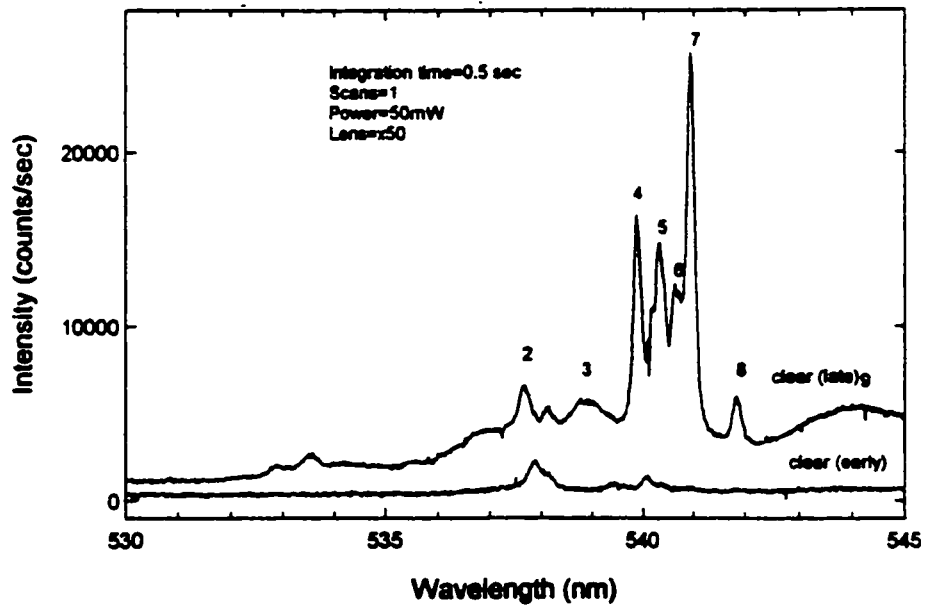
Figure 8b. Fluorescence spectra of late vs early clear fluorite from sample 51 (530 - 545 nm).
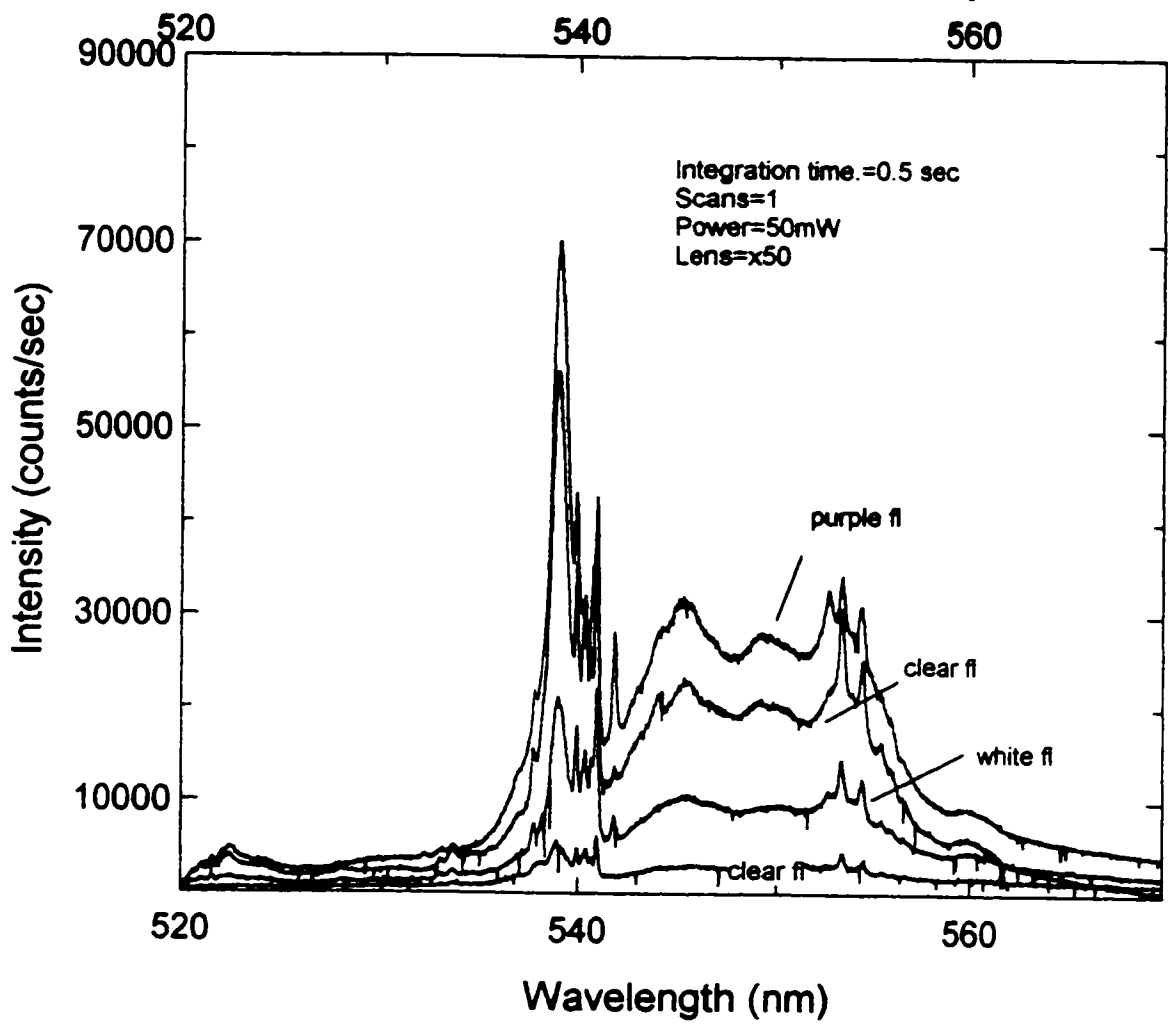
Figure 9a. Fluorescent spectra from sample 82.
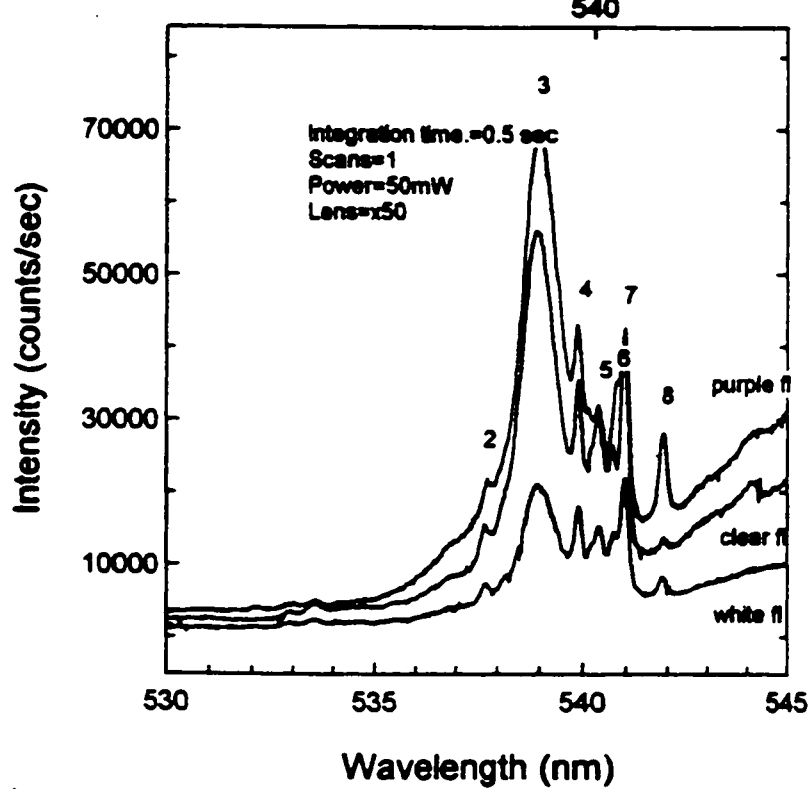
Figure 9b. Fluorescence spectra from 538 to 542 nm (sample 82).
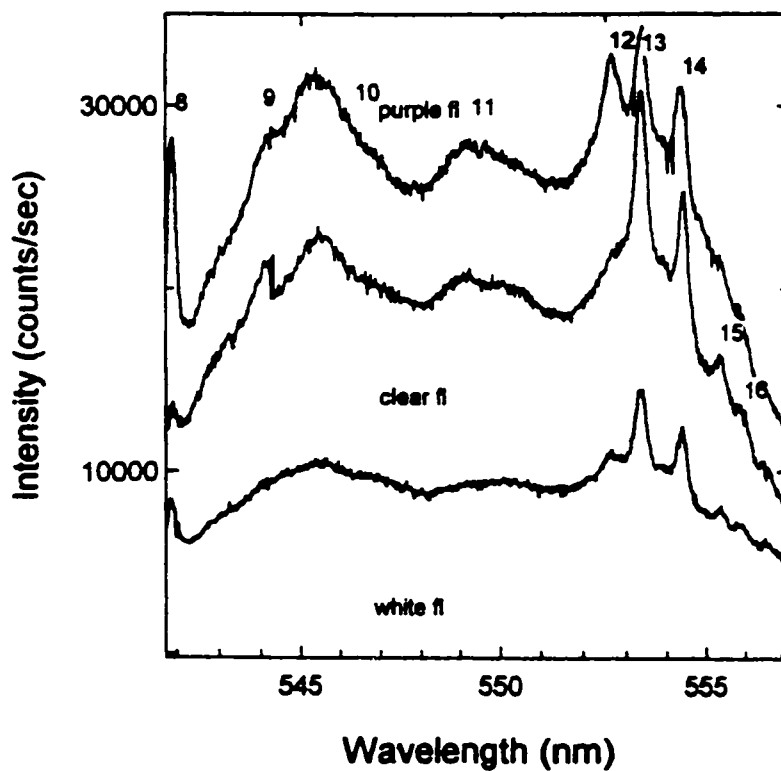
Figure 9c. Fluorescence spectra from 545 to 555 nm (sample 82).

Figure 10 shows the white massive fluorite from White Cloud (sample 82) and a green fluorite from Oregon 3 (sample 52a), collected unde the same conditions. It can be seen that the green fluorite response is significantly greater than that of the white fluorite, and in fact, is more intense than the clear and purple fluorites from sample 82. In addition, peak 3 is relatively less intense in all of the Oregon 3 spectra than in the White Cloud spectra (Figs. 7, 8 and 9).
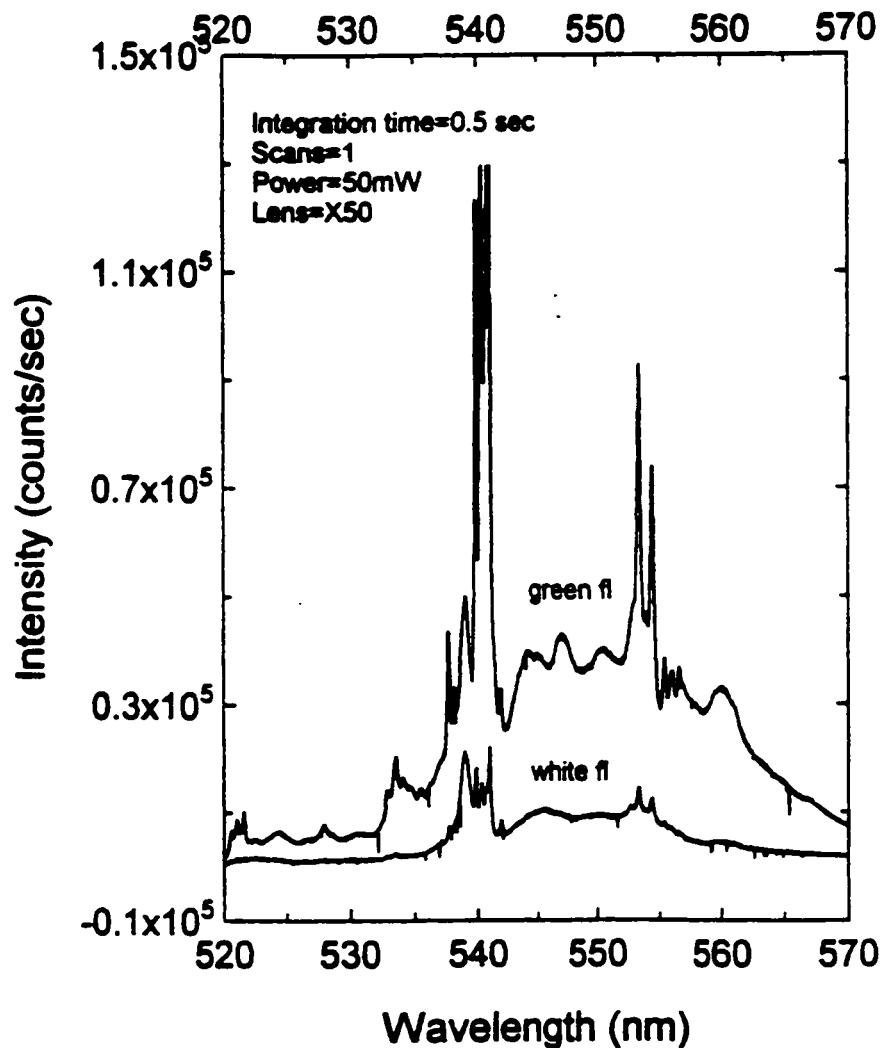
Figure 10a. Fluorescence spectra of early white and green fluorite.
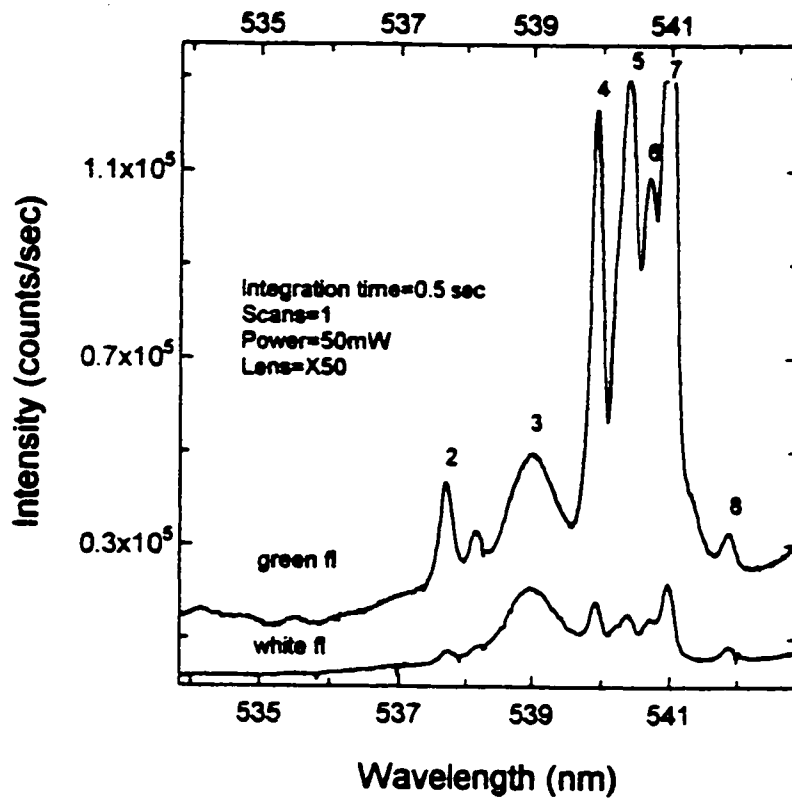
Figure 10b. Fluorescence spectra from 536 to 543 nm for white vs green fluorite.
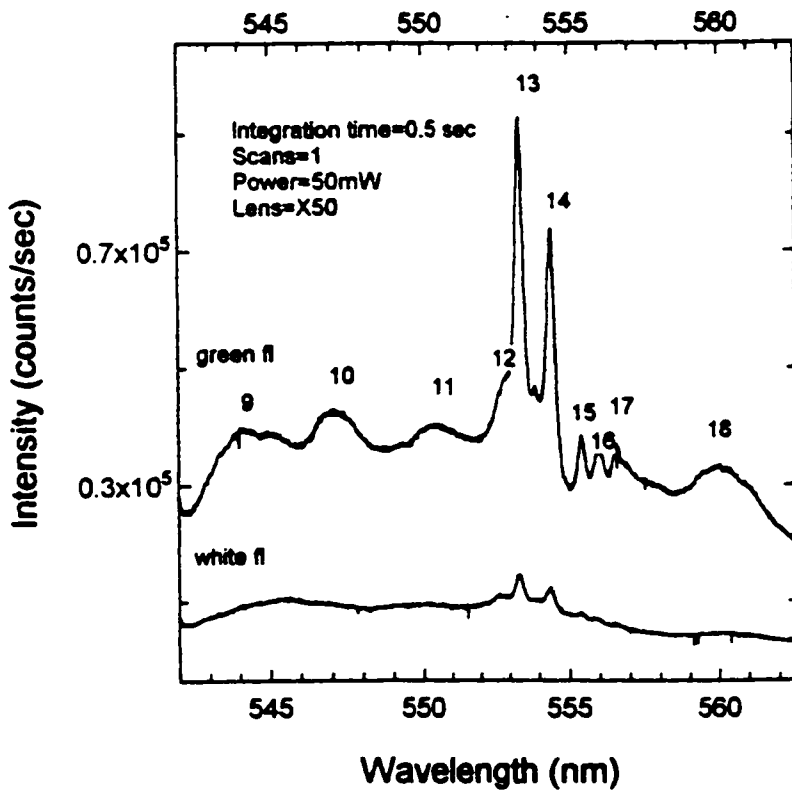
Figure 10c. Fluorence spectra from 544 to 562 nm for white vs green fluorite.

Table 3. Fluorescence peak positions and possible assignments to trivalent REE ions

Peak	λ (nm)	Possible Assignments
1	533.6	
2	537.7	Ho 537.6
3	538.9[B]	Er, Ho
4	539.9	Ho
5	540.37	Eu, Ho 540.5
6	540.72	
7	540.95	Ho
8	541.85	
9	544.5[B]	
10	546.94[B]	
11	550.41[B]	
12	552.77	
13	553.37	
14	554.4	
15	555.4	Eu 555.6 (weak)
16	555.98	
17	556.6	
18	560.3[B]	Sm?

[B] broad peak
*From Burruss et al. (1992).

Fluid Inclusion Characteristics

Minerals suitable for fluid inclusion studies (quartz and fluorite) are present in the wall, core and core-margin zones. Fluid inclusions were classified according to the type and proportion of phases present at room temperature. Inclusions which were interpreted to have undergone necking were not included

35

in this classification.   Fluid inclusions are present in quartz, and a variety of

fluorite types (green, white and purple).

Four types of fluid inclusions have been identified (Fig.11):

Type LV: Aqueous liquid-vapour.

Type LVS: Aqueous liquid-vapour-solid (solid is generally birefringent).

Type LVH: Aqueous liquid-vapour-halite±solid inclusions.

Type LC: Aqueous-carbonic.

Aqueous liquid-vpour

Aqueous liquid-vapour-solid
(Solid is generally birefringent)

Aqueous liquid-vapour-halite±solid
solid includes anhydrite (see Raman spectrum)

Aqueous-Carbonic

Aqueous Liquid   Aqueous Vapour   Halite

Solid   Carbonic Fluid   Carbonic Vapour
             or Liquid
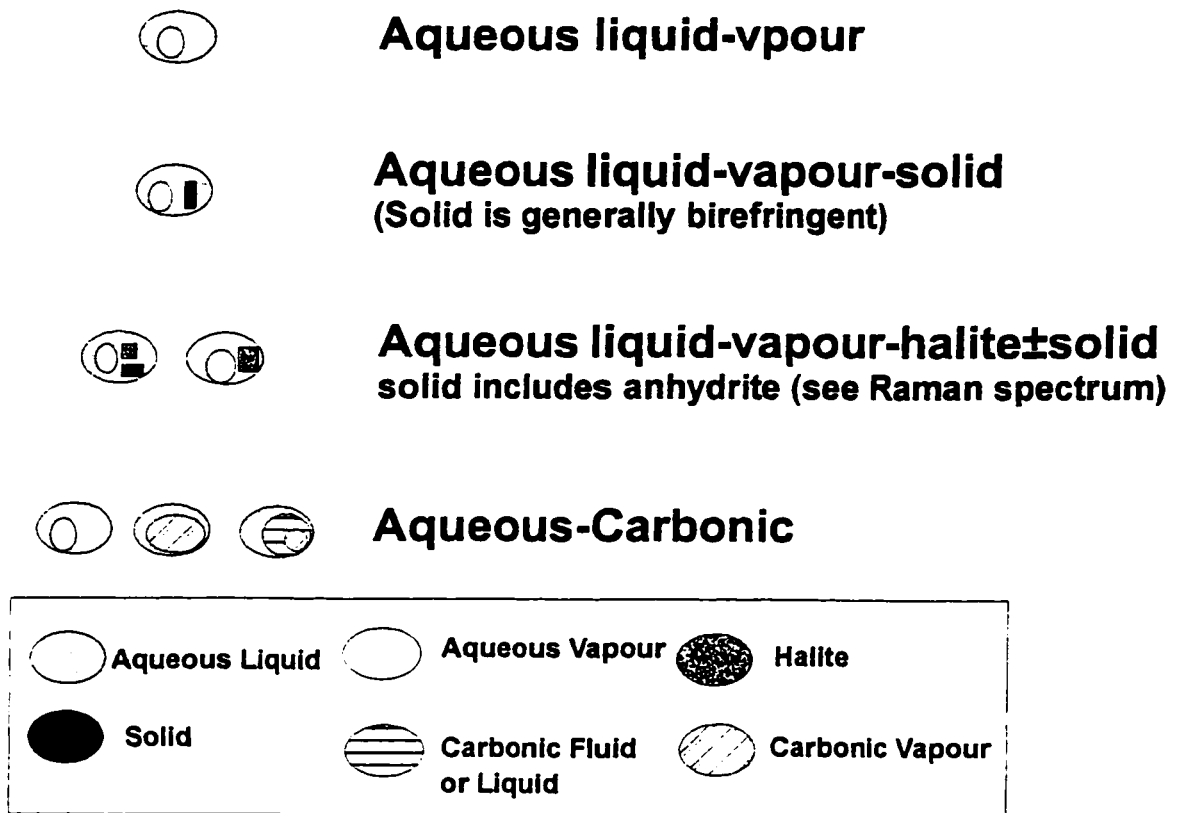
Figure 11. Fluid inclusion types.

The aqueous liquid-vapour (LV) inclusions (Fig. 12) are by far the most abundant, occurring in quartz and fluorite within the pegmatites and in the quartz vein. They typically range in size from 5 to 40 μm. The vapour bubble on average occupies 30% of the volume of these inclusions (see Appendix 2 for volume calculation methods).

LVS inclusions are typically between 20 and 50 microns in size and contain a vapour bubble which occupies between 10 and 30 % of the inclusion volume (Fig. 13). The solids within fluorite-hosted LVS inclusions are generally birefringent, anhedral, and in some cases occur as aggregates of fine grained crystals. These solids are considered to be trapped rather than daughter minerals because they are irregularly distributed amongst the inclusions and form aggregates rather than single crystals. The solids within LVS inclusions in quartz are birefringent and square or rectangular in shape (2 to 4 microns in size). Raman spectra obtained on several such crystals indicated that they are anhydrite (Fig. 14).

LVH inclusions are typically between 20 and 40 microns in size and contain a vapour bubble which occupies approximately 20 % of the inclusion volume (Fig. 15). Crystals interpreted as halite are isotropic, have a square or cubic form and are typically around 4 microns in diameter. Their identification as halite is based on their optical properties and their reaction to form another solid (hydrohalite) on cooling. Some LVH inclusions contain equant, prismatic or

37
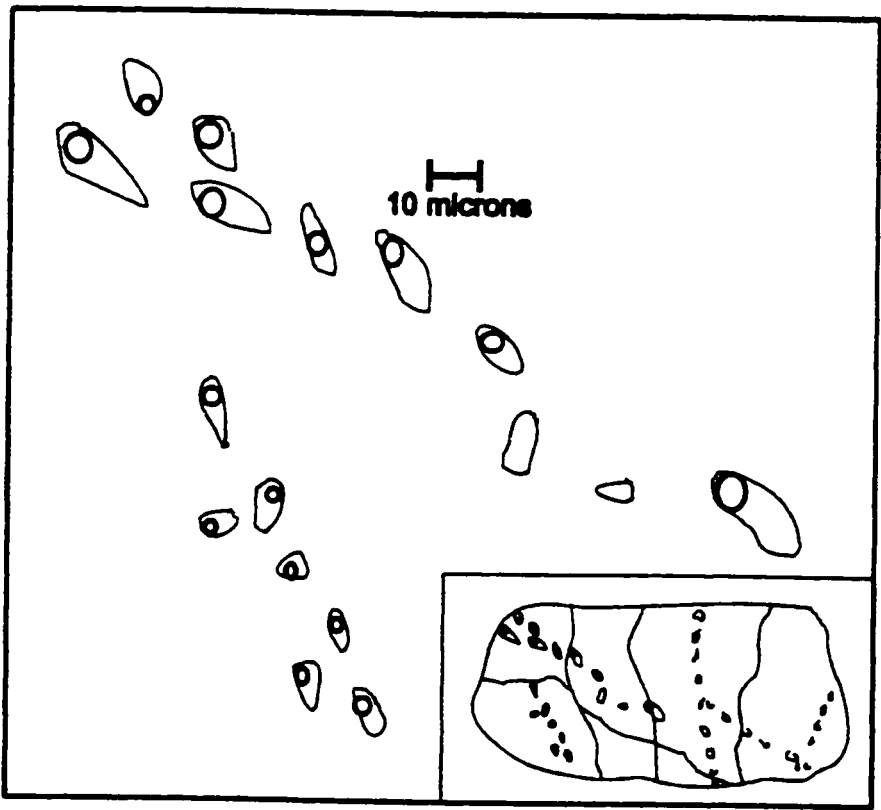
Figure 12. Camera Lucida of Secondary LV inclusions.
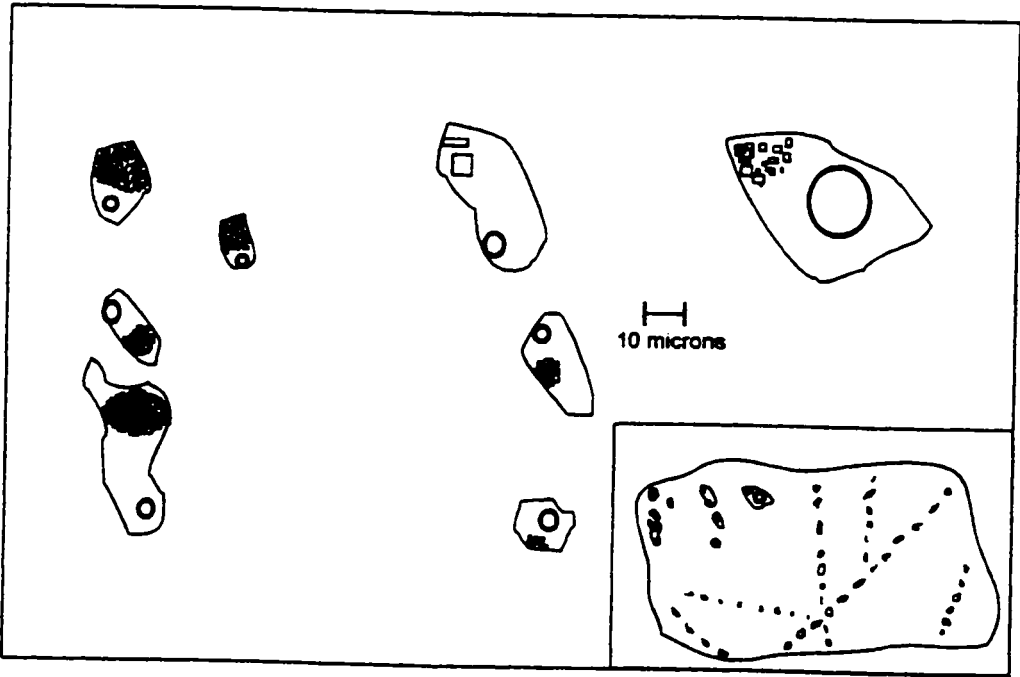
Figure 13. Camera Lucida of Primary LVS inclusions.
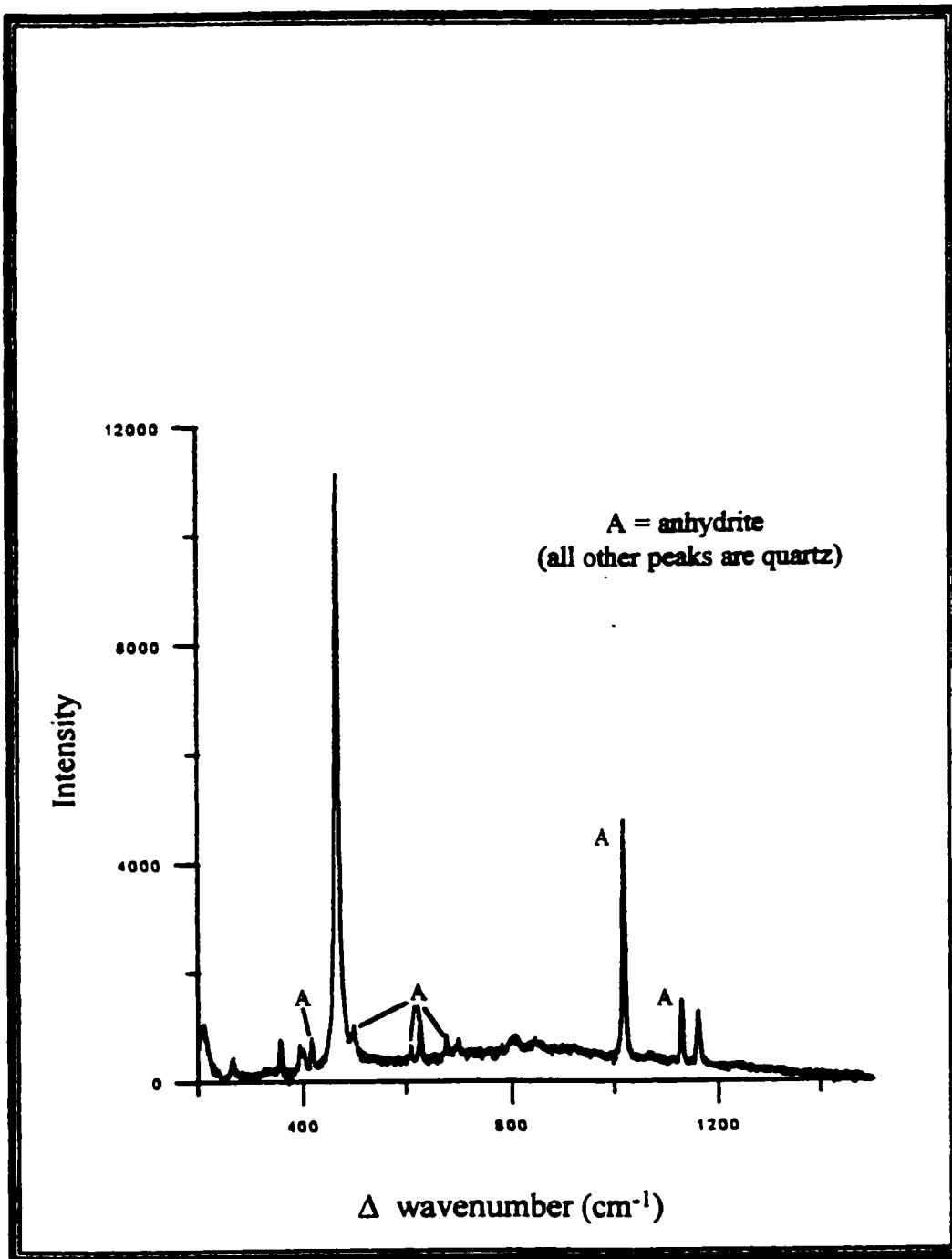
Figure 14. Raman spectrum of anhydrite in an aqueous inclusion.

acicular crystals in addition to halite. The prismatic examples are birefringent and have the same optical characteristics as the crystals identified as anhydrite from LVS inclusions. The anhydrite within the LVH inclusions is believed to be a daughter mineral as they occupy the same relative volume in the inclusions in a group. Some of the equant crystals are isotropic and also believed to be daughter minerals, possibly, sylvite. Some LVH inclusions are very large (up to 200 μm in length) and have a complex, anastomosing geometry (Fig. 16). These inclusions have complex orthogonal walls, having undergone considerable necking and averge 50 microns in length.

The aqueous-carbonic (LC) inclusions range in size from 10 to 35 microns. They consist of an outer aqueous phase and one or two inner carbonic phases which together occupy 40 to 90% of the inclusion volume (Fig. 17). One inclusion contained a trapped, birefringent solid.

Distribution of Fluid Inclusions

Primary Inclusions

Primary inclusions have been identified in core-margin, white and white-purple fluorite in Oregon 3 and White Cloud. These occur as large, isolated inclusions or as three-dimensional, non-planar arrays. The primary inclusions comprise both LV and LVS types. As this fluorite is intimately associated with the rare element mineralization and the LVS inclusions contain solids which are
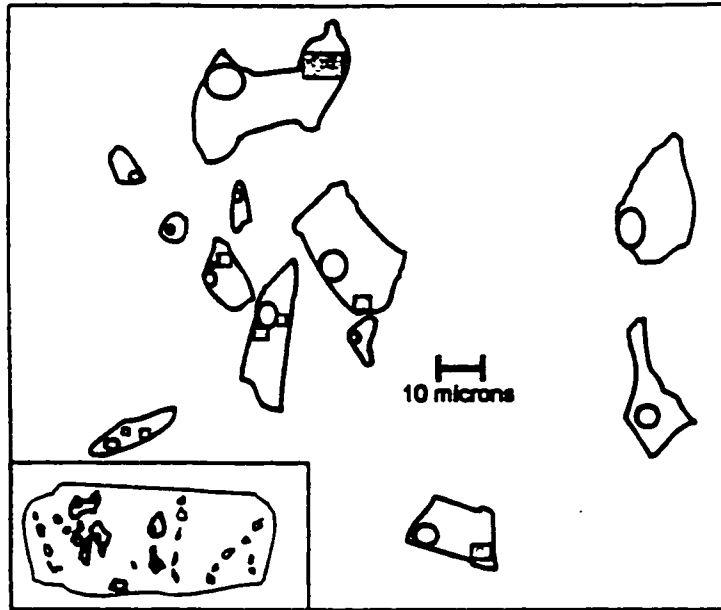
Figure 15. Camera lucida drawing of Secondary LVH inclusions.
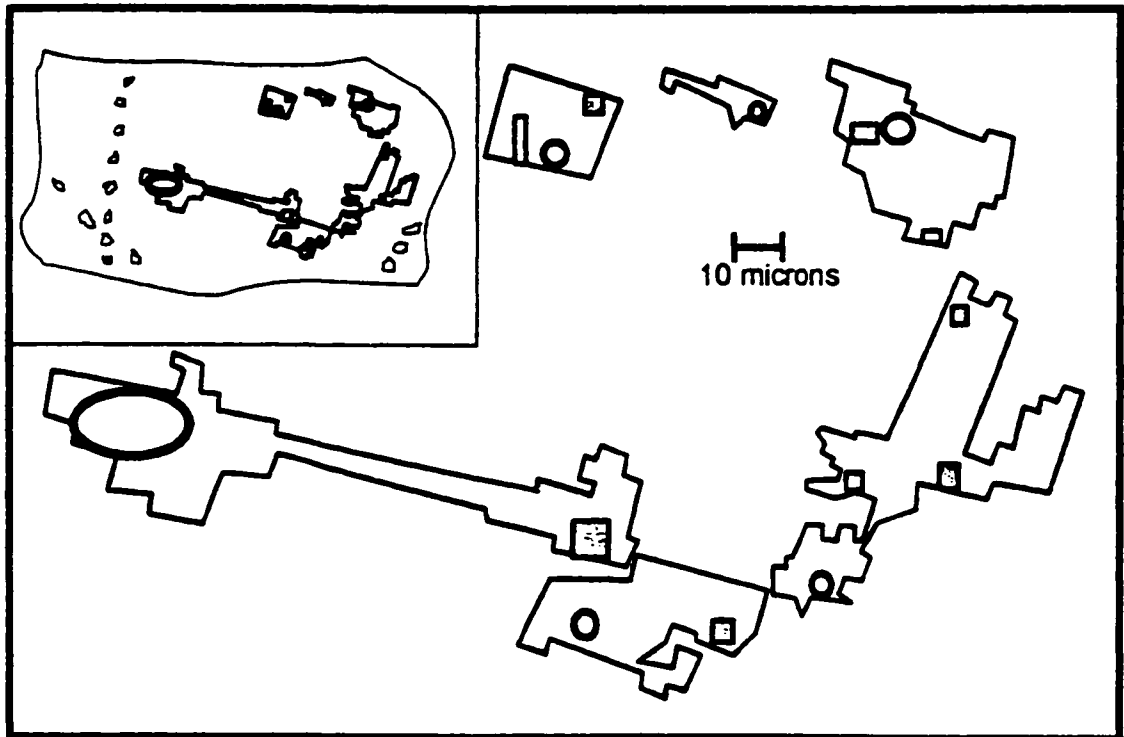
Figure 16. Camera lucida drawing of Secondary anastomosing LVH inclusions.
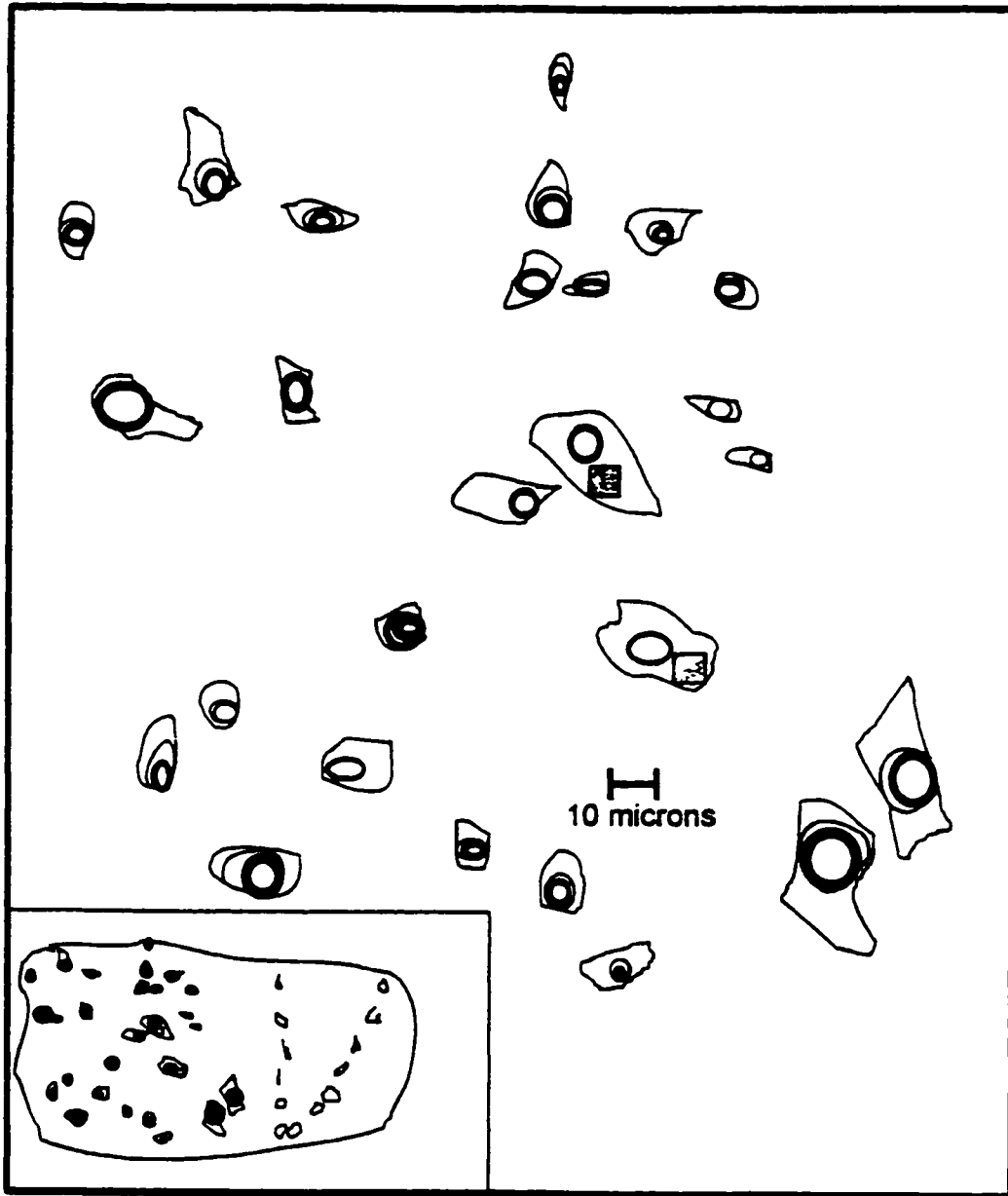
Figure 17. Camera lucida drawing of Secondary LC inclusions.

optically and morphologically the same as solid rare element mineral inclusions in the host fluorite (Fig. 6), the fluid trapped in these fluid inclusions almost certainly represents the rare element mineralizing fluid. No primary inclusions have been identified in green fluorite which is also generally devoid of solid inclusions. The origin of some inclusions in both fluorite and quartz could not be determined with certainty but the textural evidence suggests that they are more likely to be primary than secondary. These inclusions will be referred to as primary (?) and are labelled on figures as "P?".

Secondary Inclusions

Secondary inclusions are significantly more abundant than primary inclusions. LV inclusions occur in all minerals and zones. LVS inclusions are found in core and core-margin quartz and in clear fluorite from both Oregon 3, White Cloud and Lesser White Cloud. It is known that secondary LVS inclusions in quartz contain anhydrite (Fig. 14). It is possible that anhydrite-bearing inclusions also occur in fluorite (as suggested by Simmons and Heinrich (1980), but no positive identification has been made. Secondary LVH inclusions are abundant inclusions in some samples of fluorite and quartz from the core and core-margin zones of Oregon 3 and Luster 1½ but are notably absent from both White Cloud and Lesser White Cloud. LC inclusions are also abundant in some quartz and fluorite from Oregon 3 and Luster 1½, but have only been recognized

in one sample from the White Cloud pegmatites. In Oregon 3 and Luster 1½ these inclusions occur in the core, wall and core-margin zones. In most cases, secondary inclusions were easy to identify, however, as with the primary (?) inclusions, some inclusions showed equivocal textural evidence, but were probably secondary. These will be referred to as secondary (?) and are labelled on figures as "S?".

Phase Behaviour

Temperatures of initial melting (Te), final ice melting (Tm ICE), hydrate melting (Tm HYD), inclusion homogenization (Th L-V), solid mineral dissolution (Tm S) and inclusion decrepitation (Td) are presented in Figures 18 to 25 and in Appendix 3.

LV Inclusions

Upon cooling, LV inclusions froze to a dark microcrystalline mosaic at temperatures between -30 and -69°C. On warming, the ice recrystallized unitil substantial amounts of liquid had formed between -40 and -17°C. Through repeated freezing of the inclusions, the growth and melting/dissolution of ice and/or hydrate could be clearly observed, permitting temperatures of first melting (eutectic temperatures, Te) to be accurately determined. Te and Tm ICE values for these inclusions range from -44 to -10°C and -36 to -0.5°C respectively (Fig. 18). Primary inclusions have overall higher Tm ICE values (-6 to -0.5°C) than

those obtained from primary (?) or secondary inclusions. Tm ICE values for primary (?) inclusions range from -43 to -1°C, and for secondary inclusions range from -58 to 0°C. Secondary inclusions appear to define three sub-populations with Tm ICE values ranging from -44 to -34°C, -24 to -14°C and -10 to -1°C (Fig. 18). Some secondary LV inclusions in quartz from Oregon 3 contained a hydrate phase that persisted to temperatures above Tm ICE. This hydrate melted at around -3 to -4°C (Fig. 20) and has been identified as hydrohalite using Raman spectroscopy (R. Walker, pers. comm., 1996).

Homogenization temperatures (Fig. 18) of secondary (?) inclusions range from 180 to 320°C. Liquid-vapour homogenization temperatures for the primary and primary (?) LV inclusions range from 80 to 480°C whereas secondary inclusions homogenize between 80 to 410°C.
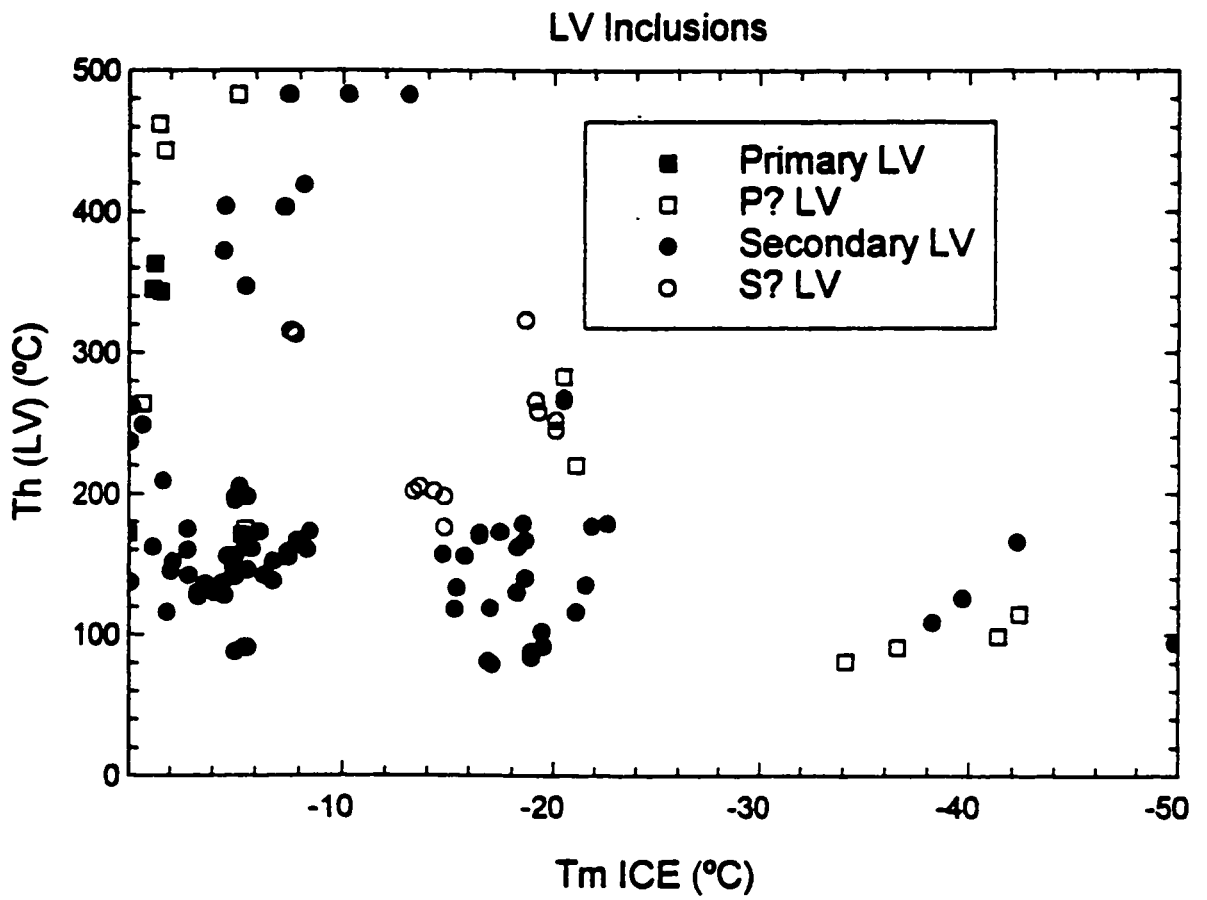
Figure 18. Tm ICE vs Th for LV inclusions.

LVS Inclusions

LVS inclusions show similar phase behaviour to the LV inclusions. Te values for these inclusions range from -11 to -57°C. Tm ICE values for LVS inclusions range from -0.5 to -50°C (Fig. 19). As with LV inclusions, primary inclusions have overall higher Tm ICE values (0 to -2°C), than secondary inclusions (-0.6 to -44°C) (Fig. 19). Primary (?) inclusions have a Tm ICE range of -39 to -5°C and a homogenization temperature range of 140 to 200°C. Secondary (?) inclusions have Tm ICE values of -19 to -0.2°C and a homogenization temperature range of 180 to 333°C. As with some LV inclusions, some secondary LVS inclusions in quartz contained a hydrate phase that became obvious once the ice had melted. Tm HYD values for these inclusions range from -4 to 13°C (Fig. 19). No hydrates were identified within the primary LVS inclusions in fluorite. Th L-V values for secondary LVS inclusions range from 160 to 340°C (Fig. 19). No change was observed in the solids up to 350°C. The first four primary LVS inclusions which were heated decrepitated at temperatures of between 440 and 490°C with no change in the size of the solids. Because of this behaviour and the low abundance of these inclusions, no high temperature experiments were carried out on other LVS inclusions.
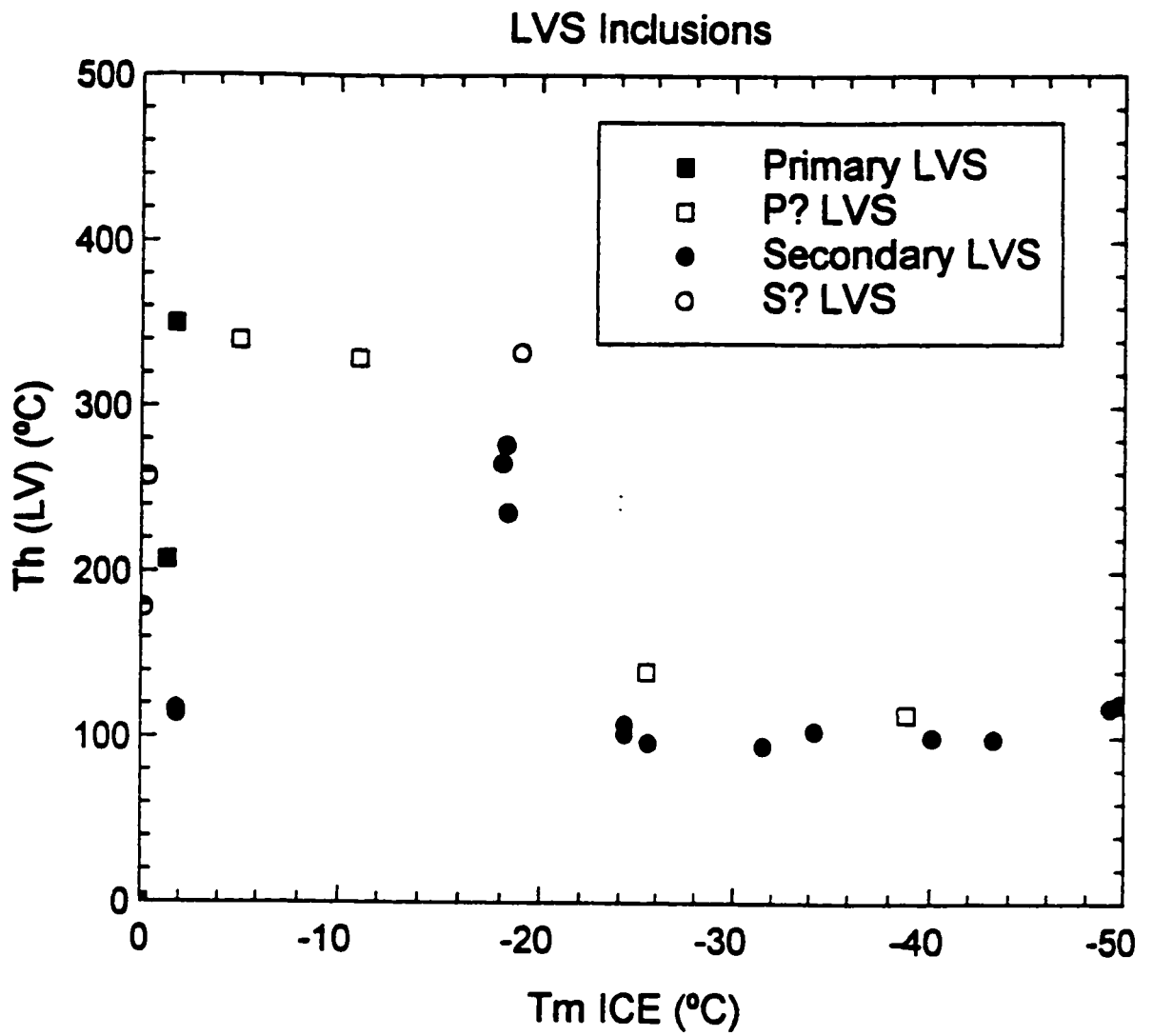
Figure 19. Tm ICE vs Th for LVS inclusions.
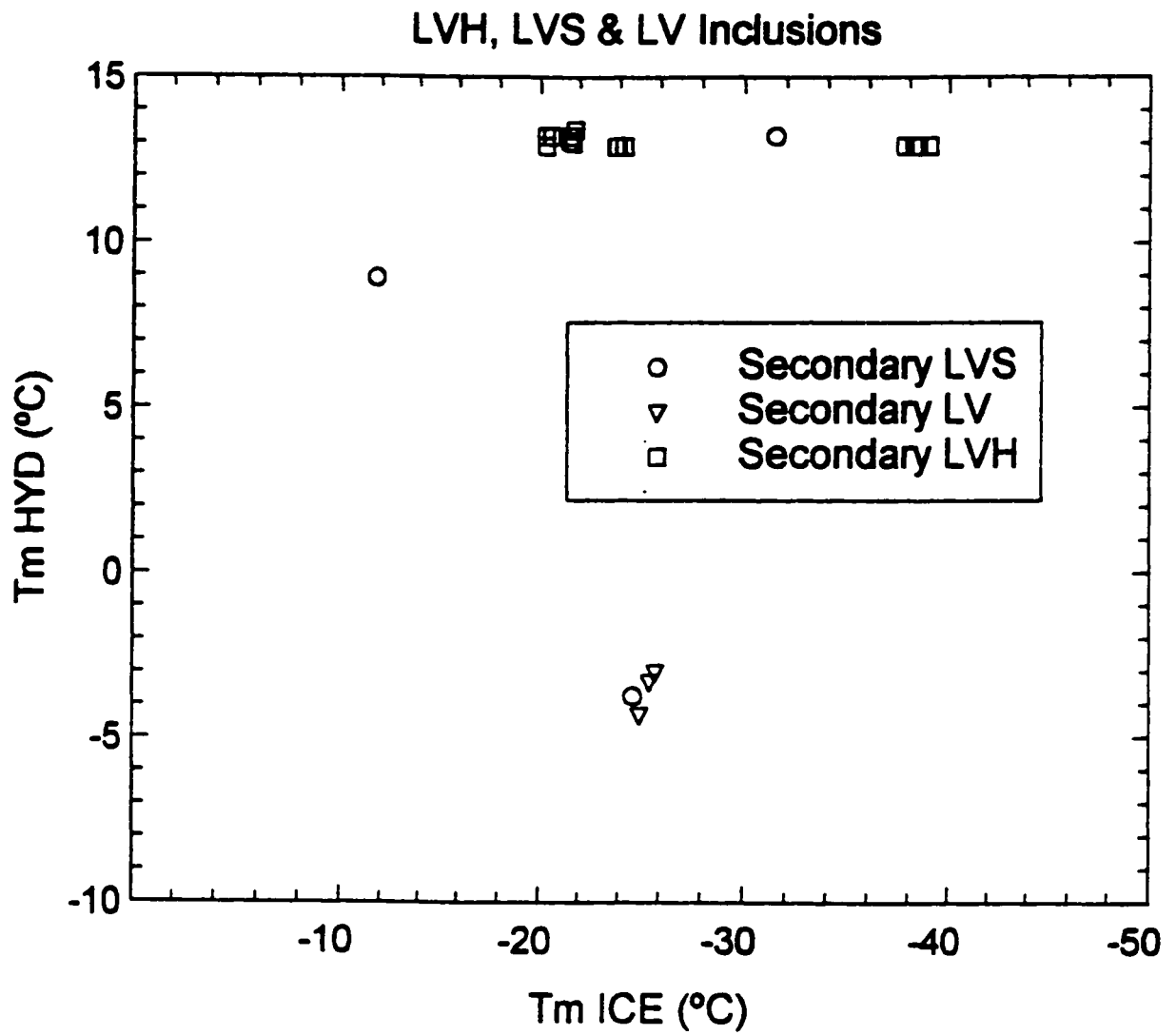
Figure 20. Tm ICE vs Tm HYD for LVS, LVH & LV inclusions.

LVH inclusions

Due to the metastable melting relations between hydrohalite and halite, temperature cycling was used to determine the temperatures of equilibrium phase changes in all LVH inclusions. The equilibrium assemblage at the eutectic should be ice + hydrohalite + other salt hydrates (e.g., see Crawford, 1981). Subsequent warming should produce an assemblage comprising ice, hydrohalite, liquid and vapour (Fig. 21). In halite-saturated inclusions (at room temperature) ice should then melt in the presence of hydrohalite, which should subsequently incongruently react to form halite. On initially freezing the South Platte inclusions, halite did not completely react to form hydrohalite, as it should. This metastability was remedied by heating a frozen inclusion slowly until the ice melted and the halite cube reacted with the remaining liquid to form hydrohalite. The inclusion was then re-frozen and heated a second time during which the eutectic and 'equilibrium' melting temperatures for ice and hydrohalite were measured.

Upon heating (2nd cycle) the solid assemblage began to melt (Te) between -57 and -27 °C. The ice melted at between -44 and -21°C (Fig. 22). With further heating the hydrate became more noticeable (-26 to -24°C) and slowly shrank in size until it finally melted at between 12 and 14 °C (Fig. 20). After the hydrate melted, the halite cube reappeared. Some LVH inclusions contain a second, isotropic, subhedral equant solid with a lower relief than the halite. This solid dissolves at between 92 and 102°C (Fig. 23), and is interpreted to be sylvite. Halite dissolution temperatures range from 150 to

170°C (Fig. 23). Liquid-vapour homogenization temperatures (to liquid) for the

LVH inclusions range from 60 to 125°C (Fig. 22).

■ **Fluorite**

● **Quartz**
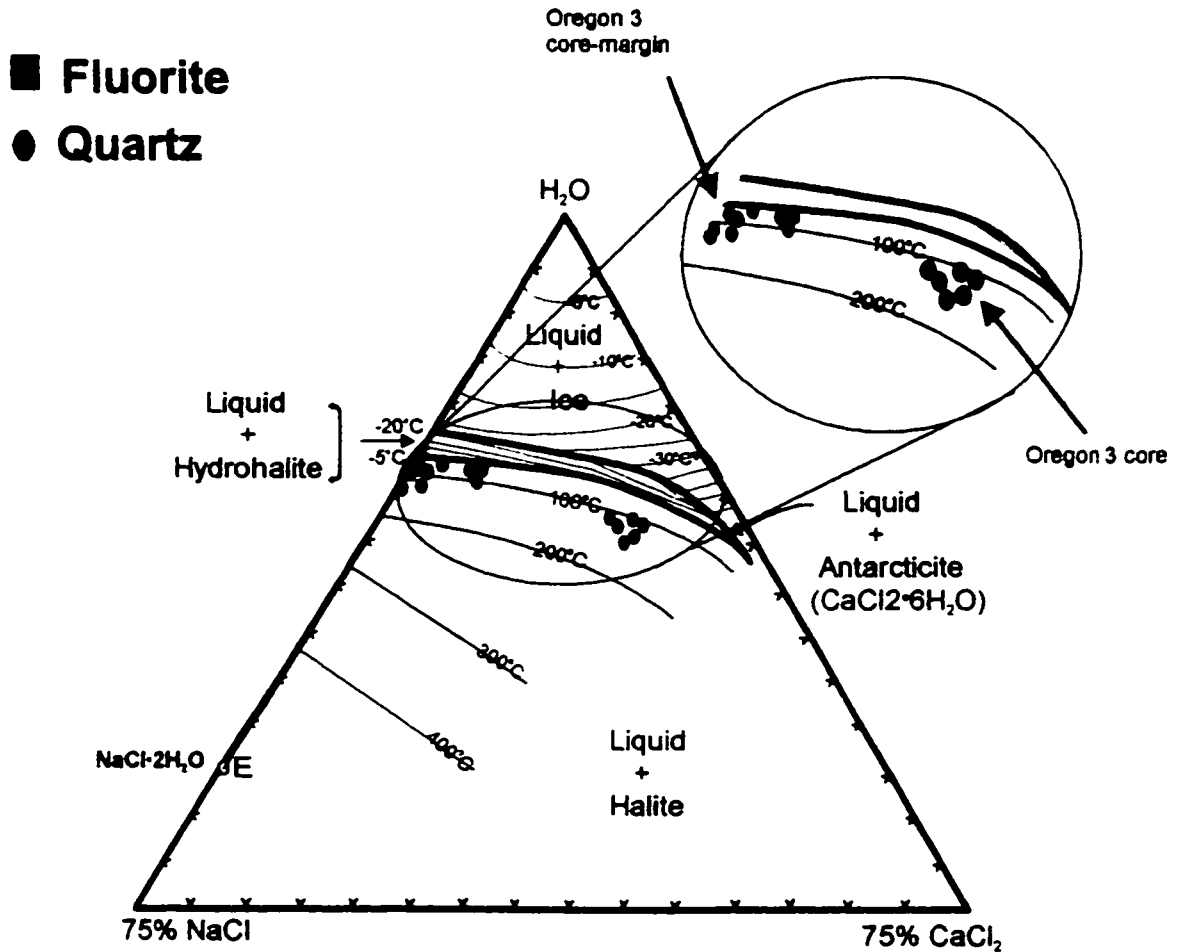
Figure 21. A phase diagram for the ternary system NaCl-CaCl₂-H₂O showing the modelled composition of LVH inclusions.
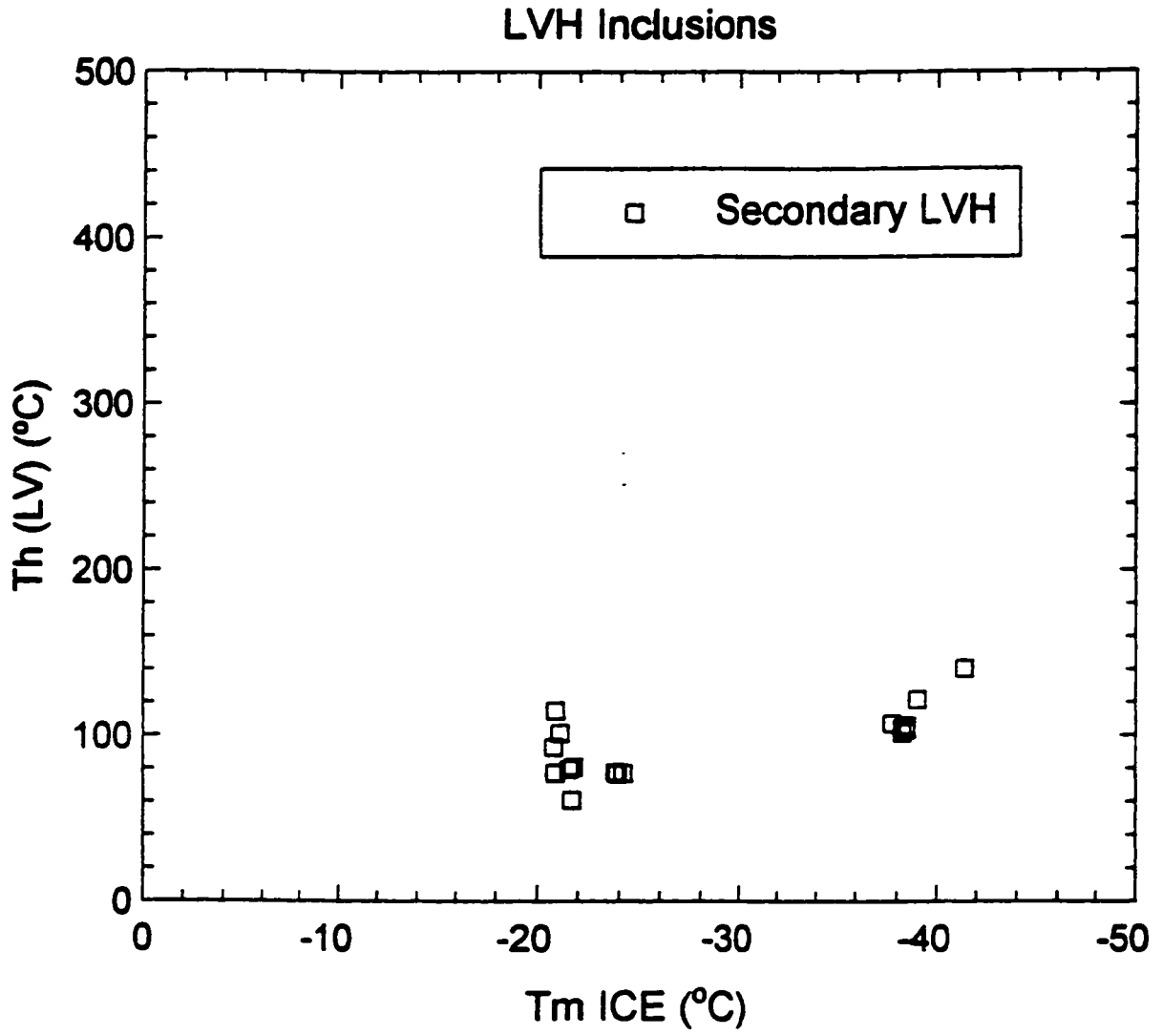
Figure 22. Tm ICE vs Th(LV) for LVH inclusions.
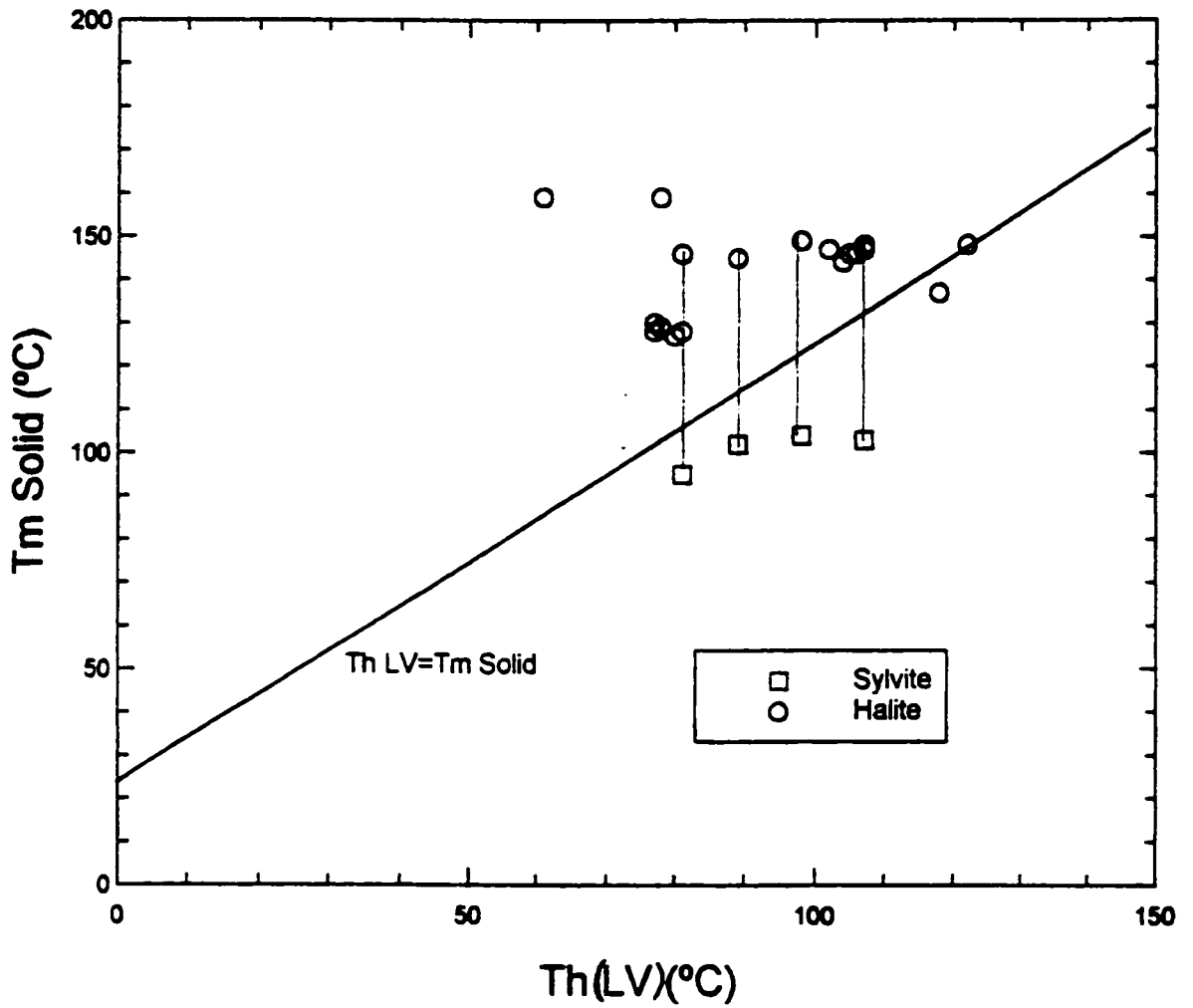
Figure 23. Th(LV) vs Tm Solid for LVH inclusions.

LC inclusions

The LC inclusions were cooled at a slower rate than the other inclusions in order to identify clathrate and solid CO_2 formation. As the inclusions were being frozen, clathrate nucleated at -47 to -28°C and the aqueous portion of the inclusion froze at -50 to -35°C. CO_2 in the carbonic portion of the inclusions froze at -107 to -70°C. Upon heating, CO_2 melted at between -56.6 and -57.7°C (Fig. 24). The aqueous portion of the inclusion began melting at temperatures of between -37 and -24°C, with final ice melting temperatures between -32 and -1°C (Fig. 25) and final clathrate melting temperatures of 5 to 10°C (Fig. 25). Upon heating, most LC inclusions homogenized to liquid between 27 and 30°C (Fig. 24). One group of LC inclusions exhibited critical homogenization (fading of the meniscus between liquid and vapour) at 30.6°C.

Fluid Composition and Density

For halite-saturated inclusions (LVH), salinities were calculated using the $NaCl-CaCl_2-H_2O$ system using the method outlined by Williams-Jones and Samson (1990) and Vanko et al. (1988)(Fig. 21). This system was used because Te and Tm ICE values below ~-21°C cannot be interpreted in the H_2O-NaCl system, which has a eutectic at -20.8 °C. For those inclusions in which sylvite

54
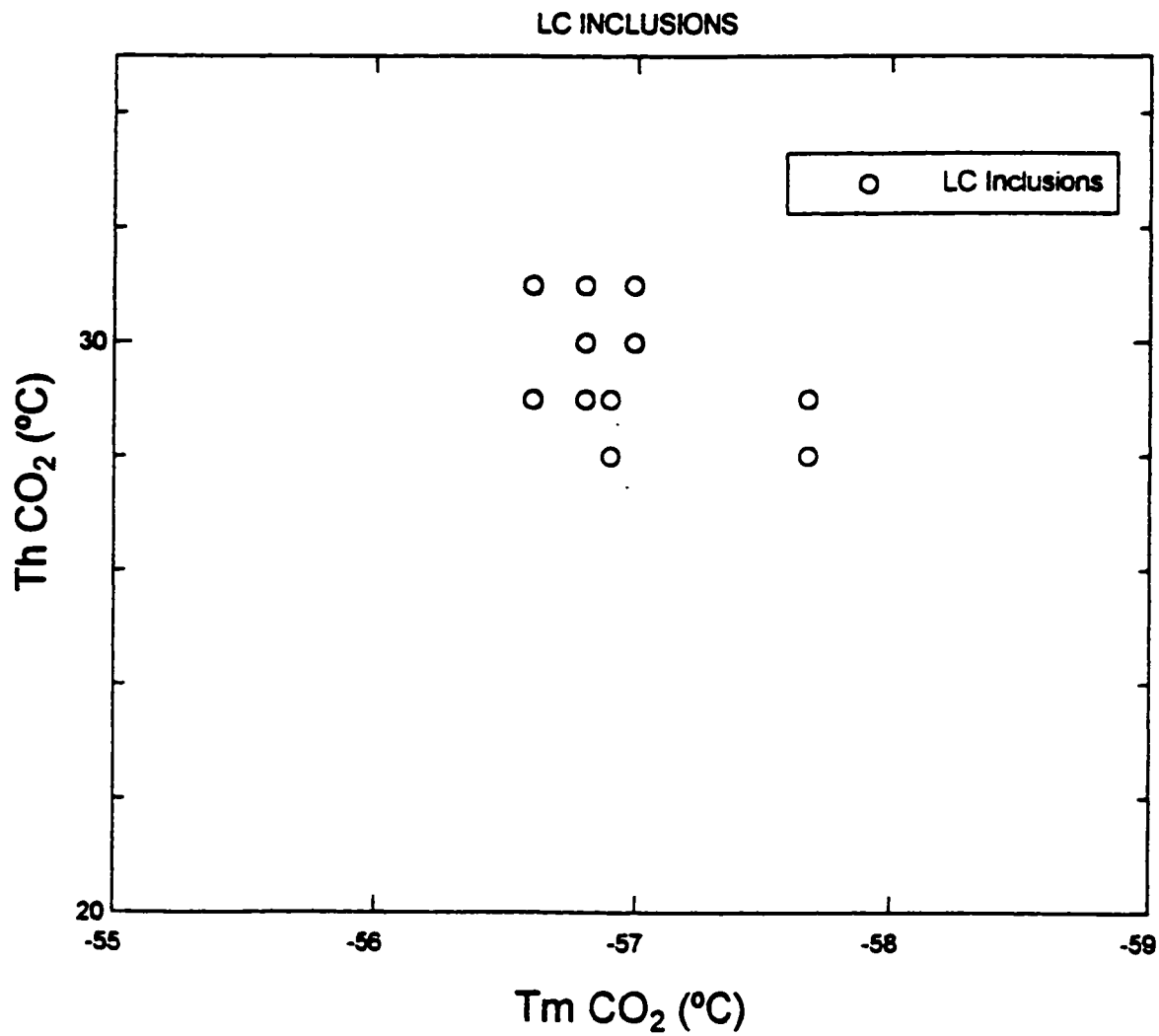
Figure 24. $TmCO_2$ vs Th CO_2 for LC inclusions.
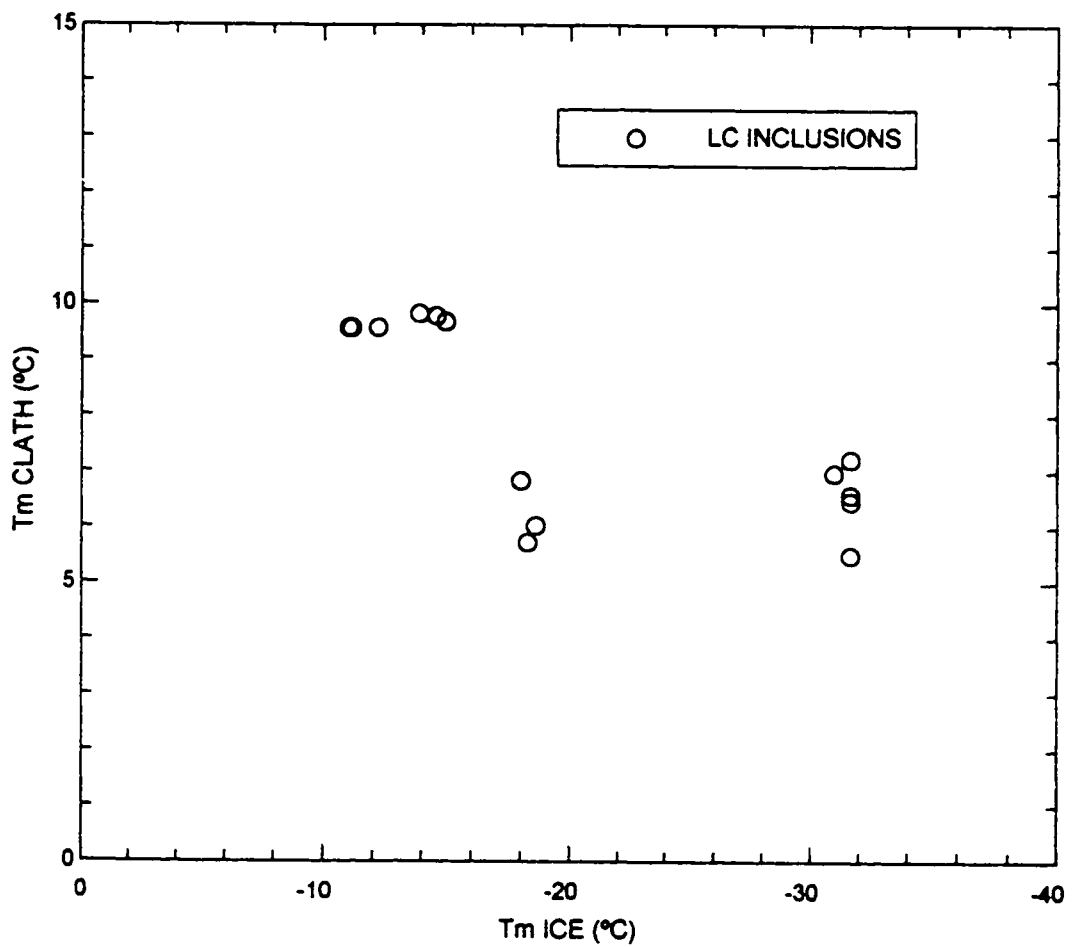
Figure 25. TmCO₂ vs Tm CLATH for LC inclusions.

ispresent,the dissolution temperatures of sylvite and halite were used to estimate KCl contents (Fig. 26)(e.g., see Roedder, 1984). Salinities of halite-undersaturated inclusions (LV and LVS) were determined from Tm ICE values using the system $NaCl-CaCl_2-H_2O$ (see Appendix 2). This system was used because of the low Te values, the fact that some LV inclusions had Tm ICE values below the eutectic in the $H_2O-NaCl$ system (-20.8 °C), and for consistency with the LVH inclusions. The use of the $NaCl-CaCl_2-H_2O$ system is also considered reasonable given the abundance of fluorite in the pegmatites. However, because $NaCl/CaCl_2$ ratios are not known for the LV and LVS inclusions, bulk densities for LV, LVS, and LVH inclusions were all calculated assuming NaCl as the only salt, using the equation of state of Zhang and Frantz (1987).

The compositions of LC inclusions were estimated in the $NaCl-CO_2-H_2O$ system because there is no appropriate experimental data for CO_2-bearing systems involving $CaCl_2$, and there appears to little or no CH_4 or N_2 in these inclusions (see below). Salinities were estimated from clathrate melting temperatures using the data of Bozzo et al. (1973). Bulk compositions and densities of LC inclusions were calculated using the computer program FLINCOR (Brown, 1989) from $ThCO_2$ values in conjunction with volumetric estimates of the proportions of aqueous and carbonic phases in the inclusions (see Appendix 2). Densities of LC inclusions were calculated using the equation of state of Brown and Lamb (1989).

When all fluid inclusion types are considered, fluid salinities cover a wide

range, from 0.2 to 36 equivalent wt. % (Fig. 27). Densities range from 0.2 to 1.4

g/cm^3 with most values above 0.7 g/cm^3 (Fig. 27). Three broad sub-populations

are evident on Figure 27: a high salinity group (26 to 30 wt. % and 1.25 to 1.4

g/cm^3),

H₂O

0

ICE

Hydrohalite

-10.7

NaCl.2H₂0

Halite

Sylvite

70 % NaCl

70 % KCl
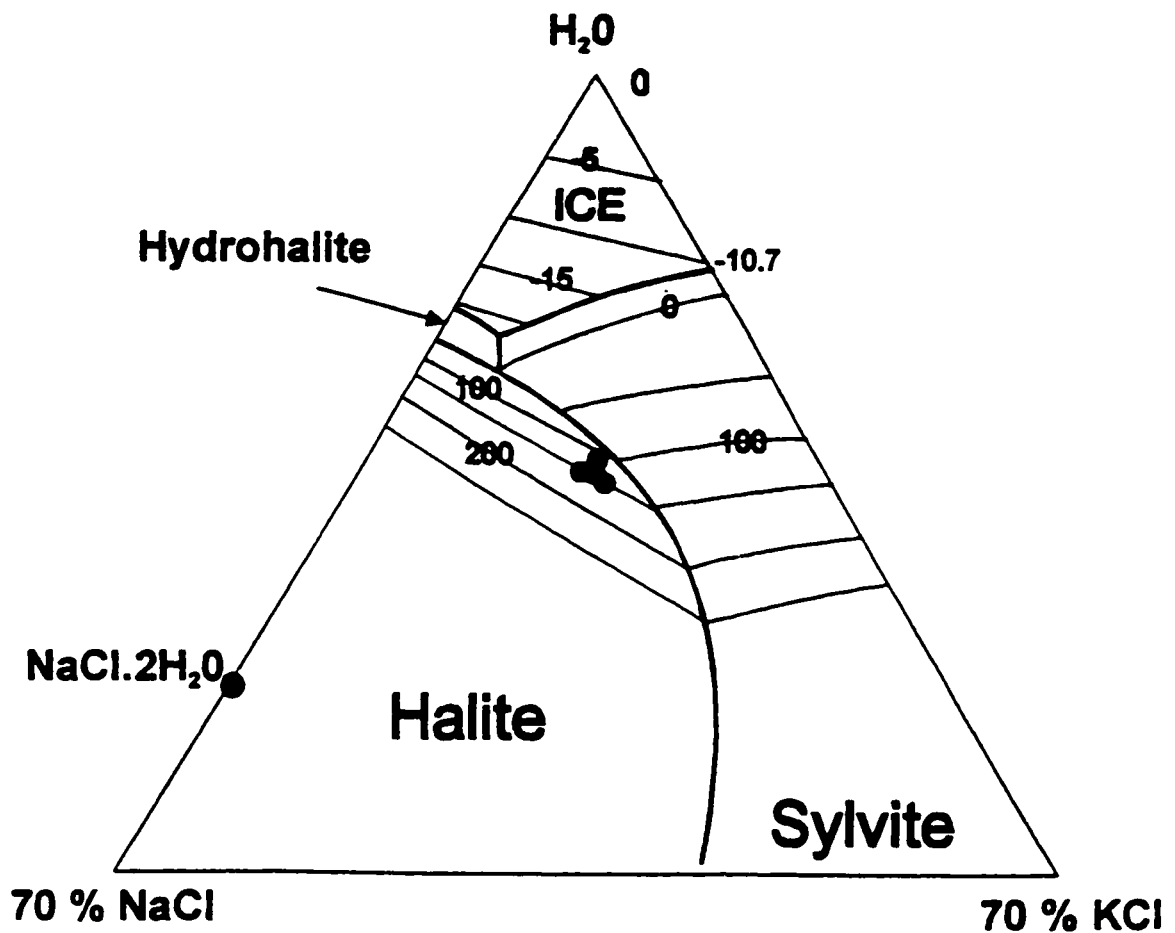
Figure 26. A phase diagram for the ternary system NaCl-KCl-H₂O showing
modelled compositions of sylvite(?)-bearing LVH inclusions.
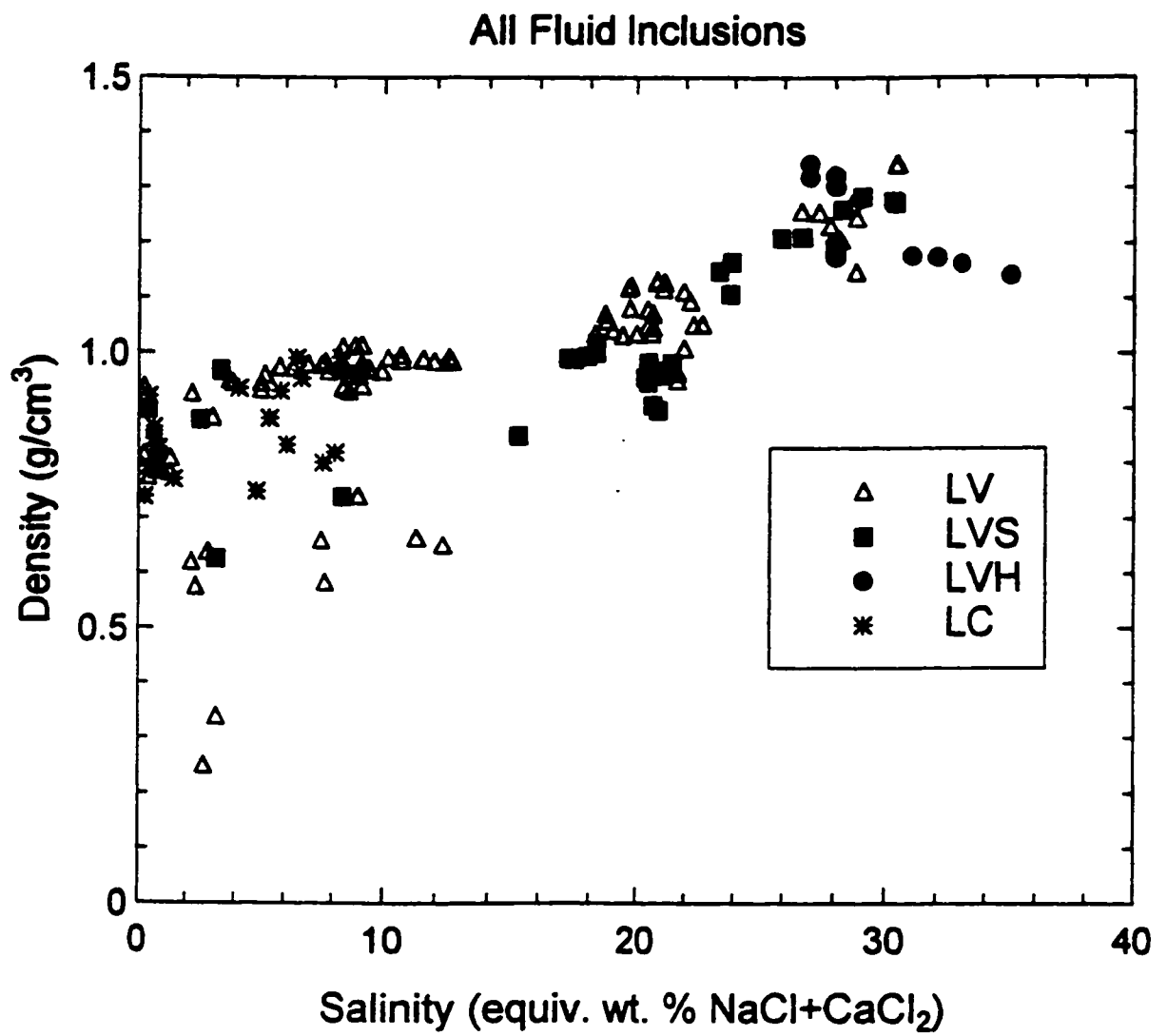
Figure 27. Salinity vs Density for all fluid inclusions.

comprising LV, LVS and LVH inclusions; a moderate salinity group (~18 to 24 wt. % and 0.9 to 1.2 g/cm^3) comprising LV and LVS inclusions, and a low salinity group (0 - 12 wt. % and 0.2 to 1.05 g/cm^3) comprising LV, LVS and LC inclusions.

Figure 28 shows differences in inclusions by host mineral. The most noticeable difference is that some inclusions in fluorite have considerably lower densities than inclusions in quartz for the same salinity. Both inclusion types exhibit an overall trend of increasing density with salinity. Primary, fluorite-hosted inclusions have uniformly low salinities (< 10 wt %; mostly < 4 wt. %) but show a wide variation in density (Fig. 29). These include inclusions from both White Cloud and Oregon 3. Note that relatively few inclusions were homogenized to yield densities but all primary inclusions in fluorite yielded low salinities. Secondary and primary (?) fluorite-hosted inclusions by contrast cover a much wider range (0 to 30 wt. %) (Fig. 29), similar to the range exhibited by quartz-hosted inclusions, which are all secondary (Fig. 28).

There are some differences in the salinities of secondary inclusions between the various pegmatites studied. Most notably, inclusions from Oregon 3 dominate the high salinity group (> 26 wt. %)(Fig. 30). Such high salinity inclusions appear to be absent from Luster 1½ and are rare in the eastern pegmatites. Figure 31 shows the salinities and densities of quartz-hosted inclusions from different zones within the pegmatites, excluding the LC inclusions. As can be seen, there are essentially no differences between inclusions hosted by the various types of quartz. This distribution is comparable to that shown by

secondary and primary (?) inclusions in fluorite (which also cover a wide range but are restricted to the core-margin fluorite),

Host Mineral
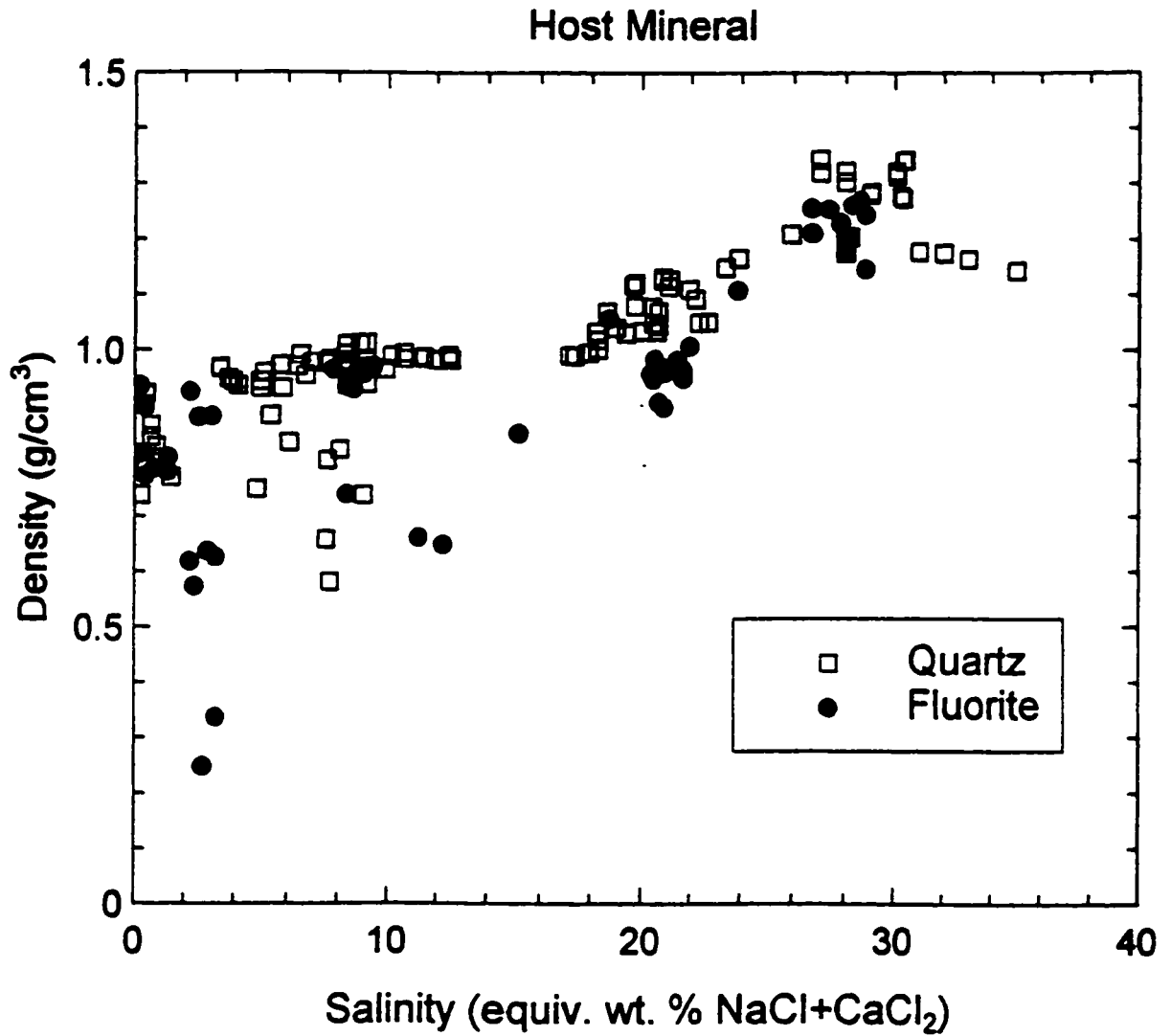
Figure 28. Salinity vs Density for inclusions subdivided by mineral.
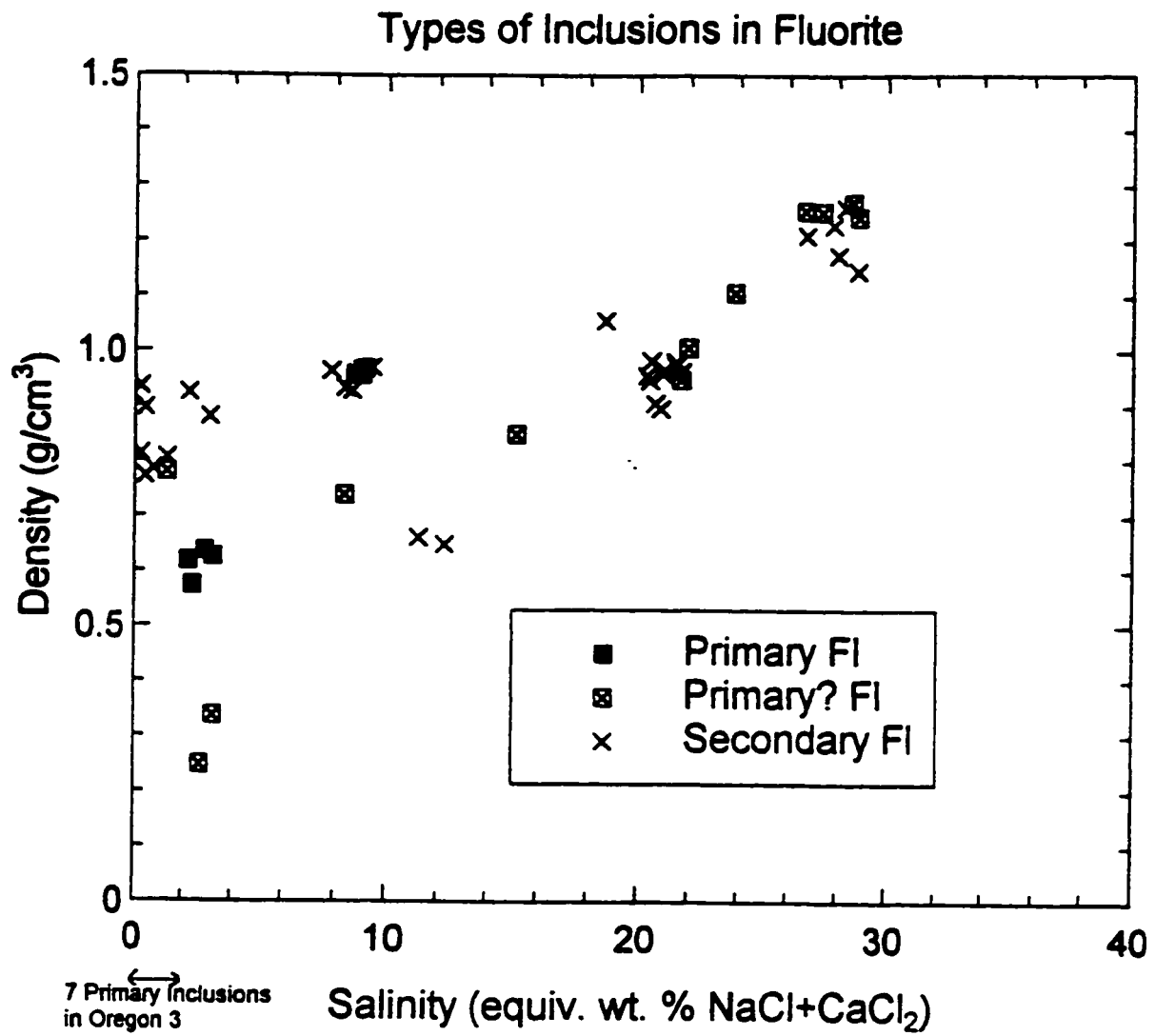
Figure 29. Salinity vs Density for various types of inclusions in fluorite.
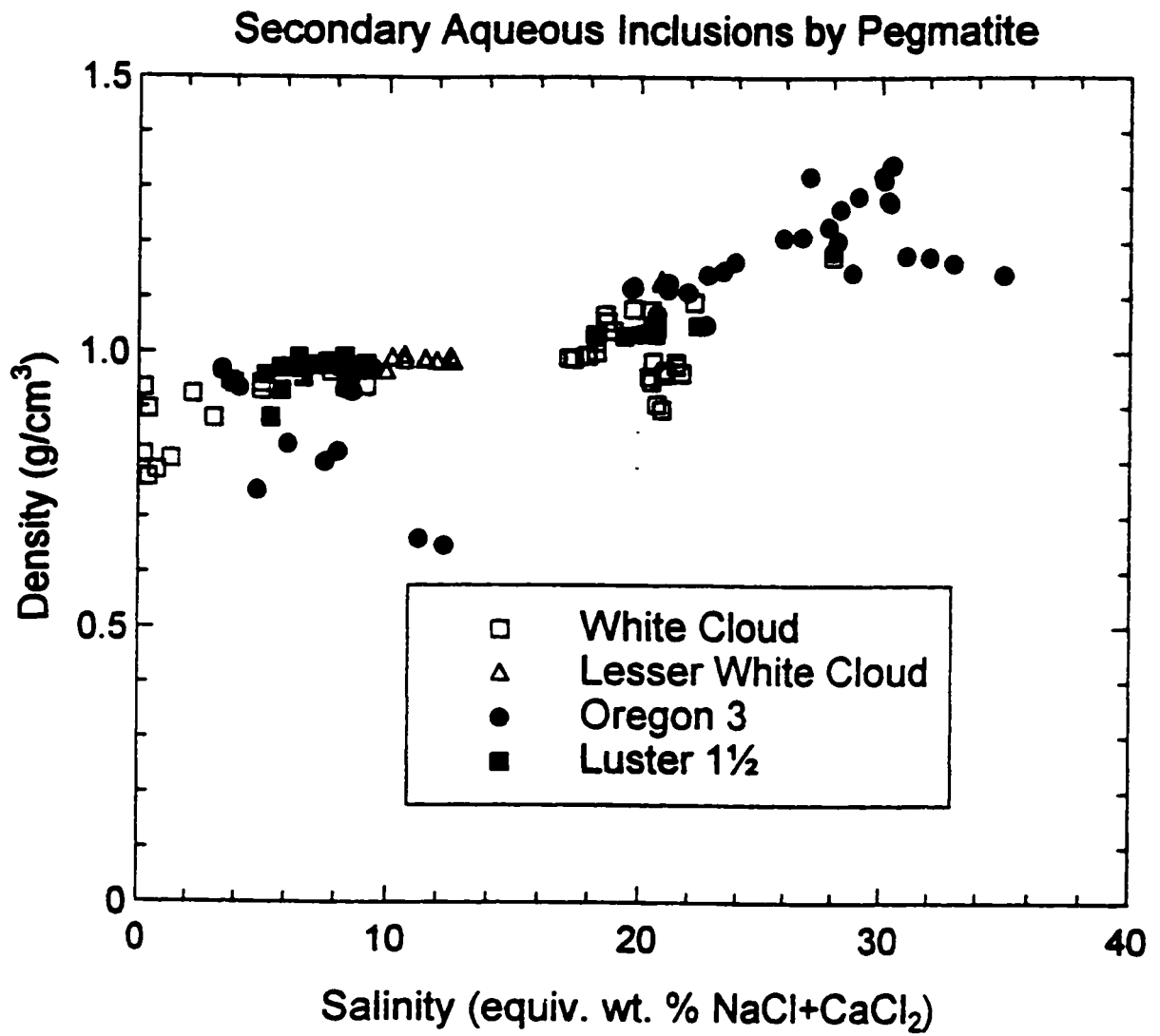
Figure 30. Salinity vs Density for secondary aqueous inclusions by pegmatite.

but does not include very low salinity inclusions (< 4 wt. %). Inclusions from the quartz vein lie within the low salinity group (at ~ 8 - 10 wt. %) and have somewhat variable densities (0.55 to 1.05 g/cm^3)(Fig. 31).

$TmCO_2$ values for both quartz and fluorite inclusions are near the CO_2 triple point (-56.6 °C)(Fig. 24) suggesting low concentrations of miscible gases such as CH_4 or N_2. Tm Clathrate values are between 5 and 10°C indicating salinities of between 0 and 8 wt. % NaCl. Thermometric data was only obtained from LC inclusions which contain relatively high volume proportions of aqueous liquid. The bulk composition of these inclusions indicate that they are H_2O-rich with between 5 and 30 mole % CO_2 and between 1 and 5 mole % NaCl (Fig. 32). LC inclusions with higher volume proportions of carbonic fluid exist, however, no thermometric data has been obtained from these inclusions to date.
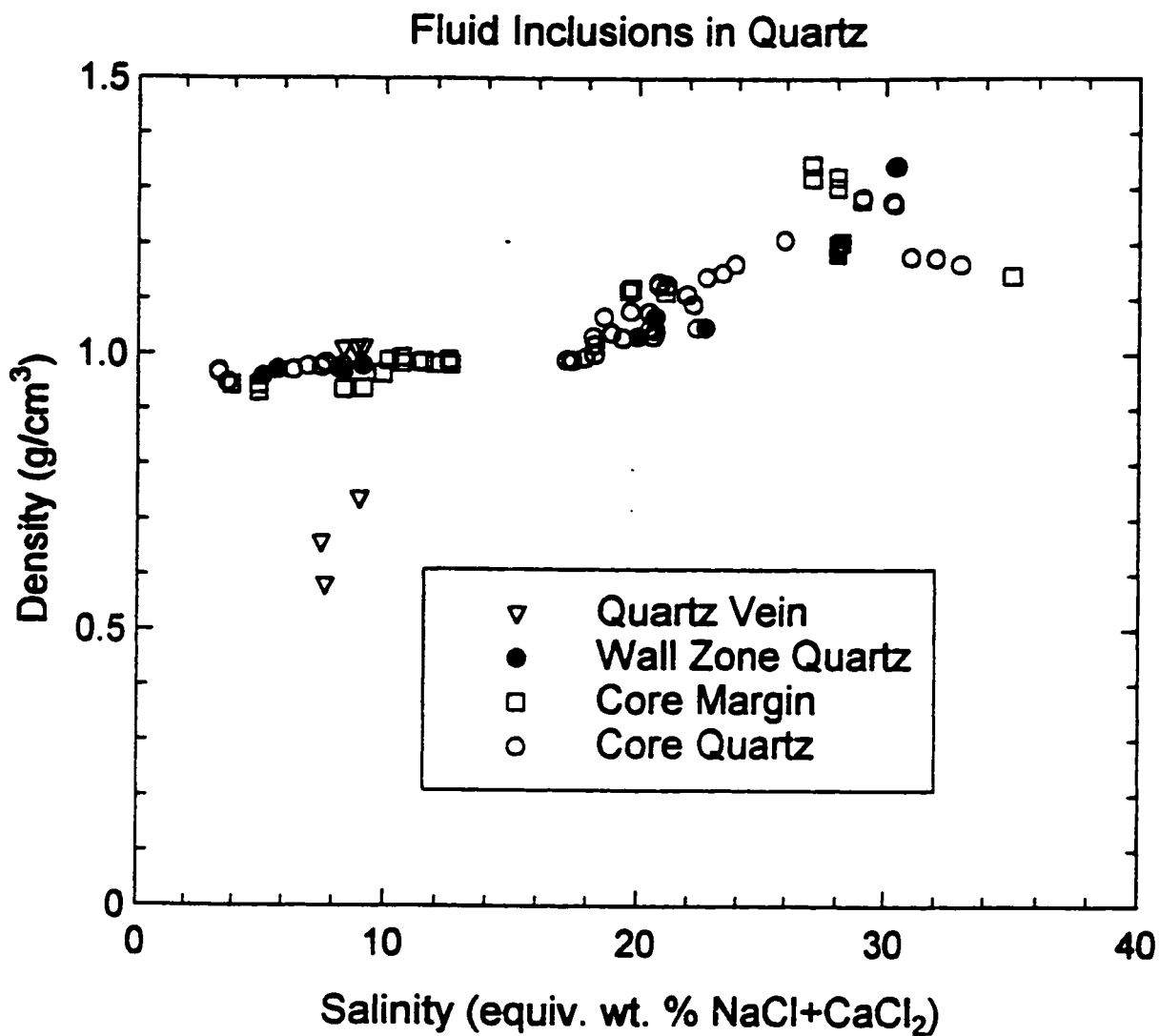
Figure 31. Salinity vs Density in pegmatites for fluid inclusions in quartz, subdivided by location.
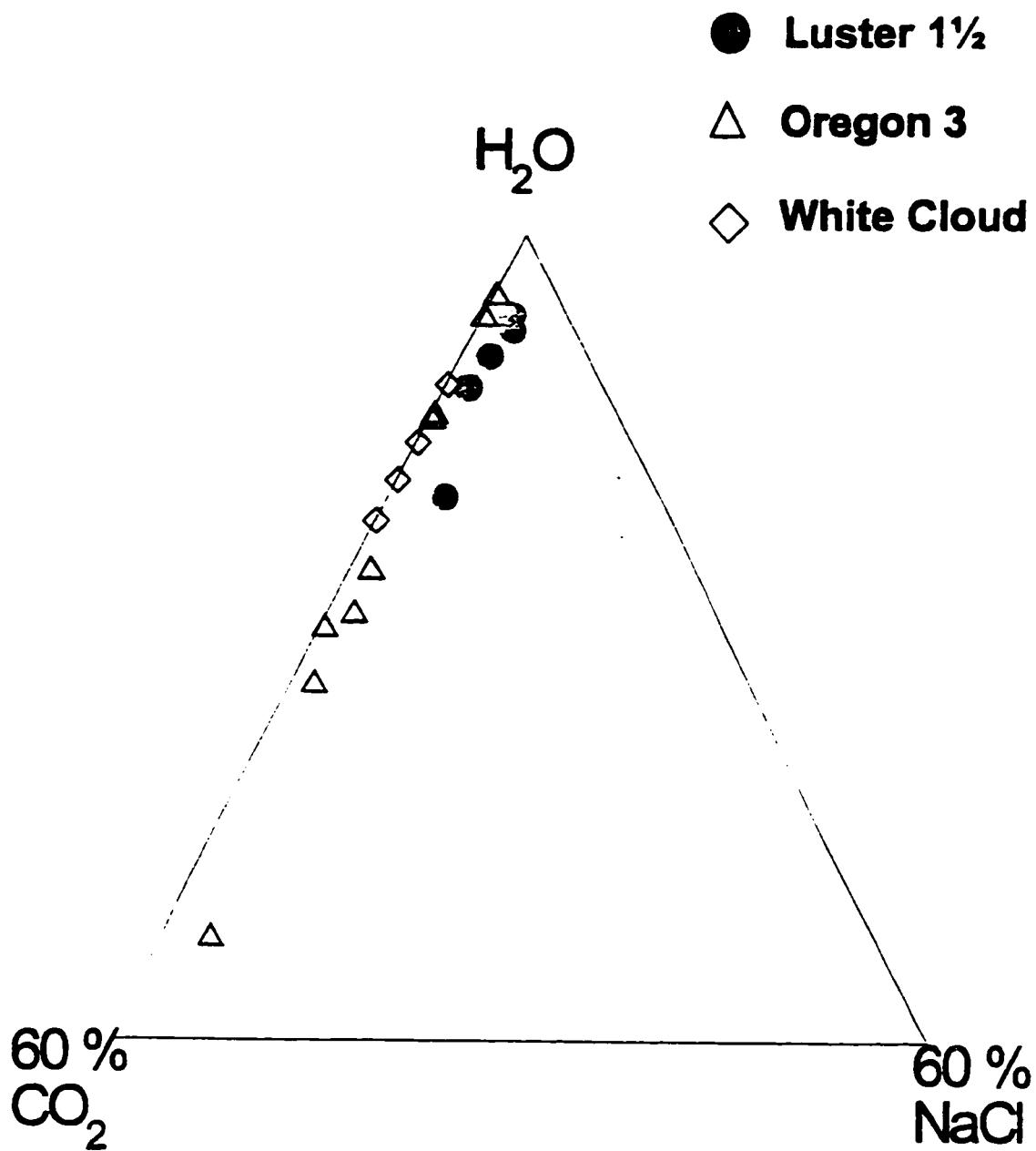
Figure 32. Relative molar proportions of H_2O, CO_2 and NaCl in LC incluisons

Chapter 4: Discussion And Interpretation

Paragenetic sequence for the South Platte District pegmatites

The four REE-enriched pegmatites investigated in this study are internally zoned, ellipsoidal bodies, consisting of at least four zones. The wall, intermediate, core-margin and core zones crystallized approximately sequentially from a F and rare element- enriched granitic magma. There is no evidence to contradict the conclusion made by Simmons and Heinrich (1980) that the massive core-margin fluorite is magmatic. After crystallization of the intermediate, core-margin and at least the outer parts of the core zone, hydrothemal fluids precipitated a variety of secondary minerals in veins and through replacement of primary minerals, mainly in the the intermediate zone feldspar and core-margin fluorite. This mineralization comprises a complex mineral assemblage dominated by albite and fluorite. A wide variety of rare-element minerals were precipitated at this time, the most abundant of which include monazite, gadolinite, allanite, samarskite and bastnaesite. The last stage of hydrothermal activity resulted in the deposition of muscovite and hematite throughout the pegmatites.

An important question pertaining to these pegmatites is whether the hydrothermal fluids were internally or externally derived. The lack of albitization or rare-element mineralization outside of the pegmatites, along with the apparent concentration of the replacement zones towards the tops of pegmatites (Simmons and Heinrich, 1980), suggests that the fluids were internally derived and that they

ponded below the already crystallized outer zones in the roof of the pegmatites. This orthomagmatic hydrothermal fluid appears to have been exsolved during the early to intermediate stages of core formation, as only the outer parts of the core have been veined and replaced by secondary minerals.

REE distribution and Source in fluorite and the Source of the REE

As is evident from the fluorescence spectra, the REE are distributed differently with respect to the types of fluorites within the pegmatites. In Oregon 3, the magmatic green fluorite contains higher concentrations of REE than the hydrothermal purple and white fluorites that replace it, whereas at White Cloud it would appear that the later clear fluorites can either have hogher or lower concentrations than the earlier, massive fluorite. These data indicate that REE were initially concentrated in the pegmatites during magmatic crystallization of the massive core-margin fluorite. In Oregon 3, during subsequent replacement of green fluorite, the REE were not transferred to the new white and purple fluorite. However, later, clear fluorite contains higher REE concentrations than the green fluorite. The presence of abundant solid inclusions in the replacement fluorite and the general association of rare-element minerals with the purple fluorite suggests that REE which were released during replacement were preferentially partitioned into REE-rich minerals such as monazite and bastnaesite, accounting for the low REE contents of the associated fluorite. The later clear fluorite does

not appear to be associated with other minerals (no solid inclusions) so that any available REE were incorporated into the fluorite. Similarly, in sample 82 from White Cloud, the clear fluorite which gave the highest intensities does not appear to contain solid inclusions, whereas the fluorite which provided the lower intensity spectrum does. This again suggests that the concentration of REE in the fluorites is determined by the presence or absence of coexisting minerals that may sequester the REE. It should be emphasized that these spectra must be considered preliminary. Better petrographic characterization of the fluorite types and associated rare element minerals, probably using cathodofluorescence, will be required to fully understand the distribution of REE between the various fluorite types.

It is not known whether the REE and other rare elements in the hydrothermal minerals were entirely or mostly derived from leaching of the massive core-margin fluorite or whether the fluids contained high rare element contents when they exsolved from the magma. The fluorescence data clearly suggests that at least some of the REE were derived by leaching, but it cannot be ruled out at present that the fluids had high rare element contents when they exsolved from the magma.

Most of the fluorites from a given pegmatite have very similar spectra (peak positions and *relative* intensities). This indicates that the *relative* concentrations of the REE causing the fluorescence are similar. However, some differences do exist indicating that the REE chemistry varies between pegmatites

and between fluorites in the same pegmatite. Further analysis and better assignment of peaks will be required to fully understand these relationships. Emission in the 530 to 570 nm band has been ascribed by Burruss et al. (1992) principaly to Ho^{3+} and Er^{3+} (Table 3) although it is possible that Eu^{3+} is also causing some of the emmision lines. The wavelength of an emission line is dependant on the element, its oxidation state and its structural site. Those peaks with narrow band widths are almost certainly attributable to 4f-4f electronic transitions of trivalent REE ions in the fluorite lattice (Burruss et al., 1992). Most of the assignments made by Burruss et al. (1992) were calculated from absorbtion and emmision energies of REE in LaF_3 and are site dependent. Natural fluorites ar likely to be more complex, so that it is possible, if not likely, that the REE occupy sites and defects not predicted by Burruss et al. (1992), accounting for the peaks not assigned by Burruss et al. (1992). The prominant peak at ~ 539 nm (peak #3) coincides with a likely emission line for both Ho^{3+} and Er^{3+} (Burruss et al., 1992) but is probably too broad to be assinged to a 4f-4f transition in a trivalent REE. Broader peaks in emmision spectra from natural fluorites have been attributed to transitions other than 4f-4f by Burruss et al. (1992), such as 4f-5d transitions in divalent REE, and may account for this peak in the South Platte spectra.

70

Fluid Inclusions in Fluorite

Primary inclusions within the fluorites comprise LV and LVS types which homogenized between 200 and 480°C and contain a low salinity fluid (from 2 to 10 wt. % $NaCl$ + $CaCl_2$). Some secondary LV and LVS inclusions within the fluorites have similar salinities to the primary inclusions, but also include more saline fluids (up to 30 wt. % $NaCl$ + $CaCl_2$). Homogenization temperatures cover a similar range to the primary inclusions (137 to 483 °C) but include a substantial number of lower values. In addition, some secondary inclusions are CO_2-rich (LC type), however no thermometry data was collected on fluorite-hosted LC inclusions.

The primary(?) inclusions show a wide range in homogenization temperatures from 91°C to 483°C. Their composition is also variable with salinities ranging from 3 to 28 wt. % $NaCl$ + $CaCl_2$. The density for these fluids is higher than that of the primary inclusions within fluorite, ranging from 0.5 to 1.2 g/cm^3. Given their salinities and densities, it is likely that these inclusions are in fact secondary in origin.

Primary fluid inclusions have only been observed in the white/purple fluorite, which is closely associated with the rare element minerals. The fluid responsible for rare element transport would therefore appear to be of relatively low salinity (<10 wt. %). Homogenization temperatures indicate that the minimum temperatures at which these assemblages could have been precipitated were between 200 and 480°C. Possible reasons for the wide range in

71

homogenization temperatures for inclusions in the fluorites could be: (1) the fluorite crystallized over a wide range of temperatures; (2) the inclusions underwent various degrees of necking; or (3) the inclusions underwent post-entrapment stretching (Bodnar and Bethke, 1984).

The time necessary for a closed system such as these pegmatites to cool over ~ 300°C would require fluorite crystallization over an extended time period. The main line of evidence which argues against such a scenario is that very low salinity aqueous (CO_2-free) fluids (< 4 wt. %) are restricted to primary inclusions in the fluorite. If such fluids were still precipitating fluorite at low temperatures, they should be present in the core, which would have completely solidified by 200 to 300°C (this is also consistent with a general lack of fluorite in the centres of the cores).

Stretching would likely only have occurred if the inclusions had been heated after entrapment. This is unlikely as the pegmatites represent that last stage of intrusion in the batholith and, once emplaced, would simply have cooled. If stretching had occurred we might expect to see a positive correlation between inclusion volume and Th (Bodnar and Bethke, 1984). Figure 33 shows inclusion volumes of LV inclusions (calculated using the method described by Bodnar (1983) plotted against Th for a variety of salinities and, as can be seen, there is no indication that a correlation exists between the two parameters.

The most likely explanation for the wide range in homogenization temperatures is therefore necking. Ascertaining the true temperatures of

precipitation will require further analysis of these inclusions. However, there appears to be a distinct low salinity (<10 wt. %) -high temperature population of fluorite-hosted inclusions in both the eastern (340-410°C) and western (400-500°C) pegmatites (Fig. 34), which most likely represents the fluid responsible for the fluorite and rare element mineralization.

Overall, the fluorite-hosted inclusions indicate deposition of the rare element assemblages at temperatures above 350°C from low salinity fluids. Subsequently, higher salinity (LV, LVS and LVH inclusions) and CO_2-rich (LC inclusions) fluids infiltrated the pegmatites and were trapped as secondary inclusions.

Fluid Inclusions in Quartz

No unequivocally primary inclusions were identified within any of the quartz samples from the pegmatites. Secondary inclusions have homogenization temperatures of 97 to 202 °C with compositions varying from 1 to 36 wt. % NaCl + $CaCl_2$. These secondary inclusions comprised LV, LVS, LVH and LC types. The highest salinity inclusions include LV, LVS and LVH types and the LC inclusions are all low salinity (<10 wt%). Intermediate salinity fluids are represented by both LV and LVS inclusions. As noted above, very low salinity aqueous inclusions appear to be absent from the quartz. The bulk composition of the LC inclusions appears to be highly variable with XCO_2 values ranging from
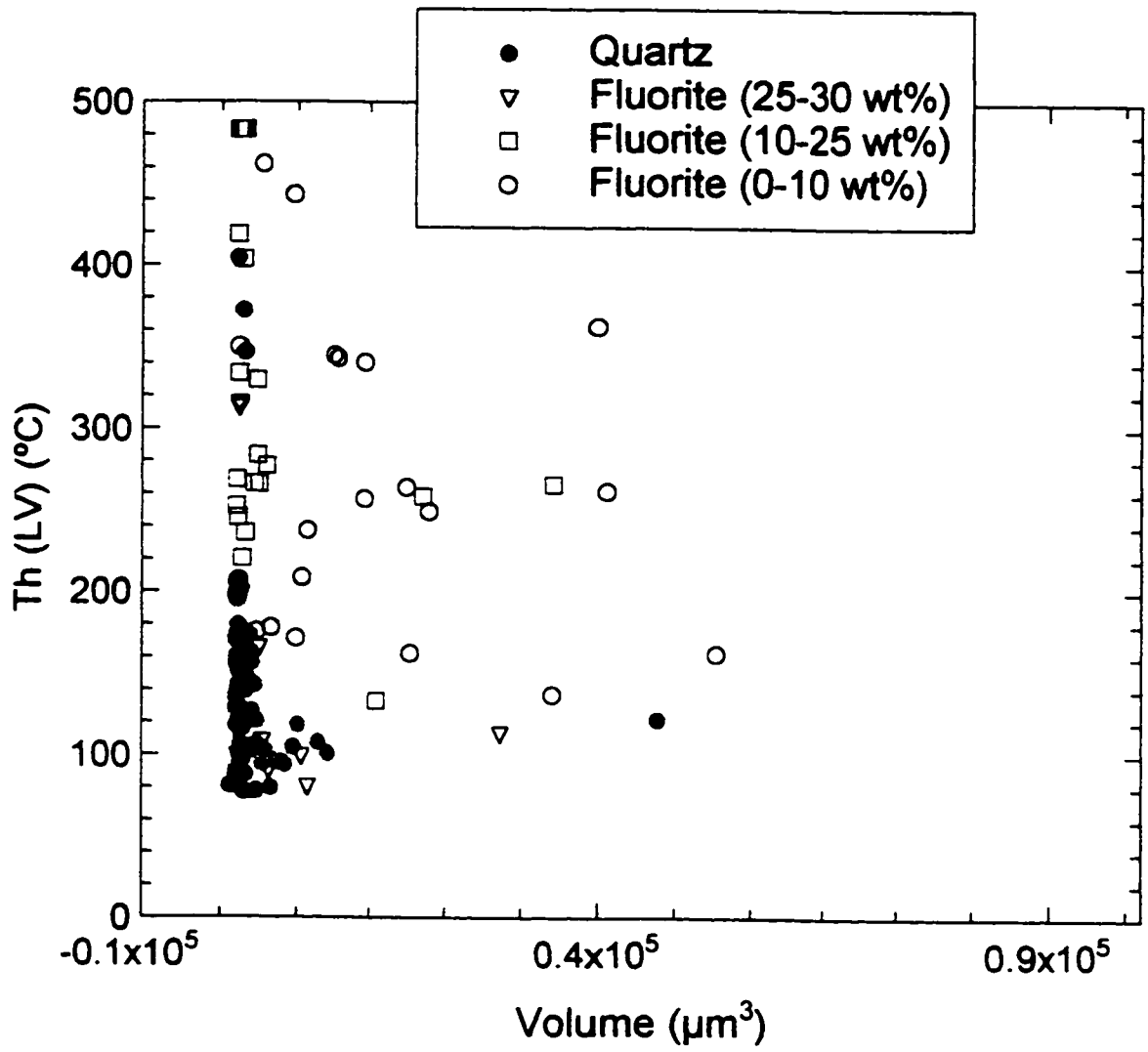
Figure 33. Volume vs Th for LV inclusions.
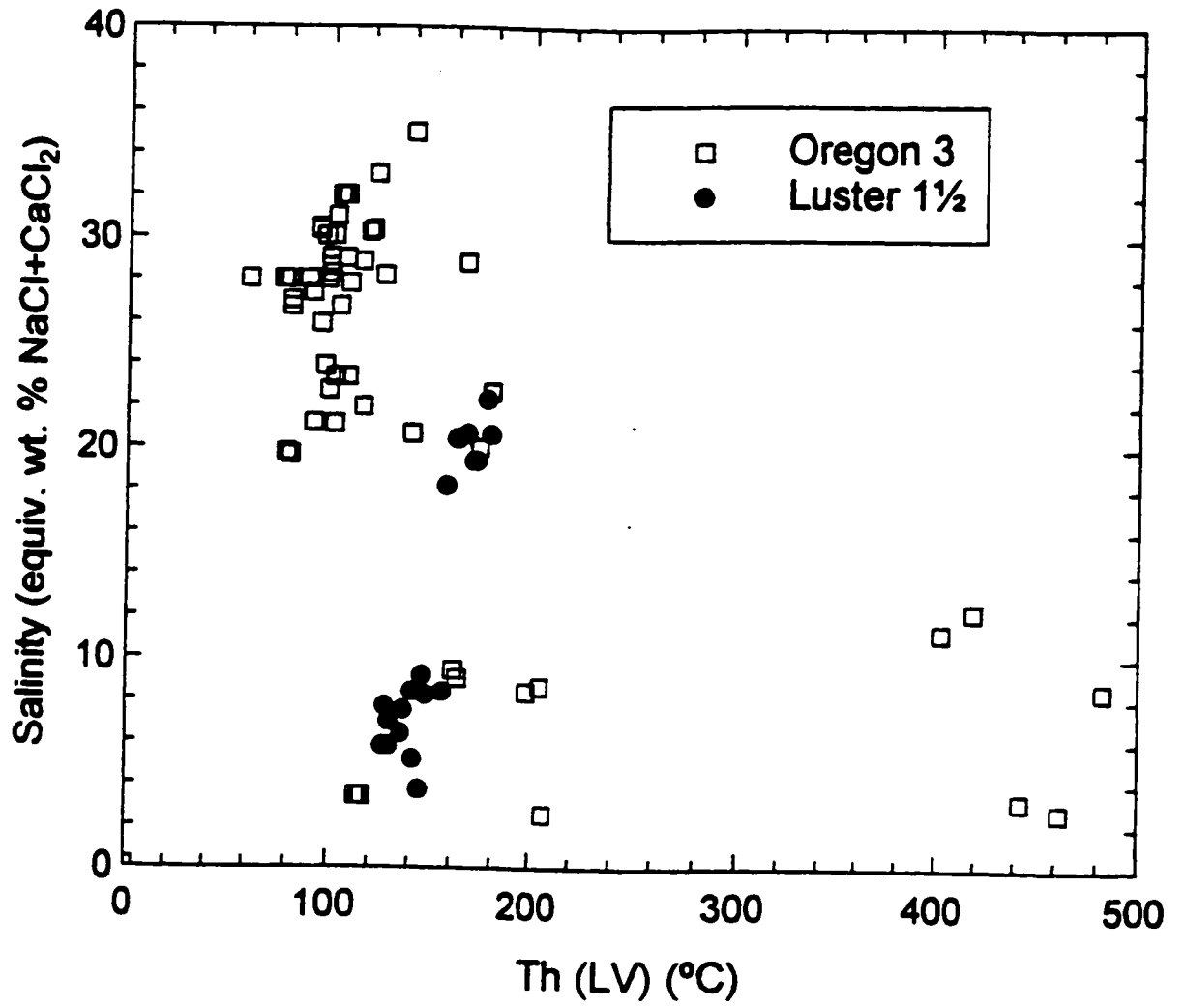
Figure 34a. Th vs Salinity for the Western pegmatites.
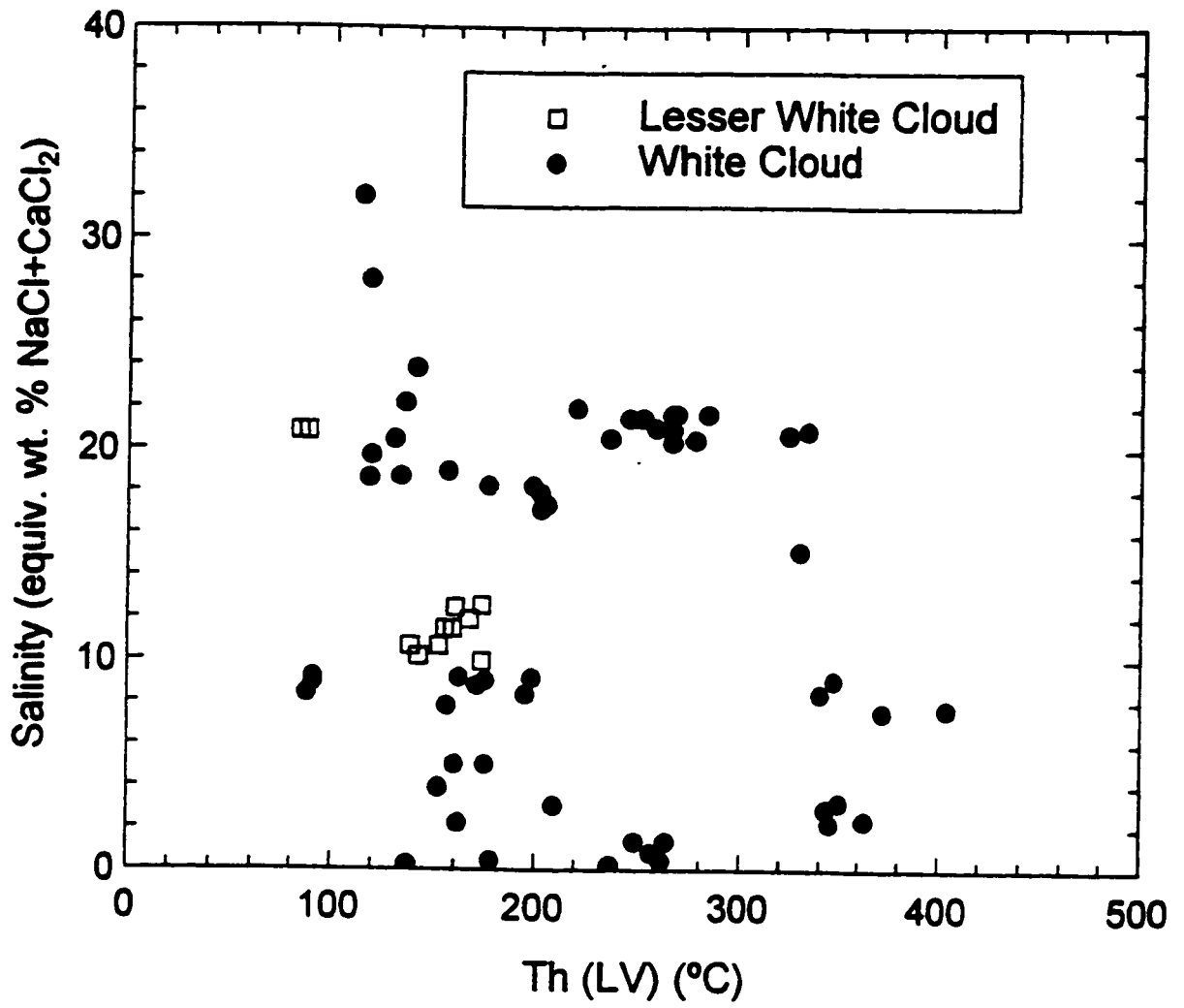
Figure 34b. Th vs Salinity for the Eastern pegmatites.

0.05 to at least 0.30. Some inclusions almost certainly contain higher mole fractions of CO_2 but no thermometry data was collected on such inclusions. The higher salinity fluids (>10 wt%) are widely distributed as secondary inclusions, particularly in core quartz, suggesting that they represent a later fluid that was trapped after widespread fracturing.

Two populations of LVH inclusions are present: one hosted by core-margin quartz and fluorite and the other by core quartz (Fig. 20). The first population is contained within the core-margin and has a composition of 25 to 30 wt. % NaCl, 1 to 6 wt. % $CaCl_2$ and 65 to 70 wt. % H_2O. The second population represents inclusions from the quartz core. Here the composition is more Ca rich: 20 to 25 wt. % $CaCl_2$, 10 to 12 wt. % NaCl and 65 to 70 wt. % H_2O. The difference in these two populations may reflect their location within the pegmatite. Ca contents may be buffered to lower values in the core-margin compared to that in the core because of equilibrium with fluorite.

Inter-pegmatite variations

Although the overall zonation is very similar for both the eastern and western pegmatites, differences exist in the replacement mineralogy. The most important rare element minerals in the eastern pegmatites are allanite, gadolinte, thalenite, bastnaesite and synchysite, whereas in the western pegmatites, samarskite is the most pronounced (Brewster, 1986; Wayne, 1986). Within the South Platte District as a whole, there appears to be a correlation between high

concentrations of fluorite and heavy REE (HREE) mineralization (Simmons and Heinrich, 1980). The pegmatites in the northern part of district (including those studied here) are polyzonal and contain abundant fluorite that is enriched in HREE and yttrian phases, such as samarskite, HREE -enriched zircon and yttrian fluorite. The pegmatites to the south are bizonal and contain sparse or no fluorite and are characterized by the LREE (light REE) phase allanite.

The fluid inclusion data presented in this thesis show that there are also differences in the nature of the fluids that permeated the eastern and western pegmatites. It would appear that, in both cases, the earliest fluids (those responsible for fluorite deposition) had low salinities and similar high temperatures, although Th values for inclusions in the west are somewhat higher than for those in the east (Fig. 33). This temperature difference could reflect real temperature variations but, as noted earlier, could be related to necking. Another possibility is that

the difference in homogenization temperatures reflects differences in the pressures of entrapment (i.e. depth). The present elevation of the eastern pegmatites is approximately 300 m lower than the western pegmatites (2100 vs. 2400 m). Higher pressures of entrapment in the eastern pegmatites would result in lower homogenization temperatures relative to inclusions in the western pegmatites. The validity of such an explanation would depend on whether any post-emplacement tilting of the batholith has occurred. However, the geometry of the pegmatites suggests that this has not occurred (their vertical tear-drop

shape) and the pegmatites are probably close enough to one another that minor tilting would not result in significant elevation changes.

A more significant difference is that CO_2-rich fluids (LC inclusions) and high salinity aqueous fluids (LVH and high salinity LV and LVS inclusions) are abundant in some samples from the western pegmatites, whereas LVH inclusions are absent from the eastern pegmatites and only one sample contains LC inclusions. This difference will be discussed in the next section in the context of fluid evolution in the pegmatites.

Fluid Evolution

There are four distinct compositional types of fluids within these pegmatites, based on fluid inclusion analysis:

(1) Low salinity aqueous fluids (0 - 12 wt. %)

(2) Intermediate salinity aqueous fluids (18 to 24 wt.%)

(3) High salinity aqueous fluids (26 to 30 wt. %)

(4) Low salinity, CO_2-bearing fluids

The evidence presented above indicates that the low salinity aqueous fluids were the first to circulate within the pegmatite and that these fluids, in particular ,those with salinities of less than 4 wt. %, were responsible for fluorite-rare element mineralization at temperatures of at least 340-500°C. It is likely that these fluids represent an internally-derived orthomagmatic fluid. These fluids were also trapped within secondary inclusions in fluorite and quartz, generally at

lower temperatures. The existence of higher salinity (4 - 12 wt. %) members of this population in core quartz suggests that this fluid was exsolved after much of the quartz core had crystallized.

The other fluid types circulated at a later time, as is indicated by their restriction to secondary inclusions and their widespread distribution in the pegmatites. There are several possible relationships between these three later fluids that have to be considered:

(1) They represent temporally distinct fluid infiltration events in which the fluids are genetically unrelated to one another.

(2) They are all related to one another through immiscibility

(3) Two of the three are related through immiscibility and the third represents a temporally distinct event.

In any of these models, the lack of a continuum in composition with the low salinity fluids probably requires that these later fluids were externally derived because the pegmatites were largely crystallized during circulation of the lower salinity fluids.

The density and salinity of the intermediate salinity fluids are very similar in the two groups of pegmatites, i.e. it would appear that the same fluid circulated through both sets of pegmatites. If the other fluids (high salinity and LC) were related to these fluids through immiscibility, we would expect them to be present in both pegmatite groups, which, by and large, they are not. In addition, if phase relationships in the $H_2O-NaCl-CO_2$ are considered (e.g. Bowers and Helgeson,

1983), it is clear that the three fluids cannot be related through immiscibility.

Production of the LC fluids by boiling the intermediate salinity fluid would require the latter to contain CO_2, and given that there is no evidence for this, this model is untenable. Even if the intermediate salinity fluid contains some undetected CO_2, boiling would produce an H_2O-rich fluid with higher salinities that that of the parent (the high salinity fluid would satisfy this fluid) and a CO_2-rich fluid with lower salinities than the parent (possibly the very CO_2-rich fluids for which no data is available). However, the bulk of the LC inclusions, which are H_2O-rich, cannot be explained in such a model.

It is conceivable, from a phase equilibrium standpoint, that the intermediate and high salinity fluids were both produced by unmixing of the LC fluid. However, this model seems unreasonable given the paucity of LC and high salinity inclusions at White Cloud. It is therfore concluded that the intermediate salinity fluid represents a regional, temporally-distinct fluid infiltration event and that is unrelated to the LC and higher salinity fluids.

Conversely, the association of LC and high salinity fluids in the western pegmatites suggests that they are genetically and temporally related. Again, considering phase relations in the H_2O-NaCl-CO_2 system, the only possible relationship is that the H_2O-rich LC fluid is the parent, and that this fluid ummixed to produce the CO_2-poor, high salinity fluids and the CO_2-rich, LC fluids. The lack of such fluids in the eastern pegmatites indicates that this fluid infiltration event was largely restricted to the western part of the pegmatite district. This model

81

can only be properly tested with quantitative data on the more CO_2-rich LC inclusions. Whether this event pre- or post-dated the infiltration of the intermediate salinity fluid is undetermined.

Other Studies

The types of inclusions identified in this study are essentially the same as those described by Simmons and Heinrich (1980), namely aqueous inclusions with highly variable salinities and aqueous-carbonic inclusions. However, this study has expanded on their work in terms of documenting in more detail the distribution of inclusion types in four of the pegmatites in the district, and on the compositions of the inclusions. One noticeable difference is that CO_2-bearing inclusions are not restricted to core quartz but occur in all the zones. Also, they state that CO_2-rich inclusions "are present in all the quartz examined with only one exception". The one exception is Oregon 3, where, in fact, CO_2-rich inclusions are abundant in some samples. It is not clear from their descriptions how many samples were examined from each pegmatite, but it is suspected that they examined one or two samples from each pegmatite. Similarly, the observation made here that CO_2-rich inclusions are rare at White Cloud is contradictory to the above statement.

The only compositional comparison that can be made is in the salinity range of the aqueous inclusions, which is the same. They do not show any detailed compositional data, so that further comparisons cannot be made.

Whereas they found anhydrite in fluorite-hosted inclusions, it was only confirmed in quartz-hosted inclusions in this study. This suggests that these fluids are late, and widespread throughout the pegmatites, although they do not state from which pegmatite the anhydrite occurred. They interpreted the anhydrite as a daughter mineral, whereas its distribution in the quartz-hosted inclusions (this study) indicates that it is a trapped solid. As they do not describe the occurrences, it is hard to judge their conclusions, however, the presence of anhydrite as solid inclusions in fluorite is more consistent with it also being a trapped phase in the fluorite-hosted inclusions.

Simmons and Heinrich (1980) do not explicitly state whether or not they examined and measured fluid inclusions in white/purple fluorite, so that direct comparisons of their fluorite data cannot be made with any certainly. However, from their Table 8, it would appear that they only measured inclusions in massive green fluorite. No primary inclusions were seen in massive core-margin fluorite, which is consistent with their suspicions that they misinterpreted secondary inclusions as primary inclusions. As with the salinity data, the range of Th values obtained on quartz core-hosted aqueous inclusions is grossly similar to that reported here, but again, the distributions cannot be compared because of a lack of detail in Simmons and Heinrich (1980).

Their conclusion that the core was precipitated at higher temperatures than the core-margin is based on the higher Th values obtained from what they interpreted to be primary LC inclusions compared to Th values for 'primary'

83

aqueous inclusions in core-margin massive fluorite. Again, they doubted the primary origin of the LC inclusions, which is consistent with the observations made in this study. However, if the Th values they obtained from the LC inclusions are representative (no such data was collected here), than it indicates that the carbonic fluids were high temperature (>300°C) and probably represent a relatively early fluid infiltration event.

Aqueous fluid inclusions in quartz from the Strange Lake pegmatites homogenize over a similar temperature range as those in the South Platte pegmatites (~120 - 480°) but have higher salinities (14 - 27 wt. %) than the South Platte orthomagmatic fluids (Salvi and Williams-Jones, 1992). Therefore, it would appear that the composition of the orthomagmatic aqueous fluids in the two systems is different. This is also the case for the carbonic fluids as, at Strange Lake, the carbonic fluids contain significant amounts of CH_4 and higher hydrocarbons, along with N_2 (Salvi and Williams-Jones, 1992). These authors, however, conclude that, unlike the South Platte pegmatites, the carbonic fluids at Strange Lake are orthomagmatic (Salvi, 1994).

Conclusions

The principal conclusions of this study are as follows:

(1)   Laser-excited emission (fluorescence) spectra indicate that the rare earth

element content of the fluorite in the South Platte pegmatites is variable.

Specifically, early, massive, core-margin fluorite (probably magmatic) in

many instances contains higher concentration of REE than the

hydrothermal white, clear and purple fluorite which replaces it. The latter

fluorite is associated with rare element minerals such as basnaesite and

monazite which have sequestered the REE released from the massive

fluorite during fluid-fluorite interaction. This indicates that at least some of

the rare elements in the mineralized zones has been derived from earlier,

magmatic concentrations. Some later hydrothermal, rare element mineral-

free fluorite contains very high concentrations of REE, possibly requiring

intrinsically high rare element contents.

(2)   Four distinct hydrothermal fluid types have been identified from a study of

fluid inclusions within both magmatic and hydrothermal minerals within the

pegmatites:

    (i)   Low salinity aqueous fluids (0 - 12 wt. %)

    (ii)   Intermediate salinity aqueous fluids (18 to 24 wt.%)

    (iii)   High salinity aqueous fluids (26 to 30 wt. %)

    (iv)   Low salinity, CO_2-bearing fluids

(3)   Data from primary inclusions within hydrothermal fluorite indicate that the rare-element mineralization was formed from low salinity (<10 equiv. wt. % NaCl + $CaCl_2$), orthomagmatic fluids at temperatures of at least 340 to 500°C.

(4)   The other fluid types occur exclusively in secondary inclusions, and post-dated the early, low-salinity fluid.

(5)   The intermediate salinity fluid is present in all the pegmatites studied and likely represents a distinct, district-wide fluid infiltration event.

(6)   The high salinity and carbonic fluids are, for the most part, restricted to the same pegmatites and are possibly genetically related to one another through immiscibility.

(7)   Two, compositionally-distinct high-salinity fluids are present, one with around 3 wt % $CaCl_2$ and another with around 11 wt % $CaCl_2$. These two fluids are distributed differently within the pegmatites and their compositional differences are thought to reflect separate fluid-rock interaction histories, the Ca-poor fluid having interacted with fluorite-rich assemblages.

References

Barker, F., Wones, D.R., Sharp, W.N., and Desborough, G.A., 1975, The Pikes Peak Batholith, Colorado Front Range, and a model for the origin of the gabbro-anorthosite-syenite-potassic granite suite. Precambrian Research, v.2, p.97-160.

Bill, H. and Calas. G., 1978, Color centers, associated rare-earth ions and the origin of coloration in natural fluorites. Phys. Chem. Minerals, v.3., p.117-131.

Bodnar, R.J., 1983, A method of calculating fluid inclusion volumes based on vapor bubble diameters and P-V-T-X properties of inclusion fluids. Econ. Geol., v.78, p.535-542.

Bodnar, R.J. and Bethke, P.M., 1984, Systematics of stretching of fluid inclusions I: Fluorite and sphalerite at 1 atmosphere confining pressure. Econ. Geol., v.79, p.141-161.

Bowers, T.S. and Helgeson, H.C., 1983, Calculation of the thermodynamic and geochemical consequences of nonideal mixing in the system H_2O-CO_2-NaCl on phase relations in geologic sytems: Equation of state for H_2O-CO_2-NaCl fluids at high pressures and temperatures. Geochim. Cosmochim. Acta, v.47, p.1247-1275.

Bozzo, A.T., Chen, J.R. and Barduhn, A.J., 1973, The properties of hydrates of chlorine and carbon dioxide. In Fourth International Symposium on Fresh Water from the Sea, A. Delyannis and E. Delyannis. eds.3, p.437-451.

Brewster, R.H., 1986, The distribution and chemistry of rare-earth minerls in the South Platte pegmatite district, Colorado, and their genetic implications. M.S. thesis, Univ. of New Orleans, 139p.

Brown P.E., 1989, FLINCOR: A microcomputer program for the reduction and investigation of fluid inclusion data. Amer. Mineral, v.74, p.1390-1393.

Brown, P.E. and Lamb, W.M., 1989, P-V-T properties of fluid in the system H_2O ±
CO_2 ± NaCl: New graphical presentations and implications for fluid
inclusion studies. Geochim. Cosmochim. Acta, v.53, p.1209-1221.

Burruss, R.C., Ging, T.G., Eppinger, R.G., and Samson, I.M., 1992, Laser-
excited fluoriexcence of rare earth elements in fluorite: Initial observations
with a laser Ramam microprobe. Geochim. Cosmochim. Acta, v.56,
p.2713-2723.

Campbell, A.R., Banks, D.A., Phillips, R.S., and Yardley, B.W.D., 1995,
Geochemistry of Th-REE Mineralizing Magmatic Fluids, Capitan
Mountains, New Mexico. Econ. Geol. v.90, p.1271-1287.

Cerny, P., 1991, Rare-element Granitic Pegmatites. Part I: Anatomy and Internal
Evolution of Pegmatite Deposits. Geoscience Canada, v.18, No.2., p.49-
67.

Crawford, M.L., 1981, Phase equilibria in aqueous fluid inclusions. In, Fluid
inclusions: applications to petrology, Hollister, L.S. and Crawford, M.L.
(editors), p.75-100.

Hedge, C.E., 1970, Whole rock Rb-Sr age of the Pikes Peak Batholith, Colorado.
US Geol. Surv. Prof. Pap., 700B: p86-p89.

Hutchinson, R.M., 1972, Pikes Peak batholith and Precambrian basement rocks
of the central Colorado Front Range: their 700-million-year history. Int.
Geol. Congress, 24th (Montreal) v.1, p.201-212.

Iliev, M., Liarokapis, E. and Sendova, M.Bl., 1988, Laser excited luminescence of
rare earth impurities in natural and synthetic CaF_2. Physics and Chemistry
of Minerals. v.15, p.597-600.

Lira, R, and Ripley, E.M., 1990, Fluid inclusion studies of the Rodeo de Los
Molles REE and Th deposit, Las Chacras batholith, central Argentina, GCA
v.54, p.663-671.

London D., 1986a, Magmatic-hydrothermal transition in the Tanco rare0element pegmatite: Evidence from fluid inclusions and phase equilibrium experiments. Amer. Mineral., Jahns Mem. Issue 71, p.376-395.

London D., 1986b, Formation of tourmaline-rich gem pockets in miarolitic pegmatites, Amer. Mineral., Jahns mem. Issue 71, p.396-405.

London D., 1986c, Holmquisite as a guide to pegmatic rare-metal deposits. Econ. Geol. v.81, p.704-712.

London, D., 1987, Internal differentiation of rare-element pegmatites, Effects of boron, phosphorus, and fluorine. Geochim. Cosmochim. Acta. v.51, p.403-420.

Oakes, C.S., Bodnar, R.J. and Simonson, J.M., 1990, The system $NaCl-CaCl_2$-H_2O: I. The ice liquidus at 1 atm. total pressure. Geochim. Cosmochim. Acta, v.54, p.603-610.

Peterman, Z.E. and Hedge, C.E., 1968, Chronology of Precambrian events in the Front Range, Colorado, Can. J. Earth Sci., v.5, p.749-756.

Peterson, W.L., 1964, Geology of the Platte Canyon Quadrangle Colorado, U.S. Geological Survey Bulletin 1181-C, 23p.

Roedder, E., 1984, Fluid inclusions. Reviews in Mineralogy v. 12 (P.H. Ribbe, series ed.), Min. Soc. Amer., Washington D.C., 644p.

Salvi, S., 1994, Magma degassing and wall rock alteration in rare metal-rich peralkaline granite at Stange Lake, Quebec/Labrador. PhD thesis, McGill Univ., Montreal, Quebec.

Salvi, S., and Williams-Jones. A.E., 1990, The role of hydrothermal processes in the granite-hosted Zr, Y, REE deposit at Strange Lake, Quebec/Labrador: Evidence from fluid inclusions. Geochim. Cosmochim. Acta. v.54, p.2403-2418.

Salvi, S., and Williams-Jones. A.E., 1992, Reduced orthomagmatic C-O-H-N-NaCl fluids in the Strange Lake rare-metal granitic complex, Quebec/Labrador, Canada. Eur. J. Mineral., v.4 ,p.1155-1174.

Simmons, W.B., Jr., 1973, Mineralogy, petrology and trace-element geochemistry of the South Platte granite-pegmatite system: Univ. Michigan unpubl. Ph.D. thesis, 143p.

Simmons, W.B., Jr. and Heinrich, E.W., 1971, Rare-earth-fluorine pegmatites of the South Platte district, Jefferson County, Colorado [abs.]: Canadian Mineralogist, v.10, p.919.

Simmons, W.B., Jr. and Heinrich, E.W., 1975, A summary of the petrogenesis of the granite-pegmatite system in the northern end of the Pikes Peak batholith: Fortschritte Mineralogie 52, Spec. Issue, IMA-Papers 9th Meeting Berlin-Regensburg, 1974, p.251-264.

Simmons, W.B., Jr. and Heinrich, E.W., 1980, Rare-Earth pegmatites of the South Platte District, Colorado. Colorado Geological Survey, Department of Natural Resources, Resource Series 11, 131p.

Simmons, W.B., Lee, M.T. and Brewster, R.H., 1987, Geochemistry and evolution of the South Platte granite-pegmatite system, Jefferson County, Colorado. Geochim. Cosmochim. Acta. v.51, p.455-471.

Sorenson, H., 1974, The Alkaline Rocks. Wiley & Sons, New York, NY, 622 p.40.

Vanko, D.A., Bodnar, R.J., Sterner, S.M., 1988, Synthetic fluid inclusions. VIII. Vapour-saturated halite solubility in part of the system $NaCl-CaCl_2-H_2O$, with application to fluid inclusions from oceanic hydrothermal system. Geochim. Cosmochim. Acta, v.52, p.2451-2456.

Wayne D.M., 1986, Electron microprobe analysis of rare-earth-element-bearing phases from the White Cloud pegmatite. South Platte district, Jefferson County, Colorado. M.S. thesis, Univ. of New Orleans, 122p.

Williams-Jones A.E. and Samson I.M., 1990, Theoretical estimation of halite solubility in the system $NaCl-H_2O-CaCl_2$: Applications to fluid inclusions. Canadian Mineral. v.28, p.299-304.

Zhang Y. and Frantz J.D., 1987, Determination of the homogenization temperatures and densities of supercritical fluids in the system $NaCl-KCl-CaCl_2-H_2O$ using synthetic fluid inclusions. Chem. Geol. v.64, p.335-350.

Replacement unit

Core (quartz)

Wallzone (quartz-microcline-biotite)

0   60 FEET

30

N
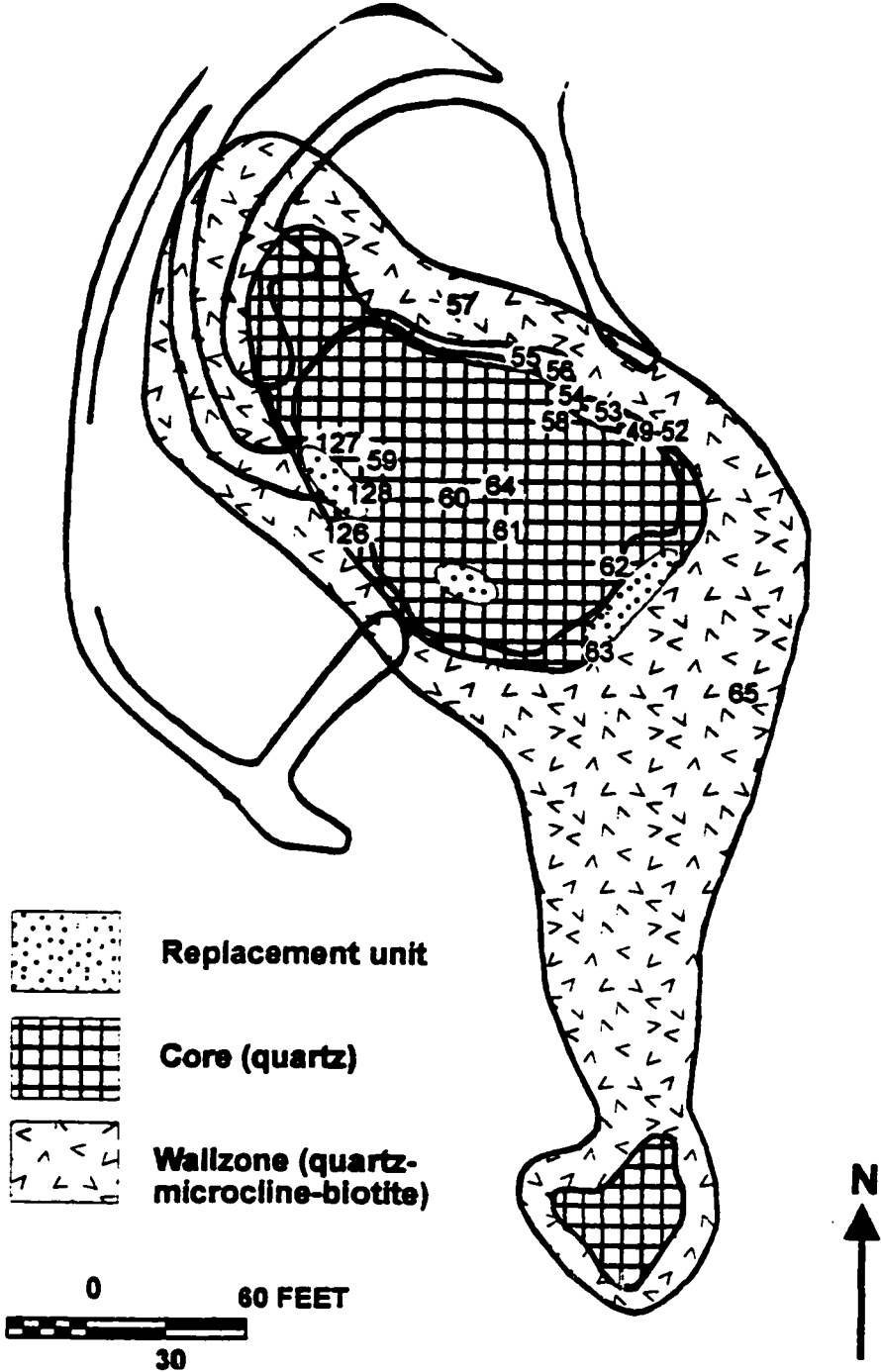
Figure A1 1. Oregon 3 Pegmatite
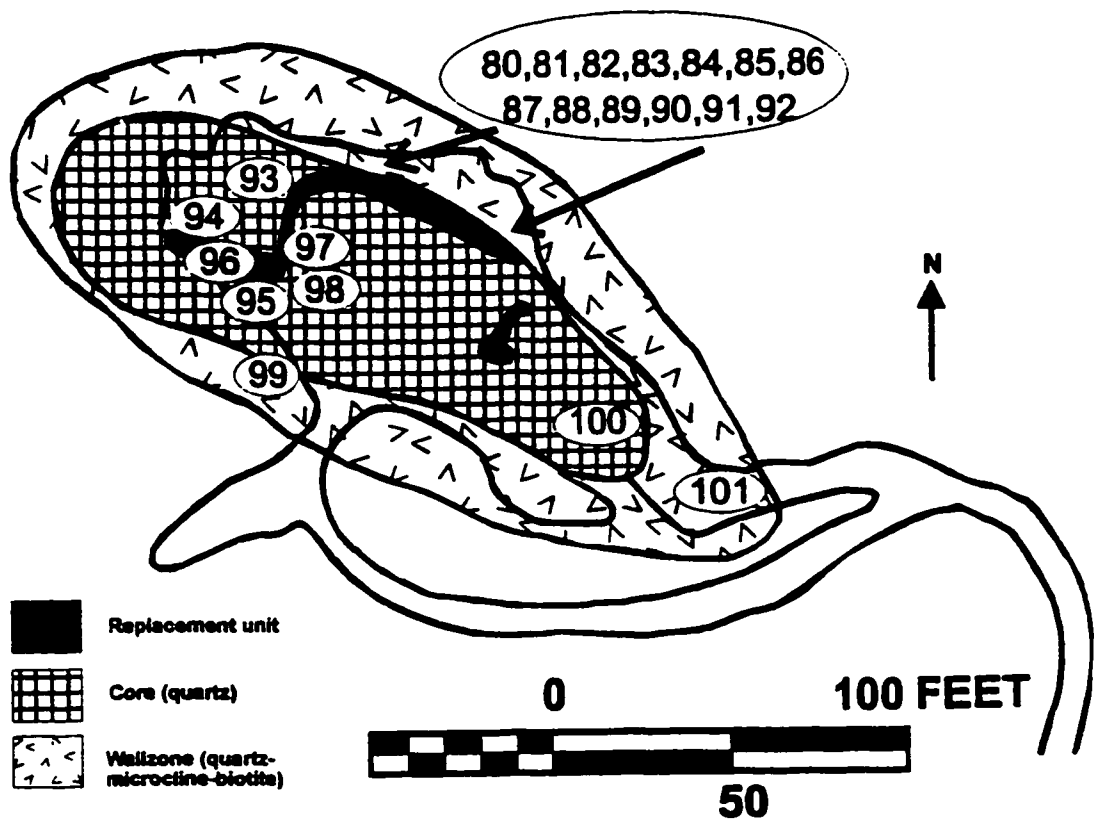
Figure A1 2. White Cloud Pegmatite
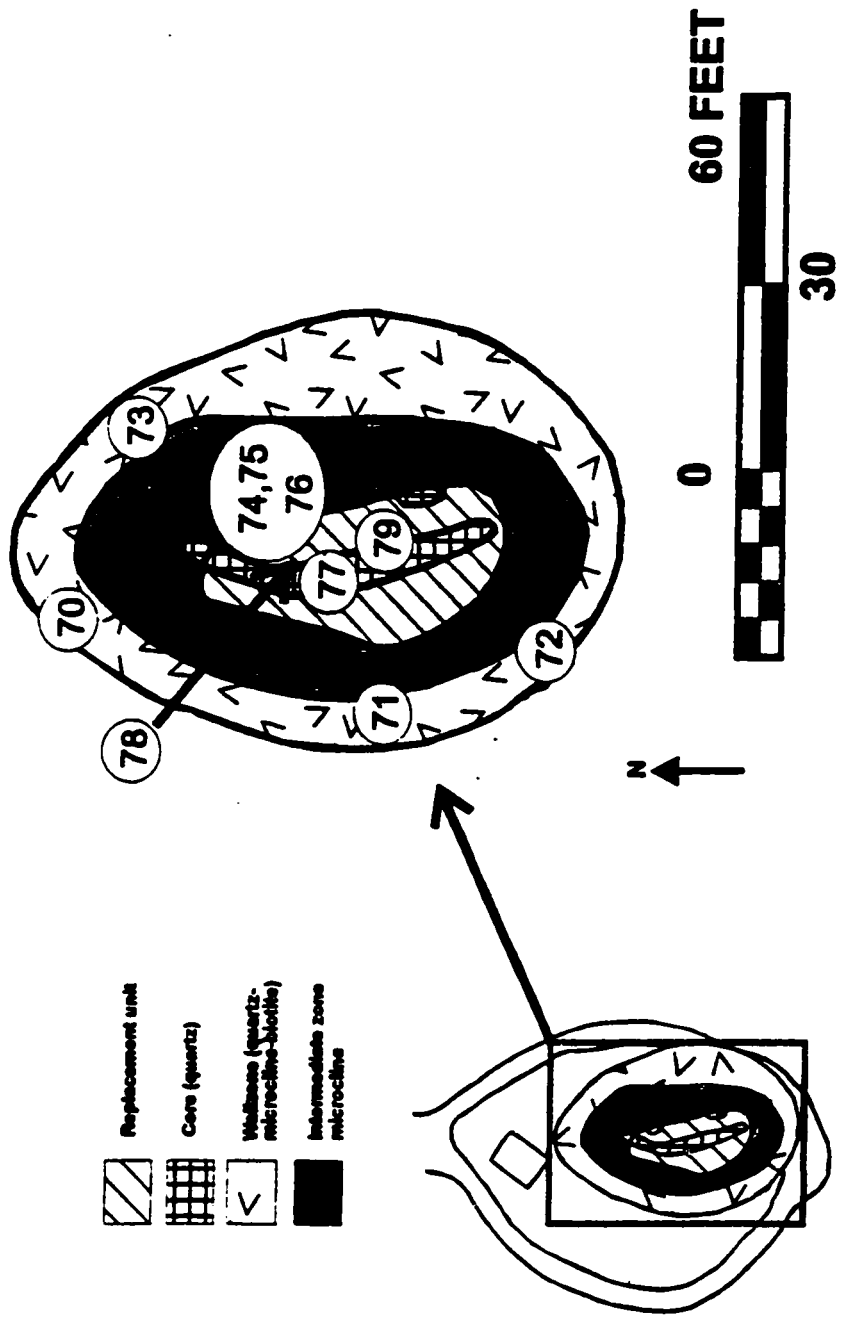
Figure A1 3. Lesser White Cloud Pegmatite
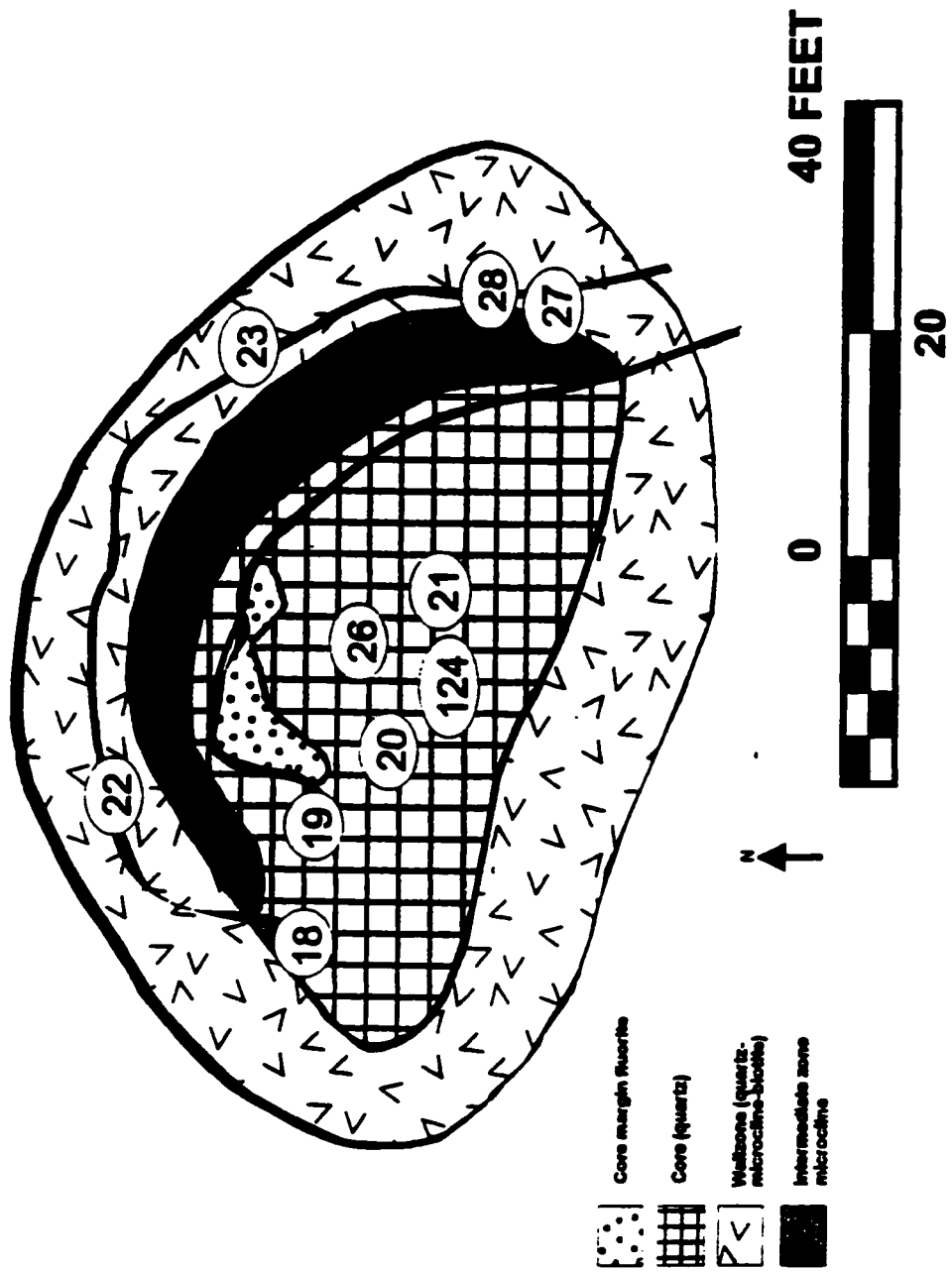
Figure A1 4. Luster 1 ½ Pegmatite

95

APPENDIX 2. METHODS

Microthermometry

All thin sections and doubly-polished wafers were examined with a transmitted light microscope in order to determine the types of fluid inclusions present. Fluid salinities and densities were calculated from the phase behaviour of fluid inclusions over the temperature interval -180 to 500°C, measured with a Linkam THMS 600 heating-freezing stage. The stage was repeatedly calibrated using a variety of organic and inorganic liquids and solids. The accuracy of measured temperatures range from $<\pm 0.3°C$ below 0°C to $\pm 2.5°C$ at 300°C. Heating rates were normally lower than $10°C/min$ and were 0.1 to $0.5°C/min$ during phase changes. The precision of measurements depends on the temperature of the phase transition: , $\pm 0.3°C$ for ice melting temperatures and , $\pm 2°C$ for vapour or solid disappearance temperatures.

Fluorescence Spectroscopy

Spectra were obtained from polished wafers between 517 and 557 nm using a THR 1000 Laser Raman Spectrograph. Excitation was achieved with the 514.5 nm line of an argon ion laser. A CCD detector recorded the response.

X-ray Diffraction

X-ray powder diffraction patterns were collected from several samples for mineral identification purposes using a Phillips PW 1140 X-ray diffractometer fitted with a Sietronics 122D automated interface. Portions of the sample containing the minerals in question were powdered for analyses. Diffraction patterns were analyzed with μPDMS identification software.

Salinity of LV and LVS inclusions

Salinities of LV and LVS inclusions were calculated from Tm ICE values using the following equation:

Salinity = -0.00000654*(-Tm ICE^4)+0.000995*(-Tm ICE^3)-0.05948*(-Tm ICE^2)+1.91*(-Tm ICE^1)+0.0872

This equation represents a regression through the median salinity value for a given Tm ICE value in the H_2O-NaCl and H_2O-$CaCl_2$ systems (Oakes et al., 1990). It thus represents an "average" salinity in the H_2O-NaCl-$CaCl_2$ system.

Bulk composition and density of LC inclusions

Calculation of the bulk composition of LC inclusions was achieved in the following manner:

1. Images of inclusions were captured via a video camera and saved directly to disk.

2. The relative areas of the aqueous and carbonic phases were calculated using Sigma Scan software.

3. Volumes of the two phases were calculated by either assuming that the areas were equivalent to volumes for flat inclusions or that the thickness of the inclusions was equal to the vapour bubble diameter for thicker inclusions.

4. These data were input into FLINCOR along with Th CO_2 and salinity data, which allowed calculation of thef bulk composition and density.

APPENDIX 3. THERMOMETRY DATA

Table A1: Thermometry data for LV and LVS inclusions

Abbreviations for Table A1

OR3	Oregon 3
WC	White Cloud
L1½	Luster 1½
LWC	Lesser White Cloud
FI	Fluorite
Qtz	Quartz
S	Secondary
P	Primary
P?	Primary?
LV	Liquid Vapour
L	Liquid
LVS	Liquid Vapour Solid
LVH	Liquid Vapour Halite
Te	Eutectic temperature
Tm ICE	Ice melting temperature
Th (LV)	Liquid vapour homogenization temperature
Tm HYD	Hydrate melting temperature
d at Th	Density at homogenization temperature
vb diam (μm)	vapour bubble diameter
vb vol	vapour bubble volume
incl vol	inclusion volume
Tm CO2	CO2 melting temperature

Tm CLATH   Clathrate melting temperature

All temperatures are in degrees Celsius

Vapour bubble diameters are in cubic microns

Table A1. Thermometry data for LV and LVS inclusions

sample #	Incl #	Pegmatite	Zone	Mineral	Min Type	Type	Origin	Te	Tm ICE	Th(L-V)	Tm HYD	Salinity (C)	d at Th	vb diam (um)	vb vol	Incl vol
RL-94-018	1-1-1	L1%	core	Qtz	milky	LV	S	-36	-18.63	179		20.62	1.034	4	34	239
RL-94-018	1-1-2	L1%	core	Qtz	milky	LV	S	-39	-16.48	172		19.36	1.030	2	4	34
RL-94-018	1-1-3			Qtz	milky	LV	S	-39	-16.48	170		19.38	1.031	2	4	34
RL-94-018	1-2-2	L1%	core	Qtz	milky	LV	S	-30	-18.24	162		20.45	1.047	7	180	1423
RL-94-018	2-1-1	L1%	core	Qtz	milky	LV	S	-28	-21.85	177		22.31	1.050	4	34	216
RL-94-018	2-1-2	L1%	core	Qtz	milky	LV	S	-31	-18.63	167		20.67	1.045	6	113	658
RL-94-018	2-2-1	L1%	core	Qtz	milky	LV	S	-31	-14.73	157		18.19	1.035	3	14	134
RL-94-019	1-1-1	L1%	core	Qtz	milky	LV	S	-22	-4.09	130		6.96	0.978	1	1	10
RL-94-019	1-1-2	L1%	core	Qtz	milky	LV	S	-23	-4.48	137		7.63	0.977	2	4	78
RL-94-019	1-1-3	L1%	core	Qtz	milky	LV	S	-21	-4.57	128		7.67	0.983	1	1	10
RL-94-019	1-1-4	L1%	core	Qtz	milky	LV	S	-22	-3.96	138		6.38	0.971	2	4	77
RL-94-022	1-1-1	L1%	wall	Qtz	smoky	LV	S		-4.98	144		8.22	0.928	4	34	498
RL-94-022	1-1-2	L1%	wall	Qtz	smoky	LV	S		-4.98	148		9.15	0.973	5	65	1030
RL-94-022	1-1-3	L1%	wall	Qtz	smoky	LV	S	-15	-5.65	146		9.60	0.960	4	34	529
RL-94-023	1-1-1	L1%	wall	Qtz	smoky	LV	S	-15	-2.91	142		5.17	0.969	6	113	1916
RL-94-023	1-1-2	L1%	wall	Qtz	smoky	LV	S	-15	-3.30	127		5.78	0.975	3	14	292
RL-94-023	1-1-3	L1%	wall	Qtz	smoky	LV	S		-3.30	130		5.78	0.971	3	14	282
RL-94-026	1-1-1	L1%	core	Qtz	milky	LV	S	-32	-2.03	145		3.73	0.948	5	65	1051
RL-94-026	1-1-2	L1%	core	Qtz	milky	LV	S	-32	-5.08	156		8.36	0.968	6	113	1640
RL-94-026	1-1-3	L1%	core	Qtz	milky	LV	S	-32	-5.08	141		8.36	0.979	4	34	571
RL-94-051	5-1-1	OR3	core-margin	Fl	clear	LV	S		-5.28	205		8.62	0.929	5	65	
RL-94-051	5-1-2	OR3	core-margin	Fl	clear	LV	S	-28	-5.08	198		8.36	0.934	3	14	139
RL-94-052a	2-1-1	OR3	core-margin	Fl	white	LVS	S	-88	-40.10	100		28.26	1.281	6	113	
RL-94-052a	2-2-1	OR3	core-margin	Fl	white	LV	S	-68	-42.24	166		28.81	1.146	12	905	7132
RL-94-052a	2-2-2	OR3	core-margin	Fl	white	LV	P	-11	-1.35	207		2.56	0.619	10	524	2364
RL-94-052a	2-2-3	OR3	core-margin	Fl	white	LVS	S	-60	-43.22	98		29.04	1.265	4	34	287
RL-94-052b	1-1-1	OR3	core-margin	Qtz	milky	LVS	S	-60	-39.71	128		28.18	1.205	5	65	499
RL-94-052b	1-1-2	OR3	core-margin	Qtz	milky	LV	S	-28	-16.88	81		19.63	1.116	8	268	1639
RL-94-055	1-1-1	OR3	core-margin	Qtz	milky	LV	S	-28	-19.41	102		21.10	1.115	5	65	1169
RL-94-055	1-1-2	OR3	core-margin	Qtz	milky	LV	S	-25	-17.07	79		19.75	1.120	8	268	3314
RL-94-055	1-1-4	OR3	core-margin	Qtz	milky	LV	S	-32	-7.01			10.96		2	4	78
RL-94-055	1-1-1	OR3	core-margin	Fl	white	LV	S	-23	-5.84	161		9.41	0.971	15	1767	1639
RL-94-055-c	3-1	OR3	core-margin	Fl	white	LV	S	-23	-5.55	153		8.02	0.887	6	113	861
RL-94-055-c	3-2	OR3	core-margin	Fl	white	LV	S	-22	-7.41			11.38		5	65	
RL-94-055-c	2-1-3	OR3	core-margin	Fl	white	LVS	P?		0.02			0.08		15	1767	
RL-94-055-c	2-1-4	OR3	core-margin	Fl	white	LVS	P		-0.37			0.76		5	524	
RL-94-055-c	2-1-5	OR3	core-margin	Fl	white	LVS	P		-0.37			0.76		5	524	
RL-94-055-c	2-1-6	OR3	core-margin	Fl	white	LVS	P					0.76		9	3054	
RL-94-055-c	2-1-7	OR3	core-margin	Fl	white	LV	S	-21	-7.11			11.00		3	14	
RL-94-055-c	2-1-8	OR3	core-margin	Fl	white	LV	S	-28	-6.92			10.77		21	4849	
RL-94-055-c	2-2-1	OR3	core-margin	Fl	white	LV	S	-28	-7.70			11.70		10	524	
RL-94-055-c	2-2-2	OR3	core-margin	Fl	white	LV	S	-28	-7.70			11.70		4	34	
RL-94-055-c	3-1-1	OR3	core-margin	Fl	white	LVS	S	-35	-11.80		0.91	15.65		32	17157	
RL-94-055-c	3-1-2	OR3	core-margin	Fl	white	LV	S	-45	-38.24	109		27.60	1.230	9	382	2606
RL-94-055-c	3-1-4	OR3	core-margin	Fl	white	LV	S	-58	-34.25	104		28.71	1.212	7	180	1475
RL-94-055-c	3-5-2	OR3	core-margin	Fl	white	L	S	-42	-9.75	483		13.62	0.534			
RL-94-055-c	3-5-3	OR3	core-margin	Fl	white	LV	S	-30	-13.07	483		18.92	0.613	8	268	583
RL-94-055-c	3-6-1	OR3	core-margin	Fl	white	LV	S	-40	-20.39	483		21.61	0.710	9	382	600
RL-94-055-c	3-6-2	OR3	core-margin	Fl	white	LV	S	-41	-7.50	483		11.47	0.481	7	180	317
RL-94-055-c	3-6-2	OR3	core-margin	Fl	white	LV	S	-43	-10.24	483		14.40	0.547	6	113	225
RL-94-055-c	3-7-1	OR3	core-margin	Fl	white	LV	S	-34	-7.31	403		11.24	0.662	8	268	710

100

Table A1. Thermometry data for LV and LVS inclusions

sample #	locl #	Pegmatite	Zone	Mineral	Min type	Type	Origin	Tc	Tm ICE	Th (L-V)	Tm HYD	Salinity (C)	d of Th	vb diam (um)	vb vol	Incl vol
RL-94-055-b	3-7-2	OR3	core-margin	Fl	white	LV	s	-20	-8.19	419		12.25	0.649	5	65	165
RL-94-060	1-1-1	OR3	core	Qtz	clear	LVS	s	-20	-1.84	117		3.40	0.967	23	6371	150268
RL-94-060	1-1-2	OR3	core	Qtz	clear	LVS	s	-20	-1.84	114		3.40	0.966	22	5676	136709
RL-94-060	1-1-3	OR3	core	Qtz	clear	LV	s	-20	-1.84	116		3.40	0.967	20	4189	98833
RL-94-060	2-1-1	OR3	core	Qtz	clear	LVS	s	-28	-24.29	108		23.37		21	4849	
RL-94-060	2-1-2	OR3	core	Qtz	clear	LVS	s	-28	-24.29			23.37		10	524	
RL-94-060	2-1-3	OR3	core	Qtz	clear	LVS	s	-48	-31.51	95	13.21	25.90	1.209	10	524	5021
RL-94-060	2-1-4	OR3	core	Qtz	clear	LV	s	-28	-21.07	116		21.94	1.110	5	65	656
RL-94-060	2-1-5	OR3	core	Qtz	clear	LV	s	-28	-19.51	92		21.15	1.128	3	14	195
RL-94-060	2-1-6	OR3	core	Qtz	clear	LV	s	-28	-24.29	102		23.37	1.149	4	34	351
RL-94-060	2-1-9	OR3	core	Qtz	clear	LVS	s	-28	-25.56	97		23.67	1.165	5	65	706
RL-94-060	2-1-0	OR3	core	Fl	white	LVS	P?	-43	-34.15	81		28.68	1.256	11	667	7817
RL-94-063	1-1-2	OR3	core-margin	Fl	white	LV	P?	-43	-36.59	91		27.36	1.254	9	362	3543
RL-94-063	1-1-3	OR3	core-margin	Fl	white	LV	P?	-48	-41.37	99		28.60	1.271	4	34	260
RL-94-063	1-1-4	OR3	core-margin	Fl	white	LV	P?	-48	-42.34	115		28.63	1.244	4	34	210
RL-94-074	1-1-1	LWC	core	Qtz	milky	LV	s	-24	-18.93	88		20.84	1.128	5	65	664
RL-94-074	1-1-2	LWC	core	Qtz	milky	LV	s	-24	-18.93	84		20.84	1.131	3	14	225
RL-94-078	1-1-1	LWC	core-margin	Qtz	milky	LV	s	-13	-7.50	159		11.47	0.966	6	113	1499
RL-94-078	1-1-2	LWC	core-margin	Qtz	milky	LV	s	-13	-7.50	155		11.47	0.966	2		57
RL-94-078	2-1-1	LWC	core-margin	Qtz	milky	LV	s	-14	-9.48	173		12.58	0.962	5	65	743
RL-94-078	2-1-2	LWC	core-margin	Qtz	milky	LV	s	-14	-9.38	160		12.47	0.961	2	4	53
RL-94-078	1-2-1	LWC	core-margin	Qtz	milky	LV	s	-13	-7.89	167		11.92	0.962	5	65	786
RL-94-078	1-2-1	LWC	core-margin	Qtz	smoky	LV	s	-12	-6.82	138		10.65	0.964	3	14	233
RL-94-078	1-2-2	LWC	core-margin	Qtz	smoky	LV	s	-12	-6.82	152		10.65	0.965	3	14	203
RL-94-078	2-1-1	LWC	core-margin	Qtz	milky	LV	s	-24	-8.23	173		9.91	0.965	6	113	1366
RL-94-078	2-1-2	LWC	core-margin	Qtz	milky	LV	s	-25	-8.43	142		10.16	0.969	3	14	228
RL-94-080	3-1-1	WC	core-margin	Fl	white	LV	s	-28	-20.49	263		21.66	0.649	10	524	2310
RL-94-080	3-1-2	WC	core-margin	Fl	white	LV	P?	-28	-21.07	220		21.84	1.007	6	113	617
RL-94-080	A-3-1	WC	core-margin	Fl	white	LVS	S?	-27	-19.12	266		20.64	0.960	12	7238	35190
RL-94-080	3-2	WC	core-margin	Fl	white	LV	S?	-27	-19.22	258		21.00	0.987	10	4189	20847
RL-94-080	A-1-1	WC	core-margin	Fl	white	LV	S?	-25	-18.63	323		20.87	0.906	19	26731	116243
RL-94-081	A-1-2	WC	core	Fl	white	LVS	S?	-28	-19.02	333		20.89	0.897	5	65	254
RL-94-081	1-1-1	WC	core	Qtz	milky/clear	LV	s		-15.80	156		18.93	1.040	2	4	38
RL-94-081	1-1-2	WC	core	Qtz	milky/clear	LV	s		-18.24	130		20.45	1.077	1	1	5
RL-94-081	1-1-3	WC	core	Qtz	milky/clear	LV	s		-15.31	118		18.60	1.066	1		7
RL-94-082	1-2-1	WC	core-margin	Fl	clear	LVS	s	-36	-18.05	266		20.34	0.957	9	362	1906
RL-94-082	1-2-2	WC	core-margin	Fl	clear	LVS	s	-36	-18.34	236		20.51	0.964	7	180	666
RL-94-082	3-1-1	WC	core-margin	Fl	clear	LV	S2	-24	-20.10	245		21.46	0.982	4	34	171
RL-94-082	3-1-2	WC	core-margin	Fl	clear	LV	S2	-24	-20.10	252		21.46	0.975	2	4	21
RL-94-081	4-1-1	WC	core-margin	Fl	clear	LVS	S?	-4	-0.37	257		0.79	0.768	9	3054	14363
RL-94-082	4-2-1	WC	core-margin	Fl	clear	LV	s	-5	-0.18	262		0.43	0.775	13	8203	40043
RL-94-085	A-1-1-1	WC	core-margin	Fl	clear	LV	s	-10	-0.08	237		0.24	0.813	7	1437	7628
RL-94-085	A-1-1-2	WC	core-margin	Fl	clear	LV	s	-11	-0.08	137		0.24	0.635	8	2145	35124
RL-94-085	A-3-1-1	WC	core-margin	Fl	clear	LV	s	-7	-1.84	208		3.07	0.681	6	905	7190
RL-94-085	A-3-1-2	WC	core-margin	Fl	clear	LV	s	-4	-1.18	162		2.22	0.625	10	4189	52976
RL-94-085	A-3-1-3	WC	core-margin	Fl	clear	LV	s	-5	-0.67	249		1.34	0.608	10	4189	21563
RL-94-080	1-1-1	WC	core-margin	Fl	white	LV	P?	-3	-0.67	284		1.34	0.608	10	4189	19023
RL-94-080	1-1-2	WC	core-margin	Fl	clear/green	LV	s	-33	-15.41	133		18.67	0.760	7	1437	15717
RL-94-080	1-1-3	WC	core-margin	Fl	clear/green	LV	s	-28	-20.49	266		21.66	1.057	5	524	2457
RL-94-080	4-1-1	WC	core-margin	Fl	clear/green	LVS	s	-5	-0.57	268		1.16	0.982	3	14	66

Table A1. Thermometry data for LV and LVB inclusions

sample #	Incl. #	Pegmatite	Zone	Mineral	Min Type	Type	Origin	Te	Tm ICE	Th (L-V)	Tm HYD	Salinity (C)	d/l Th	vb diam (um)	vb vol	Incl vol
RL-94-060	4-1-2	WC	core-margin	Fl	clear/green	LVS	S	-27	-18.24	277		20.45	0.948	11	897	3331
RL-94-060	A-1-1	WC	core-margin	Fl	clear/green	LV	S	-23	-4.67	156		7.61	0.685	15	14137	205691
RL-94-060	C-1-1	WC	core-margin	Fl	clear	LVS	P?		-38.63	114		32	1.164	12	905	28369
RL-94-060	C-1-2	WC	core-margin	Fl	clear	LVS	P?	-22	-11.02	329		15.16	0.849	10	524	7244
RL-94-060	C-1-3	WC	core-margin	Fl	clear	LV	P?	-24	-5.08	340		8.36	0.759	20	4169	14465
RL-94-060	C-1-4	WC	core-margin	Fl	clear	LV			-5.75			8.28		21	4849	
RL-94-060	C-2-1	WC	core-margin	Fl	clear	LV	P	-24	-1.55	343		2.90	0.638	10	4169	11369
RL-94-060	C-2-2	WC	core-margin	Fl	clear	LV	P		-1.18	345		2.22	0.619	10	4169	10608
RL-94-060	C-2-3	WC	core-margin	Fl	clear	LV	P		-1.74	350		3.24	0.628	6	113	286
RL-94-060	C-2-4	WC	core-margin	Fl	clear	LV	P		-1.26	363		2.39	0.574	18	17157	39990
RL-94-060	C-2-5	WC	core-margin	Fl	clear	LVS	P		-1.64			3.07		12	905	
RL-94-092	1-1	WC	core-margin	Fl	clear	LV	S?	-32	-7.60	315		9.15	0.651	8	113	327
RL-94-092	1-1-2	WC	core-margin	Fl	clear	LV	S?	-31	-7.80	313		8.36	0.655	8	113	332
RL-94-092	1-2-1	WC	core-margin	Fl	clear	LVB	S?	-14	-0.18	178		0.43	0.668	9	362	3766
RL-94-092	2-1-2	WC	core-margin	Fl	clear	LV	P	-25		172		16.60		3	14	
RL-94-092	2-1-3	WC	core-margin	Fl	clear	LV	P	-24	-6.65	162		9.15	0.669	7	1437	19439
RL-94-092	2-2-1	WC	core-margin	Fl	clear	LV	P	-25	-6.35	171		8.76	0.659	10	524	6624
RL-94-092	2-3-1	WC	core-margin	Fl	clear	LVS	P	-28	-6.55	175		9.02	0.665	7	180	2156
RL-94-092	3-1-3	WC	core	Qtz	milky	LV	P?	-60	-25.48	140		23.63	1.107	5	65	477
RL-94-092	3-1-4	WC	core	Qtz	milky	LV	S		-5.65	198		9.15	0.659	3	14	139
RL-94-092	3-1-6	WC	core	Qtz	milky	LVB	S		-5.08	185		8.38	0.637	3	14	143
RL-94-092	3-2-1	WC	core	Fl	clear	LV	S	-40	-12.68			16.60		3	14	
RL-94-092	3-2-2	WC	core-margin	Qtz	milky	LV	S	-21	-2.82	160		6.02	0.644	6	113	1566
RL-94-092	3-2-4	WC	core-margin	Qtz	milky	LV	S	-21	-2.13	162		3.90	0.644	5	65	970
RL-94-092	2-1-1	WC	core-margin	Qtz	milky	LV	S?	-22	-2.62	175		5.02	0.632	3	14	166
RL-94-063	2-1-3	WC	core	Qtz	milky	LV	S?	-24	-14.83	176		18.28	1.018	5	65	550
RL-94-063	2-1-4	WC	core	Qtz	milky	LV	S7	-24	-14.34	202		17.90	0.685	4	34	249
RL-94-063	2-1-5	WC	core	Qtz	milky	LV	S?	-24	-14.83	188		18.28	1.001	4	34	250
RL-94-063	2-1-1	WC	core	Qtz	milky	LV	S7	-25	-13.65	205		17.38	0.966	3	14	108
RL-94-063	2-1-3	WC	core	Qtz	milky	LV	S?	-25	-13.38	202		17.15	0.960	5	65	507
RL-94-063	2-1-4	WC	core	Qtz	milky	LV	S	-40	-21.58	135		22.16	1.092	1	1	4
RL-94-064	1-1-1	WC	core	Qtz	milky	LV	S	-41	-16.97	119		19.66	1.076	1	1	6
RL-94-004	1-1-1	WC	vein	Qtz	vein	LV	S	-34	-4.48	372		7.53	0.655	6	266	738
RL-94-102a	1-1-2	WC	vein	Qtz	vein	LV	S	-35	-4.57	404		7.87	0.581	5	65	149
RL-94-102a	1-1-3	WC	vein	Qtz	vein	LV	S	-34	-4.96			8.22		1	1	
RL-94-102a	1-1-4	WC	vein	Qtz	vein	LV	S	-36	-5.65	347		9.02	0.738	6	266	613
RL-94-102a	3-1-1	WC	vein	Qtz	vein	LV	S	-38	-5.08	88		8.36	1.010	8	16	16
RL-94-102a	3-1-3	WC	vein	Qtz	vein	LV	S	-36	-5.65	91		9.15	1.013	2	4	132
RL-94-102a	2-1-1	WC	vein	Qtz	vein	LV	S	-38	-6.45	91		8.60	1.012	1	1	17
RL-94-126	2-1-2	OR3	core	Qtz	milky	LV	S	-24	-17.48	173		19.99	1.034	5	65	503
RL-94-126	2-1-3	OR3	core	Qtz	milky	LV	S	-25	-22.63	179		22.67	1.051	4	34	208
RL-94-126	2-3-3	OR3	core-margin	Qtz	vein	LV	S	-24	-18.63	140		20.67	1.070	6	113	1022
RL-94-126	2-3-4	OR3	core	Qtz	milky	LV	S	-60	-49.85	94		30.36	1.342	11	897	5287
RL-94-127	1-1-1	OR3	core	Qtz	milky	LVS	S	-61	-50.34	94		30.44	1.342	9	362	2849
RL-94-127	1-1-6	OR3	core	Qtz	milky	LV	S	-71	-58.72			30.86		11	897	
RL-94-127	1-1-7	OR3	core	Qtz	milky	LVS	S	-48	-49.28	118		30.27	1.277	13	1150	6717
RL-94-128a	2-1-1	OR3	core-margin	Fl	clear	LV	P?	-48	-49.75	120		30.35	1.274	9	362	2172
RL-94-128a	2-1-3	OR3	core-margin	Fl	clear	LV	P?	-17	-1.74	443		3.24	0.537	10	4169	8260
RL-94-126a	2-2-2	OR3	core-margin	Fl	clear	LV		-18	-1.45	462		2.73	0.248	8	2145	2845
								-22	-5.18	483		8.49		8	266	

102

Table A2: Thermometry data for LC inclusions

sample #	Incl #	Pegmatite	Zone	Mineral	Min Type	Type	Origin	Te	Tm Ice	Th(L-V)	Tm CO2	Tm CLATH	Th CO2	Salinity	d of Th
RL-94-018	1-2-3	L1%	core	Qtz	milky	LC	s		-31.68		-56.90	8.48	29	6.7	0.854
RL-94-018	1-2-4	L1%	core	Qtz	milky	LC	s		-31.88		-56.90	8.58	29	6.5	0.851
RL-94-018	1-2-5	L1%	core	Qtz	milky		s		-30.98		-56.90	8.97	28	5.82	0.831
RL-94-018	1-2-6	L1%	core	Qtz	milky	LC	s		-31.88		-56.90	7.22	28	5.37	0.882
RL-94-018	1-2-7	L1%	core	Qtz	milky	LC	s		-31.88		-56.90	8.49	29	6.31	0.902
RL-94-060	2-1-7	OR3	core	Qtz	clear	LCV	s	-23				7.90	28		
RL-94-060	2-1-8	OR3	core	Qtz	clear	LCV	s	-23				7.51	28	4.13	0.908
RL-94-060	2-4-1	OR3	core	Qtz	clear	LCVHs	s	-26	-18.41		-57.00	-9.57	28	4.65	0.749
RL-94-060	2-4-2	OR3	core	Qtz	clear	LCV	s	-26	-18.02		-57.88	8.82	28	6.08	0.833
RL-94-060	2-4-3	OR3	core	Qtz	clear	LCV	s	-26	-18.31		-57.88	5.72	29	8.08	0.820
RL-94-060	2-4-4	OR3	core	Qtz	clear	LCV	P?		-18.61		-57.68	8.02	28	7.58	0.802
RL-94-060	A-1-2	WC	core-margin	Fl	clear/green	LCV	s		-0.93			9.87			
RL-94-092	3-1-1	WC	core-margin	Qtz	milky	LCv	s				-56.60	9.87	31	0.28	0.738
RL-94-092	3-1-2	WC	core-margin	Qtz	milky	LCv	s				-56.80	9.67	29	0.66	0.643
RL-94-092	3-1-5	WC	core-margin	Qtz	milky	LCV	s		-14.97			9.67	30	0.66	0.864
RL-94-092	3-1-7	WC	core-margin	Qtz	milky	LCV	sKs				-56.99	9.79	30	0.44	0.792
RL-94-126	2-3-1	OR3	well	Qtz	milky	LCV	s	-59	-49.18	101					0.875
RL-94-126	2-3-2	OR3	well	Qtz	milky	LCV	S?	-59	-49.00	97					0.826
RL-94-127	1-1-3	OR3	core	Qtz	milky	LCV	s				-56.60	9.28	29	0.66	0.805
RL-94-127	1-1-4	OR3	core	Qtz	milky	LCV	s				-56.60		29	0.66	0.822
RL-94-126Q2	1-1-1	OR3	core-margin	Qtz	smoky	LCV	s		-11.14		-56.60	9.58	30	0.46	0.801
RL-94-126Q2	1-2	OR3	core-margin	Qtz	smoky	LCV	s		-12.22		-56.60	9.58	31	16.22	
RL-94-126Q2	1-3	OR3	core-margin	Qtz	smoky	LCV	s		-11.05		-56.99	9.77	31	15.17	
RL-94-126Q2	1-4	OR3	core-margin	Qtz	smoky	LCV	s	-24	-14.58		-56.99	9.62	31	1.46	
RL-94-126Q2	1-5	OR3	core-margin	Qtz	smoky	LCV	s	-26	-13.09		-56.99				0.771

Table A2: Thermometry data for LVH inclusions

sample #	Incl #	Preparation	Zone	Mineral	Min Type	Type	Origin	Te	Tm ICE	Th (L-V)	Tm NaCl	Tm KCl	Tm HYD	Salinity (C)	d in Th
RL-94-052b	1-1-3	OR3	core-margin	Qtz	milky	LVH	S	-60	-41.37	140	149	102		35	1.143
RL-94-052b	2-1-1	OR3	core-margin	Qtz	milky	LVH	P?-a	-60	-20.68	88	145	100	13.21	28	1.304
RL-94-052b	2-1-2	OR3	core-margin	Qtz	milky	LVH	P?-a	-59	-20.29	91	148	93	13.21	28	1.323
RL-94-052b	2-1-3	OR3	core-margin	Qtz	milky	LVH	P?-a		-20.29	107	147	101	12.91	27	1.344
RL-94-052b	2-1-4	OR3	core-margin	Qtz	milky	LVH	P?-e	-63	-21.17	107					1.281
RL-94-052b	2-1-7	OR3	core-margin	Qtz	milky	LVH	P?-e	-68	-20.88	78	159		12.91	28	1.194
RL-94-052b	2-1-8	OR3	core-margin	Qtz	milky	LVH	P?-e	-67	-21.88	91	159		13.01	28	1.201
RL-94-052b	3-1-1	OR3	core-margin	Qtz	milky	LVH	S	-68	-21.56	80	127		13.21	28	1.184
RL-94-052b	3-1-2	OR3	core-margin	Qtz	milky	LVH	S	-60	-21.76	91	128	96	13.40	27	1.321
RL-94-052b	3-1-3	OR3	core-margin	Qtz	milky	LVH	S	-60	-23.90	77	128		12.91	28	1.185
RL-94-052b	3-1-4	OR3	core-margin	Qtz	milky	LVH	Sl		-24.20	77	130		12.91	28	1.188
RL-94-052b	3-1-5	OR3	core-margin	Qtz	milky	LVH	Sl	-60	-23.60	78	129		12.91	28	1.185
RL-94-060	1-1-4	OR3	core	Qtz	clear	LVH	S		-38.44	104	144		12.91	32	1.175
RL-94-060	1-1-5	OR3	core	Qtz	clear	LV(H?)	S		-22.73	98				27.71	1.142
RL-94-060	1-1-6	OR3	core	Qtz	clear	LVH	B	-65	-38.44	108	148		12.91	32	1.174
RL-94-060	1-2-1	OR3	core	Qtz	clear	LVH	B	-65	-39.02	122	148		12.91	33	1.184
RL-94-060	1-2-2	OR3	core	Qtz	clear	LVH	B	-52	-37.76	107	148		12.91	32	1.174
RL-94-060	1-2-4	OR3	core	Qtz	clear	LVH	B	-52	-39.24	108	148		12.91	32	1.175
RL-94-060	1-2-6	OR3	core	Qtz	clear	LVH	B		-39.24	102	147		12.91	31	1.177
RL-94-060	4-1-3	WC	core-margin	Fl	clear/green	LVH	B	-28	-20.29	118	137			28	1.175

Table A3. Thermometry data for LVH inclusions

VITA AUCTORIS

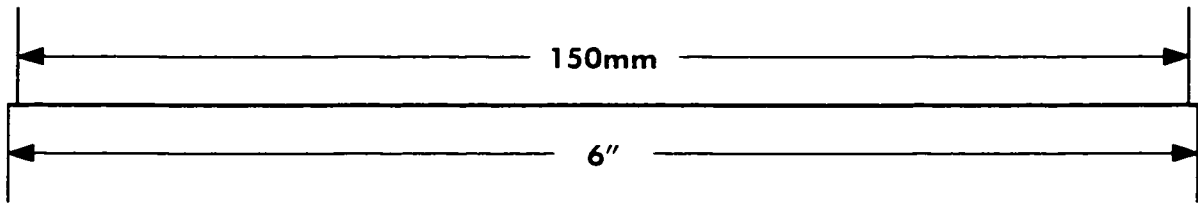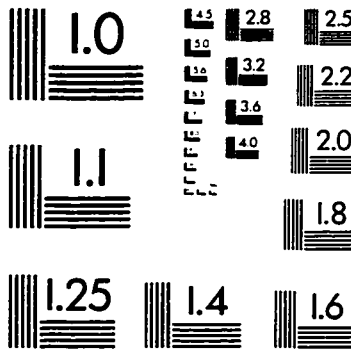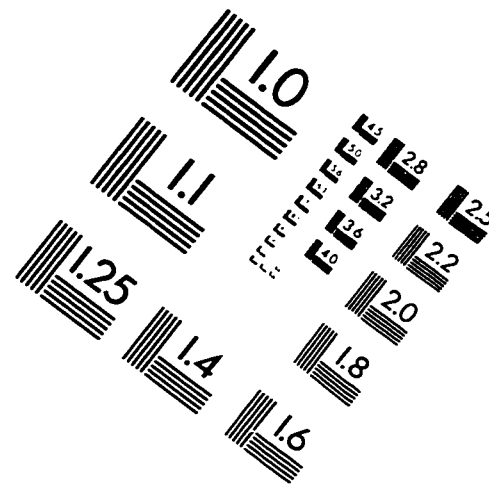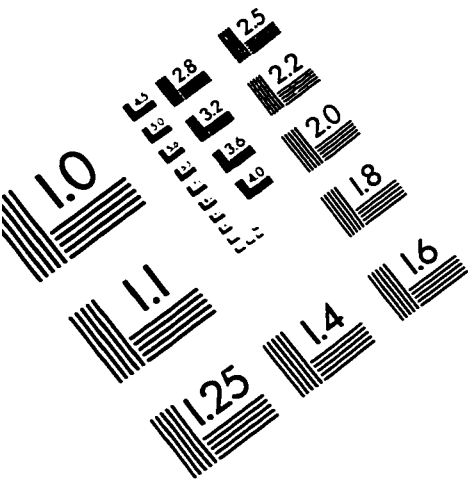|	
NAME:	Randy Levasseur
PLACE OF BIRTH	Windsor, Ontario
YEAR OF BIRTH	1969
EDUCATION	Brennan High School, Windsor 1983-1988
	University of Windsor, Windsor, Ontario 1988-1993. Honours B.Sc. (Geology)
	University of Windsor, Windsor, Ontario 1993-1997. Masters Sc. (Geology)

IMAGE EVALUATION
TEST TARGET (QA–3)

150mm

6"